Can Alterations in the Temporal Structure of Spontaneous Brain Activity Serve as a Disease-Specific Biomarker for Schizophrenia? A Multi Cohort fMRI Study

Fumika Kondo

A thesis submitted to the
Faculty of Graduate and Postdoctoral Studies
in partial fulfillment of the requirements
for the Master of Science degree in Neuroscience

Department of Neuroscience
Faculty of Medicine
University of Ottawa

Abstract

Schizophrenia (SCZ) is a complex psychiatric disorder including various symptoms. Resting-state fMRI investigations mostly focused on functional connectivity alterations in SCZ reflecting the spontaneous activity's spatial structure. Complementing its spatial structure, the brain's spontaneous activity can be characterized by a complex temporal structure such as scale-free dynamics or long-range temporal correlations (LRTCs). However, it remains an open question whether the temporal structure of spontaneous brain activity, as indexed by the power-law exponent (PLE), can provide biomarkers specific to SCZ as distinguished from other psychiatric disorders like major depressive disorder (MDD) and bipolar disorder (BP). Here, we studied a large-scale cohort (n = 244) of two independent schizophrenic data sets (n = 45), MDD (n = 28), and BP patients (n = 73, in manic, depressed, and euthymic phases) and 98 healthy controls. We found significant PLE reduction in specifically the medial prefrontal cortex (mPFC) in SCZ. This was replicated in an independent sample and was shown to be specific when compared to MDD and different phases of BP. Due to its disease-specific nature, the mPFC PLE reduction may eventually serve as a biomarker for SCZ.

List of Contents:

List of Figures and Tables:

List of abbreviations:

ALFF: Amplitude of Low Frequency Fluctuations

ApEn: Approximate entrophy

BDI: Beck Depression Inventory

BOLD: Blood-Oxygenation-Level-Dependent

BP: Bipolar Disorder

CON: Control

CPZ: Chlorpromazine

DLPFC: Dorsolateral Prefrontal Cortex

DMN: Default Mode Network

DSM: Diagnostic and Statistical Manual of Mental Disorders

EEG: Electroencephalography

ETC: Effort to compress

fALFF: fractional Amplitude of Low Frequency Fluctuations

FC: Functional Connectivity

fMRI: Functional Magnetic Resonance Imaging

HC: Healthy Controls

LRTC: Long Range Temporal Correlation

LV: Lempel-Ziv

MADRS: Montgomery–Åsberg Depression Rating Scale

MDD: Major Depressive Disorder

MEG: Magnetoencephalography

mPFC: Medial Prefrontal Cortex

PACC: Perigenual Anterior Cingulate Cortex

PANSS: Positive and Negative Syndrome Scale

PCC: Posterior Cingulate Cortex

PLE: Power Law Exponent

ROI: Region of Interest

SD: Standard Deviation

TE: Echo Time

TR: Repetition Time

FFT: fast Fourier transform

Statement of Contribution and Acknowledgements

The main raw data of schizophrenic patients in the resting-state fMRI experiment were originally collected at the University of Goettingen (Goettingen, Germany) and shared with us. The other two data sets were collected in Taiwan and Italy. I have conducted all the work presented here including proposing the study, processing raw data, designing and conducting the analysis, and writing this thesis under the supervision of Dr. Georg Northoff.

I would like to thank Dr. Georg Northoff for his guidance. Also, special thanks go to Dr. Zirui Huang for his supervision and for guiding me throughout the learning stages with the analysis methods. I would also like to thank my thesis advisory committee members, Dr. Paul Albert and Dr. Andre Longtin for their advice.

Most of all, I am grateful to my family and friends, who have always encouraged me to make and pursue my own goals and supported me from Japan.

Statement of the Specific Contribution to the Work

I conducted the main data analysis for this thesis. Data collection was conducted in Germany for dataset I, Taiwan for dataset II, and Italy for dataset III. I

would like to thank Dr. Niall Duncan and Dr. Nithin Nagaraj for their contribution to the additional data analysis.

1. Background and introduction

1.1. Schizophrenia and human brain's resting-state activity

Past studies have investigated schizophrenia (SCZ) from various aspects. For instance, some studies have focused on patients' perceptions of their environment (Stanghellini et al., 2015), while other studies have focused on altered affective functions which can possibly explain auditory hallucinations (Panksepp, 2004). That being said, SCZ is still one of the most unclear and unknown psychiatric disorders. According to the National Health Service (NHS), SCZ is one of the most common serious mental health conditions, and about 1 in 100 people will experience SCZ symptoms in their lifetime. The exact cause of SCZ is unknown, but most experts believe the condition is caused by a combination of genetic and environmental factors. Regarding genetic influences, adoption studies revealed that kids whose biological parents are schizophrenic were at an elevated risk for psychosis, but kids adopted into families where one of the adoptive parents has schizophrenia were not at an increased risk for developing schizophrenia (Narayan et al., 2015). Regarding environmental influences, Marcelis et al. (1999) revealed that people who were born in urban areas have a greater risk of developing schizophrenia. In addition, there is consistent evidence for a 5–8% excess of births in winter and spring of children who later develop schizophrenia (Bradbury & Miller, 1985). However, its neuronal mechanisms are still unclear and remain to be explored.

Past studies have shown that SCZ is related to some cognitive deficits, and it has been said that cognitive impairment is a core feature of SCZ (Nuechterlein et al., 2014). There are two main reasons that cognitive deficits are viewed as a core feature of SCZ. The first one centers on the fact that many studies find that cognitive deficits existed before the onset of psychosis and are capable of predicting SCZ in groups at

high risk. The second reason is that cognitive deficits persist during symptomatic remissions and are relatively stable across time in SCZ patients. Predominant cognitive deficits include memory functioning, language, executive function, and attention (Fioravanti et al., 2012).

Regarding its symptoms, SCZ is a long-term mental health condition that causes a range of different psychological symptoms, including hallucinations (hearing or seeing things that do not exist) and delusions (unusual beliefs not based on reality that often contradict the evidence). It has been found that schizophrenic patients experience positive symptoms such as hallucination and delusion as well as negative symptoms such as depression and withdrawal (Frith et al., 2000). Positive symptoms include changes in behavior or thoughts such as hallucinations or delusions. Negative symptoms include withdrawal or lack of function, such as absence of emotions. Also, SCZ is characterized by a lack of integration between thought, emotion, and behavior (Camchong et al., 2011). It has been also found that schizophrenic patients have inhibited emotion regulation. Symptoms also include ego disturbances, where patients describe an altered sense of self as well as emotional and cognitive symptoms (Leube et al., 2008). Therefore, SCZ is considered as an extreme example of abnormal consciousness (Ebisch et al., 2014). Sometimes schizophrenic patients cannot distinguish their own thoughts from reality, so SCZ can be considered a self-disorder. Self-reference is typically reduced in SCZ as a disorder of the self (Kühn & Gallinat, 2013). Thus, SCZ damages people differently, and its symptoms vary from person to person.

Theories of brain disturbances in schizophrenia: mPFC-Dopamine

When we talk about the mechanisms of SCZ, dopamine hypothesis is often mentioned (Howes & Kapur, 2009). It has been revealed that there is an increased

dopamine synthesis rate in mPFC and striatum in SCZ. Lindstrom et al. (1999) revealed a biochemical disturbance, namely, a dysregulation of the dopamine synthesis in the mPFC in SCZ. It has been known that excessive dopamine in mesolimbic system causes delusions and hallucinations. However, we do not know if their findings are primarily pathophysiological in SCZ or merely reflect subcortical neuropathological changes. Moreover, dopamine-related psychosis occurs in many disorders, not exclusively in schizophrenia. On the other hand, it has been known that autistic children have decreased mPFC dopaminergic activity (Ernst et al., 1997). As well as hypothesis of excessive dopamine, a recent study found that a gene called C4 (Complement component 4) is one of the causes for SCZ, but studies remain to be explored. Sekar et al. (2016) found that the higher the levels of C4 activity were, the greater a person's risk of developing schizophrenia was. The researchers also conducted experiments in mice, and found that the more C4 activity there was, the more synapses were pruned during the brain development.

Since the actual biological mechanisms are unclear, there are no biomarkers yet that can guide diagnosis and therapy in an objective way; diagnosis is still based on subjective judgments by psychiatrists following diagnostic manuals, such as the *Diagnostic and Statistical Manual of Mental Disorders* (DSM-V, 2015). Here, biomarkers indicate objective indications of a patient's medical state observed from outside the patient—which can be measured accurately and reproducibly (Strimb & Tavel, 2010). Currently, schizophrenia is diagnosed mostly based on DSM-IV, which contains diagnostic criteria for schizophrenia such as delusions, hallucinations, disorganized speech, and social/occupational dysfunction. In addition, the Positive and Negative Syndrome Scale (PANSS) is a medical scale used for measuring the symptom severity of patients with schizophrenia. For treatment, medications are the cornerstone of schizophrenia treatment, and antipsychotic medications are the most

commonly prescribed drugs. They're thought to control symptoms by affecting the brain neurotransmitter dopamine. Chlorpromazine is a very effective antagonist of D2 dopamine receptors.

Although there has been much research investigating the underlying mechanisms of mental illness by using psychophysiological and neuro-imaging techniques, the results of past research have shared limited consistency where the actual mechanism remains to be investigated. By understanding and knowing the actual mechanisms, we will be able to develop personalized treatments for mental illness.

Resting-state brain activity and past research

Recently, the brain activity that is independent of external stimuli has become a focus of research (Raichle, 2015). This spontaneous brain activity is called "resting-state" brain activity. Normally, in the resting-state experiment, participants are told to relax and not to think about anything in particular during the experiment. Blood-Oxygenation-Level-Dependent (BOLD) fMRI provides an indirect measure of neural activation from such activation's neurovascular influence on local blood oxygen levels (Logothetis, 2001). The current study investigated the neural mechanisms occurring in the resting-state brain of a person with SCZ.

In the past years, the resting-state functional magnetic resonance imaging (rs-fMRI) technique has been used frequently in medical science, such as in cancer screening (e.g., Kesler et al., 2011). However, the use of rs-fMRI in the area of psychiatric neuroimaging is relatively uncommon. Resting-state fMRI signals reflect the brain's spontaneous activity; therefore, it gives us an idea about the mechanisms when the brain is not engaged in any specific task (Lee et al., 2013). Resting-state brain mechanisms are meaningful to investigate in psychiatric research as they can

reveal abnormal neuronal mechanisms independent of the brain's cognitive functions. To investigate the mechanisms of mental illnesses, previous studies have used different metrics by using rs-fMRI brain signals, especially functional connectivity (FC) and temporal variability (e.g., Huang et al., 2016). Functional connectivity refers to a pattern of statistical dependencies between distinct units within a nervous system (Lynall et al., 2010). In other words, FC is defined as the statistical association or dependency among two or more anatomically distinct time-series (Friston 1994). Temporal variability describes the degree of change in the signal amplitude over time and can be calculated by standard deviation (SD). Although there have been many studies on FC, metrics such as SD have not been investigated further yet, and the results are inconsistent.

Resting-state fMRI studies of SCZ have also typically focused on FC—i.e., the degree of temporal correlation of the BOLD signal among anatomically distributed brain regions (Turner et al., 2013). According to Moran et al. (2011), investigation of resting-state, low-frequency fluctuation is essential to study internal mental processes. Also, studying the full spectrum and the low-frequency oscillations may be critical for deciphering the complex brain signal abnormalities observed in SCZ patients.

1.2. Functional connectivity of resting-state activity and DMN

Default-mode network (DMN)

As indicated above, the neural activity of one's brain is often considered in terms of its connectivity. Stephan et al. (2006) suggested that SCZ is not caused by focal brain abnormalities but by pathological connectivity between brain regions. It has been suggested that disruption in the connectivity between brain processes may underlie the symptoms of SCZ, which is called the disconnection hypothesis

(Camchong et al., 2011). The study of Uhlhaas (2013) also proposed that studies should focus on the neuronal dynamics in large-scale networks, which is compatible with the notion of disconnectivity.

Functional imaging studies have shown that certain brain regions consistently show greater activity during resting states than during engagement in cognitive tasks (Greicius et al., 2003). These areas comprise the default-mode network (DMN), which has been a focus of brain research in recent years. The DMN includes the medial prefrontal cortex (mPFC), the medial temporal lobes, and the posterior cingulate cortex (PCC). Brain areas are preferentially activated during internally focused tasks (Öngür et al., 2010), whereas the DMN reflects an ensemble of cortical regions typically deactivated during demanding cognitive tasks in fMRI studies (Raichle et al., 2001). Several studies have shown that cortical midline structures (CMS) are related to self-related processing (e.g., Northoff et al., 2006; Van der Meer et al., 2010). Especially, past studies have found that the mPFC and the PCC highly overlap with the DMN and with high levels of spontaneous activity and functional connectivity during resting-state activity (e.g., Boly et al., 2008, Wicker et al., 2003). Also, it has been found that higher levels of activity within the anterior medial regions of the DMN such as the mPFC are linked to a focus on internal mental contents, self-directed thoughts, sensations of parts of the body (like the limbs or the face), and bodily processes (such as the heartbeat; Vanhaudenhuyse et al., 2011).

Schizophrenia is also characterized by the false attribution of perceptual experience to an external source (Yu et al., 2014). The networks, including attention, visual, motor, salience, and language, showed decreases in schizophrenic patients in Yu et al.'s (2014) study; these findings are consistent with those of other studies showing deficits in cognitive, motor, and low-level sensory processing as well as

deficits in reward sensitivity in schizophrenic patients. Yu et al. (2014) assumed that those decreases may provide neuronal bases to the excessive internally directed thought processing often observed in SCZ patients and the abnormal focus on internally generated stimuli. Since schizophrenic patients often show disturbed self-reference, it is suggested that they show some abnormality in the brain regions in the DMN. Since the DMN network has been associated with internal contents, this might explain the abnormal perception of the internal contents. For this reason, researchers have suggested that this dysregulation might be associated with hallucinations. If the DMN reflects self-monitoring and stimulus-independent thought, it should not be surprising that there are anomalies in this network in schizophrenic patients. Frith (2000) has argued that a failure to recognize internally generated thought as arising endogenously is fundamental to the disorder, which can be called a failure of covert cognition in SCZ.

According to Garrity et al.'s (2007) study using tasks, healthy subjects and patients had significant spatial differences in DMN activity, most notably in the frontal and anterior cingulate. In addition, activity in patients in the medial frontal, temporal, and cingulate gyri is correlated with the severity of positive symptoms. The results indicate that SCZ is associated with altered temporal frequency and spatial location of the DMN. Garrity et al. (2007) found that schizophrenic patients have a reduced volume of activation in the anterior cingulate cortex (ACC) in DMN compared to healthy subjects. Abnormal fMRI activation of the ACC has been reported in SCZ and has been correlated with working memory deficits (Fletcher et al., 1999). The ACC is believed to play a role in modulating basic subconscious and higher cortical processing in the default mode during rest and monitoring task progress. A failure to monitor internally generated actions has been implicated in

hallucinations and delusions in SCZ. Previous research also suggests that auditory hallucinations in SCZ may be due to a failure to properly interpret inner speech (Allen et al., 2004). Therefore, the activation of the ACC in both a resting state and during a task implicates it as a modulator of default mode functioning. However, its inability to function properly to modulate internal thoughts and those related to the task may play a role in the positive symptoms of SCZ (Garitty et al., 2007).

Functional connectivity within the DMN in schizophrenia

The resting-state functional connectivity fMRI approach detects temporal correlations in spontaneous BOLD signal oscillations while subjects rest quietly in the scanner (Greicius et al., 2009). As the DMN has been considered to be abnormal in SCZ, many studies have investigated the functional connectivity within DMN in schizophrenic patients. Until now, numerous studies have shown alterations within the DMN in those patients. However, the findings of functional connectivity in SCZ have been inconsistent.

According to Micheloyannis et al. (2006), disturbances in functional connectivity have been proposed as a major pathophysiological mechanism for SCZ, such as for cognitive disorganization. During the working memory task using electroencephalography (EEG), healthy subjects exhibited small-world properties (a combination of local clustering and high overall integration of the functional networks) in the alpha, beta, and gamma bands. However, these properties were not seen in the SCZ group. These findings are in accordance with an inadequate organization of neuronal networks in subjects with SCZ.

1.3. Temporal variability of resting-state activity

In addition to examining functional connectivity, past studies have investigated the temporal variability of resting-state brain activity. Although there are

many studies focusing on the relationship between heart rate variability in mental illnesses (e.g., Akar et al., 2015), there are fewer studies investigating the temporal variability of the BOLD signal. According to Bar et al. (2007), complexity of heart rate modulation is significantly reduced in acute, untreated schizophrenia, thus indicating an increased risk for cardiovascular events in these patients.

The low-frequency fluctuations, slower than cardiac or respiratory fluctuations, are considered to be related to spontaneous neural activity within a region, and they contribute strongly to the correlations seen in BOLD signal time courses across regions (Cordes et al., 2001; Yang et al., 2007; Lui et al., 2009). Higher temporal variability in the resting state has been observed in the regions that constitute the default mode network. Here, higher temporal variability reflects a greater dynamic range of possible responses to incoming stimuli. This is beneficial to the adaptability and efficiency of neural systems as it permits a greater range of response to a greater range of stimuli (Garrett et al., 2013). In contrast, when variability is lacking, there is little capacity for the brain to explore its state space. This increases the possibility of the system to remain rigidly in a single state (Deco et al., 2009), making state-to-state transitions more difficult. It has been considered that slow fluctuations in activity are a fundamental feature of the resting brain, and their presence is the key to determining correlated activity between brain regions and defining resting-state networks. The relative magnitude of these fluctuations can differ between brain regions and between subjects, and thus may act as a marker of individual differences or dysfunction.

Temporal variability is normally calculated by SD, which describes the degree of change in the signal amplitude over time (see Fig. 1).

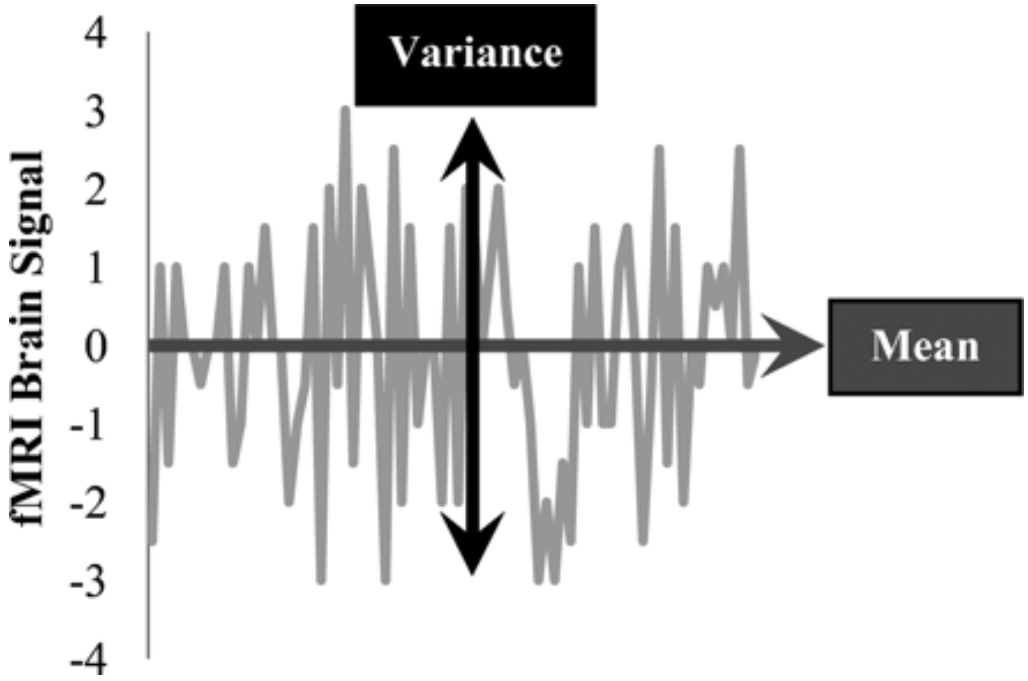

Figure 1: **Temporal variance (Garrett et al., 2010).**

X axis indicates time. Y axis indicates the amplitude of the fMRI Brain Signal. The horizontal line indicates the mean value. The vertical line indicates the variance.

The temporal SD of the activity patterns is normally used to quantify the variability of this measure as a function of time at each brain voxel (Tomashi et al., 2016). The SD of the BOLD signal describes the temporal variance of brain activity across time within a particular region. However, to investigate the amplitude of the signal fluctuations as a function of time in each individual, an alternative measure, the amplitude of the low frequency fluctuations (ALFF), has been also used widely as a similar measure to SD. It can be said that the temporal variability measured by SD is similar to values measured by ALFF and the fractional amplitude of low frequency fluctuations (fALFF). Just like SD, the ALFF and fALFF can also be measured from resting fMRI data. The SD is the square root of variance, and ALFF is the square root of power. Mathematically, variance of a time course is approximately the same as the power (by fast Fourier transform (FFT) calculation), and both of the measures tell us the temporal dynamics of brain activity. We can say that ALFF and SD measure the same thing in two different ways. The fast Fourier transform (FFT) is a common algorithm for Fourier transforms. A Fourier transform (FT) converts a signal from the time domain (signal strength as a function of time) to the frequency domain (signal strength as a function of frequency).

ALFF (Zang et al., 2007) and f/ALFF (Zou et al., 2008) quantify the amplitude of these low-frequency oscillations (LFOs). ALFF is defined as the total power within the frequency range between 0.01 and 0.1 Hz, and thus it indexes the strength or intensity of LFO. f/ALFF is defined as the power within the low-frequency range (0.01–0.1 Hz) divided by the total power in the entire detectable frequency range, and it represents the relative contribution of specific LFO to the whole frequency range (Zuo et al., 2010). Therefore, we can say that fALFF is the normalized index of ALFF.

The temporal dynamics of resting-state activity, such as the ALFF (Zang et al., 2007), and the SD of neural activity changes across time (Garrett et al., 2011) have been investigated in recent years (e.g., Huang et al., 2014). The researchers hypothesized that abnormal brain responses while processing self-referential tasks may be related to impairments not only in the spatial domain but also with temporal abnormalities in neuronal measures of resting-state activity—for example, lower ALFF and SD within the midline regions. Huang et al.'s (2014) study found that the larger the signal changes in the PACC during the self-referential condition compared with the non-self-referential condition, the higher the degree of consciousness in patients with abnormal consciousness. For the whole-brain analysis, reduced ALFF and FC were observed in the midline regions, including the PACC, the mPFC, and the PCC, in the patients with abnormal consciousness compared with the healthy group. The midline regions identified during the self-referential task (i.e., PACC and PCC) overlapped with the ones obtained from the group difference of ALFF and FC in the resting state. The researchers analyzed the SDs of resting-state activity as a relatively analogous measure, revealing similar results. This SD finding further confirmed the ALFF results. From the results, it can be said that ALFF and SD are relatively similar measures. They found that the magnitude of cortical responses in the anterior midline regions (e.g., the PACC) was significantly correlated with patients' degree of consciousness. The same midline regions displayed major resting-state abnormalities as manifested by reduced ALFF, FC, and the SD of signal changes. In healthy volunteers, there were stronger signal changes in the mPFC, PACC, and PCC while answering self-referential questions compared with nonself-referential questions. This finding is in accordance with the previous studies of the neural correlates of the self in healthy subjects. Their results revealed that the resting-state FC of the

(mPFC=)PACC-to-PCC was significantly lower for the patient group compared with the control group. The study observed a strong link between task-induced signal changes (self vs. nonself) and resting-state activity (ALFF and SD) in the precuneus in the patient group. This suggests that greater ALFF (or SD) in the resting state may be correlated with greater differentiation between self and nonself. The reduced ALFF, FC, and SD suggest a decreased propensity of resting-state activity to exhibit neural activity changes during self-referential tasks. Their findings suggest that task-related abnormalities in midline regions may be closely related to deficits in spatial (i.e., FC) and temporal (i.e., ALFF, SD) measures of resting-state activity. Therefore, it can be assumed that patients with abnormal self-consciousness, such as schizophrenic patients, may have abnormalities which can be measured by temporal measures as well as spatial measures.

Huang et al. (2015) conducted a whole brain SD of BOLD signal analysis in anesthesia; they found that the higher the inter-regional functional connectivity, the higher the degree of temporal variability in healthy people, but this relationship was broken down in anesthesia. However, the exact relationship between functional connectivity and neuronal variability remains to be determined. According to Huang et al. (2015), temporal variance as measured by the SD of the BOLD signal was significantly reduced in especially the cortical midline regions in anesthesia. Furthermore, they found significant frequency-dependent effects of SD in the thalamus, which showed abnormally high SD in Slow-5 (0.01–0.027 Hz) in the anesthetized state. Their study employed the measurement of SD of activity across time (Garrett et al., 2010, 2011) to examine the temporal variance of the brain's spontaneous activity. The SD of the BOLD signal change across the time series for each voxel was also calculated to yield an SD map for each subject. They found a

significantly reduced SD in the anesthetized state in the mPFC, PACC, PCC, and visual cortex. Decreased temporal variance in the midline regions is in line with several recent findings indicating a central role for temporal variance in shaping neural activity. The assumption of consciousness-related reduction in DMN temporal variance is consistent with previous findings in the midline regions of vegetative-state patients (Huang et al., 2014). However, mechanisms underlying the importance of midline temporal variance for the support of consciousness remain to be explored.

Although there have been a variety of studies measuring SD, ALFF, and fALFF, the findings using these measures for SCZ are inconsistent: ALFF amplitudes in mPFC were reduced in Huang et al.'s (2010) study, while Hoptman et al. (2010) found increased fALFF amplitude in medial frontal gyri. Also, larger ALFF amplitudes were found in putamen in SCZ in Huang et al.'s study but not in Hoptman et al.'s study. Here, Hoptman et al. used medicated patients, while Huang et al. used antipsychotic-naive first-episode schizophrenia patients. ALFF has recently been shown to be reduced in SCZ in cross-sectional studies, albeit with some regional inconsistencies (Hoptman et al., 2010; Huang et al., 2010). Interestingly, a recent study reported an increase of frontal and parietal ALFF in antipsychotic–naïve SCZ patients after antipsychotic drug treatment (Turner et al., 2012). Hence, ALFF may provide a relatively easy method to track antipsychotic response in clinical populations.

Hoptman et al. (2010) used ALFF and fractional ALFF (fALFF; the relative amplitude that resides in the low frequencies) to examine the amplitude of LFO in SCZ. Their findings show that schizophrenic patients showed reduced low-frequency amplitude in proportion to the total frequency band investigated (i.e., fALFF) in the lingual gyrus, left cuneus, left insula/superior temporal gyrus, and right caudate and

increased fALFF in the mPFC and the right para-hippocampal gyrus. ALFF was reduced in patients in the lingual gyrus, cuneus, and precuneus and increased in the left parahippocampal gyrus. These results suggest LFO abnormalities in SCZ. According to Hoptman et al. (2010), the reduced LFO in the precuneus is consistent with abnormalities in the DMN in SCZ. The decrease there is in contrast with increased fALFF in the mPFC, which is also a part of the DMN. It is possible that these differential effects on amplitude in patients are related to the disruption in coordination among elements of the DMN in SCZ (e.g., Garrity et al., 2007; Whitfield-Gabrieli et al., 2009).

On the other hand, Yang et al.'s (2014) study found that the temporal variability (SD) of the global brain signal is larger in schizophrenic patients. By using the power spectrum, Yang et al. (2014) investigated the cortical power and variance of the brain signal in SCZ by using the power spectrum and found an increased variance in schizophrenic patients. Yang et al.'s (2014) study used the power spectrum (the energy of the signal at each frequency that it contains) to investigate the cortical power and temporal variance in SCZ. Researchers calculated the difference in cortical power and temporal variance between healthy controls and schizophrenic patients without removing the global signal (GS), which refers to the mean BOLD signal over all voxels (Boly et al., 2008). The natural variation in breathing depth and rate during rest has a significant impact on rs-fcMRI analyses as the induced fMRI signal changes can occur at similar spatial locations and temporal frequencies. The GS correlates with respiration-induced fMRI signal fluctuations. Therefore, the GS is usually removed to better isolate functional networks, but the study revealed that GS itself is profoundly increased in schizophrenic patients when compared to both bipolar and healthy subjects. Yang et al. (2014) suggested that the GS variability averaged across

the whole brain is abnormally elevated in SCZ. Accordingly, they provided the first evidence that whole-brain GS are altered in SCZ. These abnormal increases of temporal variability in SCZ may be explained by net increases in local (recurrent self-coupling) and distant (long-range coupling) signal synchronization. Yang et al. (2014) also examined the relationship between FC and temporal variability and discovered that the temporal variability increases as a function of increasing signal synchronization. Alterations in temporal variability across the brain may form the basis for some of the resting-state FC abnormalities often observed in SCZ (Garrity et al., 2007). Other researchers revealed that the temporal variability increases as a function of increasing local and distant signal synchronization (Huang et al., decoupled). It was also suggested that the observed increase in temporal variability in SCZ may arise from increased neural coupling at both local and long-range scales, leading to a cortical network that operates closer to the edge of instability than in awake, healthy subjects (Yang et al., 2014). Importantly, these studies give us an indication that the relationship between the temporal variability and signal synchronization may be consciousness relevant.

As well as studies described above, Garrity (2007) found that SD is reduced in SCZ. Furthermore, another study (Turner et al., 2013) investigated fALFF, which found that fALFF is lower in schizophrenic patients than in healthy controls, throughout the cortex. Thus, it can be said that the results of schizophrenic brain analysis are inconsistent. Garitty et al. (2007) found that the amplitude (SD) in the DMN was lower in SCZ during the task, but the tendency was not significant. Although it was not significant, SCZ patients tend to exhibit smaller default mode changes overall than do healthy comparison subjects. Radulescu et al. (2012) showed

that the temporal variability was more restricted in schizophrenic patients than in controls.

Table 1 below shows some of the inconsistent results from the past studies on SCZ regarding temporal variability or related metrics such as ALFF and fALFF. Here, although the results are inconsistent, we can see changes tend to occur in the mPFC.

Table 1

Comparison of the Results of Past Studies on fMRI BOLD Signal Variability in SCZ. Author and year of the study, area of the brain, task or resting-state design, comparison between healthy subjects and SCZ patients, and measures of the calculation are shown from the left.

study	area	task/resting	comparison	calculation
Garrity et al. (2007)	DMN	task	healthy> schizophrenia	the amplitude
Huang et al. (2010)	mPFC	resting-state	healthy> schizophrenia	ALFF
Hoptman et al. (2010)	medial frontal gyri	resting-state	schizophrenia> healthy	fALFF
Yu et al. (2012)	mPFC	resting-state	schizophrenia> healthy	ALFF
Radulescu et al. (2012)	Brodmann's area 10	task	healthy> schizophrenia	PSSI
Turner et al. (2013)	whole brain	resting-state	healthy>schizophrenia	fALFF
He et al. (2013)	mPFC	resting-state	healthy> schizophrenia	fALFF
Yang et al. (2014)	whole brain	resting-state	schizophrenia> healthy	SD

Thus, FC and temporal variability are both investigated in SCZ, but the results are inconsistent. Here, one possibility is that the amplitudes of LFO are frequency dependent (Yu et al., 2014).

1.4. Temporal structure of resting-state activity

As indicated above, investigations of the blood-oxygen-level-dependent (BOLD) signal using non-invasive fMRI have extended our knowledge of the functional changes in schizophrenic patients' brains, such as GS power, FC, and temporal variability (Stephan et al., 2006; Yang et al., 2014, 2016) in various networks including the DMN and other regions, especially in the mPFC. Although investigated in other psychiatric disorders like bipolar disorder (Martino et al., 2016), the temporal pattern and structure of spontaneous brain activity remains to be investigated in SCZ (see Weinberger & Radulescu, 2016).

Temporal structure

Scale-free properties have been studied at the neuronal level and behavioral level in neuroscience. Recently, there has been an increasing interest in the scale-free properties of the resting-state brain. While human resting-state neural dynamics have mainly been investigated using measures of FC (Beckmann et al., 2005; Fox et al., 2005: He et al., 2009), investigations of scale-free properties have been conducted in recent years. A recent study found that when instrumental noise is carefully controlled for, by using both fMRI and electrophysiology, the brain produces $1/f^{\beta}$ power spectra on its own (He et al., 2010). This means that spontaneous brain activity can be characterized by scale-free dynamics or power-law spectra. Scale-free dynamics is an intrinsic feature of many complex processes in nature (Huang, 2016). For instance, it has been revealed that similar scale-free power-law dynamics characterize an animal's activity across intervals of several days, which indicates that scale-free behavioral

fluctuations arise also in natural settings. Also, temporal structures can be called "long-range temporal correlations." Since the correlation measures the "similarity" between two signals, the temporal correlation measures the similarity of one signal over time. Lee et al. (2010) explained that scale-free activity can be identified mathematically when a system follows a "power law," a measure of self-similarity. This scale-free property is thought to enable rapid synchronization, rapid information transfer, minimal wiring costs, and a balance between local segregation and global integration. Previous studies proved that the power spectrum of spontaneous fMRI signals follows a power-law distribution (Bullmore et al., 2001).

He et al. (2010) investigated the scale-free dynamics in the fMRI signal and its power-law exponent (PLE) across brain regions. The researchers showed that scale-free brain activity contains rich temporal structures. They revealed that spontaneous fMRI signals are scale-free, and its PLE varies across brain regions. The visual and DMN regions have the steepest power spectra, characterized by the largest PLE β. On the other end, the cerebellum and hippocampus had the shallowest power spectra, characterized by the smallest PLE β. Interestingly, it was found that when the total variance of the fMRI signal instead of the PLE was calculated, no significant effect was found. Therefore, it can be suggested that the PLE can be a more accurate measure compared to variance. Deco et al. (2013) also insisted that brain fluctuations at the resting state are not random but structured in spatial patterns of correlated activity across various brain areas.

Evidence has suggested that spontaneous brain activity can be characterized by scale-free dynamics or power-law spectra. Scale-free activity indicates the temporal structure of neural activity by describing its self-affine pattern over time (Palva et al., 2013). Temporal structure describes the power distribution across

frequencies. The term scale-free indicates that brain clusters do not have a preferred size (Palve & Palva, 2011, p. 366). Self-affine temporal structure may account for recurring or consistent patterns of neural activity across time. This suggests that the degree to which the neural activity pattern at one particular point in time can predict neural activity at subsequent points in time. Such self-affine temporal structure distinguishes scale-free activity measures (e.g., the PLE) from other resting-state activity measures (e.g., FC, temporal variability), which do not show such temporal structure. The brain's spontaneous activity can be characterized by a complex temporal structure that shows a certain order and regularity across in activity pattern across time. One feature of the spontaneous activity's temporal structure is scale-free dynamics or long-range temporal correlations (LRTCs) (He, 2014; He et al., 2010; Linkenkaer-Hansen et al., 2011; Manning et al., 2009; Palva et al., 2013, 2015). The LRTCs, as for instance, indexed by the PLE, measure the relationship in power between slower and faster frequency fluctuations. Scale-free dynamics, indicated by the power spectrum with the formula $P \alpha 1/f^{\beta}$, are widely observed in nature (Goldberger et al., 2002). Recently, it has been argued that they are relevant in investigating brain activity (He et al., 2010). Scale-free properties index long-range temporal correlations (Palva et al., 2013), which can be understood as self-affinity (Hardstone et al., 2012). Increasing evidence has suggested that spontaneous brain activity can be characterized by scale-free dynamics or power-law spectra (e.g., He et al., 2010) in fMRI signals. Huang et al. (2015) investigated how the temporal structure of spontaneous activity, or, in other words, the long-range temporal correlations of the BOLD signal, can be characterized. Interestingly, the temporal structure of spontaneous brain activity can be characterized by scale-free dynamics or LRTCs (e.g., He et al., 2010; Palva et al., 2013). Recent fMRI studies show that

infraslow spontaneous fluctuations observed in the resting state conform to a power-law distribution and hence show LRTCs (He et al., 2010). It can be said that higher LRTCs (a larger PLE) are related to a higher time-lagged autocorrelation, indicating that the past pattern of a system has a stronger influence on its future dynamics (Linkenkaer-Hansen et al., 2001).

The relationship between different frequencies can be distinguished from the degree of order or regularity; that is, similarity of dynamics signal patterns from time point to time point. This can be accounted for by complexity measures such as Lempel-Ziv complexity (LZ), effort to compress (ETC), and approximate entropy (ApEn). Although some initial studies (Akar et al., 2016; Bachiller et al. 2014, 2015; Brookes et al., 2015, Molina et al., 2016; Radulescu et al., 2012; Sokunbi et al., 2014; Yang et al., 2015) indicate abnormal dynamic patterns of neural activity in both infraslow and faster frequency ranges, the changes in the different aspects or facets of the spontaneous activity's temporal structure remain unclear in SCZ. Moreover, it remains to be elucidated whether these changes in temporal structure are specific for SCZ as distinguished from other psychiatric disorders like depression (see also Weinberger & Radulescu, 2016).

1.5. SCZ and the resting-state brain

Temporal structure, schizophrenia, and self-consciousness

In the present study, this temporal structure was mainly investigated. Now, the reason why using this temporal structure for SCZ and other psychiatric disorders is important will be discussed. First, self-reference is typically reduced in SCZ as a disorder of the self (Northoff, 2014). The concept of the minimal self refers to the consciousness of oneself as an immediate subject of experience. Furthermore,

according to recent studies, disturbances of the minimal self may be a core feature of SCZ (e.g., Martin et al., 2014).

Huang et al. (2016) found that in healthy subjects, the higher the PLE in mPFC, the higher the private self-consciousness. Huang et al. (2016) investigated various measures of resting-state activity, including the PLE, regional homogeneity (ReHo), temporal variability (SD), degree of centrality (DC), and functional connectivity (FC). Scale-free activity, as indicated by the PLE and confirmed by the Hurst exponent (*H*), was the only neural measure to correlate. As the PLE and *H* measure specifically the temporal structure of spontaneous activity, rather than signal synchrony across regions (e.g., ReHo, DC, and FC) or the overall power of signal fluctuations (e.g., SD), this may suggest that the rest-self overlap in the mPFC is mediated by the temporal structure of the spontaneous activity. Huang et al. (2016) used the measure of PLE and revealed two key regions in the CMS: the PCC and the mPFC. They investigated the association between the scale-free dynamics of rs-fMRI activity and different dimensions of self-consciousness. From the results, it was revealed that there was a significant positive correlation between the PLE in the mPFC and private self-consciousness. Thus, higher degrees of long-range temporal correlations calculated by PLE are related to higher degrees of private self-consciousness. In Huang et al.'s (2016) study, the averaged power spectra across voxels within each of the two ROIs (region of interest), the mPFC mask, and the PCC mask were extracted for each subject. The power spectrum was fitted with a power-law function $P \propto 1/f^{\beta}$ using a least-square estimation (in a log frequency by log power plot) in the frequency range of 0.01–0.2 Hz (Baria et al., 2013). Finally, the PLE, β, of each subject's ROI was defined as the slope of the linear regression of log-power on log-frequency corresponding to the straight-line regime. Two of these regions located

in the CMS, the mPFC and the PCC, are defined as our ROIs based on our primary hypothesis about self-rest overlap. The study found a significant positive correlation between the PLE in the mPFC and private self-consciousness. This result suggests that higher degrees of long-range temporal correlations (as signified by the PLE) are specifically related to higher degrees of private self-consciousness. Future studies may consider the link between self-related stimulus-induced activity and private self-consciousness at a psychological level. Since applying self-related stimuli, such as one's own name or trait adjectives. The self is generally experienced as being continuous in time. This requires that sensory information be processed and integrated in such a way that we experience continuity over time (Northoff, 2013). According to Huang et al. (2016), a central feature of the self is its continuity across time (Klein, 2014). This continuity may be related to analogous temporal continuity in the spontaneous brain activity, which is characterized by its scale-free dynamics. Their finding is in line with a recent study in which researchers found that a higher degree of scale-free dynamics was related to a lower degree of extraversion (Lei et al., 2013). A lower degree of extraversion (or a higher degree of introversion) could be indicative of a higher degree of private self-consciousness, thereby aligning with our findings that higher private self-consciousness scores correlate positively with the PLE. The study demonstrated a direct relationship between the resting state's scale-free activity and its temporal structure in the mPFC with private self-consciousness. This significantly extends previous findings of rest-self overlap, indicating self-relatedness, to be encoded in especially the temporal structure of the mPFC resting-state activity (Huang et al., 2016). Thus, it can be suggested that temporal structure as indexed by the power structure (e.g., the PLE) is related to self-consciousness (Huang et al., 2016). As it has been suggested that patients with SCZ have altered self-

consciousness (e.g., Northoff, 2014), the temporal structure of the schizophrenic brain's resting-state signal may be abnormal and will therefore be the focus in the current study.

Thus, SCZ has altered self-consciousness (e.g., Northoff, 2014), and self-reference is typically reduced in SCZ as a disorder of the self (Kühn & Gallinat, 2013). In addition, it was found that temporal structure is related to self-consciousness (Huang et al., 2016) as described above. Based on these findings, it was hypothesized that the temporal structure of the resting-state signal in schizophrenic patients may be abnormal, and so it became the focus of the present study. Based on the recent studies, temporal structure is considered to be related to self-consciousness. Past studies have found that slow cortical potentials follow a power-law distribution (He et al., 2010), slow cortical potentials are consciousness relevant (He & Raichle, 2009), and PLE has been suggested to be related to self-consciousness (Huang et al., 2016). Based on the previous study, temporal structure can be calculated by using a PLE. Therefore, it can be assumed that the temporal structure of the schizophrenic brain's resting-state signal (e.g., the PLE) may be abnormal and will therefore be the focus in the current study.

As shown earlier, past studies mostly focused on metrics such as FC and temporal variability and its changes in SCZ. However, it remains unclear if the temporal structure changes in SCZ. There has been little research on PLE in the context of mental illness. That being said, several studies have used metrics which are related to PLE and investigated the randomness of the BOLD signal in psychiatric illnesses and addictions. Changes in scale-free brain activity have been observed in mental illnesses, such as anxiety (Tolkunov et al., 2010), autism (Lai et al., 2010), as well as SCZ (Rădulescu & Mujica-Parodi, 2014). Scale-free dynamics of spontaneous brain activity have also been linked with personality traits at a psychological level,

such as extraversion (Lei et al., 2013) and trait impulsivity (Hahn et al., 2012). The randomness of time-series as mirrored by the Hurst exponent has attracted growing interest in recent years (Hahn et al., 2010). Scale-free properties of intrinsic brain activity have been linked with personality traits. The Hurst exponent was negatively correlated with extraversion (Lei et al., 2013). One study showed an association between Gray's impulsivity scale and the decreased Hurst exponent (Hahn et al., 2012). Past studies have revealed some possible relationship between SCZ and temporal structure.

So far, altered scale-free brain activity has been observed in mental illness such as anxiety, autism, and SCZ. Tolkunov et al. (2010) also used PSSI to examine the limbic dysregulation in trait anxious adults. They used the formula $S(f) \propto f^{\beta}$. The scaling parameter β (Shelhamer, 2007) serves as a measure of the auto-correlations within the signal. Estimating the β exponent for a time series provides a measure of whether the data are a pure random walk or have underlying trends. A flat spectrum ($\beta = 0$) corresponds to the uncorrelated time series (i.e., white noise). Increasing (negative) values of the scaling exponent indicate the persistence in the time series (i.e., the system's "memory") over many different time scales.

Ide et al. (2016) also used PSSI and revealed that cocaine-dependent adults showed decreased PSSI compared to healthy controls. Power spectrum densities were computed from preprocessed BOLD images on a voxel-wise basis and plotted on a log-log scale. They computed the slope of the linear fit (β) within a frequency window of 0.01–0.25 Hz using least-squares fitting; this range of frequency was adopted to exclude low fluctuations drifts (lower limit) and to avoid aliasing (upper limit) following previous experiments on PSSI computations on task data (Tolkunov et al., 2010). They used a preprocessed time-series without taking the derivative and

reported β to simplify interpretation of correlations and having PSSI represented by positive numbers. They used the formula $S(f) \propto f^{-\beta}$, where β = 0 represents a power spectrum with maximum entropy (white noise), and increasing β represents greater persistence (which can be due either to diminished excitatory inputs or tighter homeostatic constraint over the system via negative feedback (Radulescu & Mujica-Parodi, 2014)). The current study also used the same formula to calculate the temporal structure of the BOLD signal (see Method section).

Lai et al. (2010) examined the BOLD signals of autism using the Hurst exponent, which describes the complexity of endogeneous low-frequency fMRI time series on a continuum from random (H = .5) to ordered (H = 1). According to Lai et al. (2010), shifts in fractal scaling of physiological time series have been associated with neurological and cardiac conditions. In their study, the Hurst exponent was always reduced in the autism group in most regions, including cortical midline structures, medial temporal structures, lateral temporal and parietal structures, the insula, the amygdala, the basal ganglia, the thalamus, and the inferior frontal gyrus. Thus, autism is associated with a significant shift to randomness of endogenous brain oscillations. Thus, complexity measures may provide physiological indicators for autism as they have done for other medical conditions.

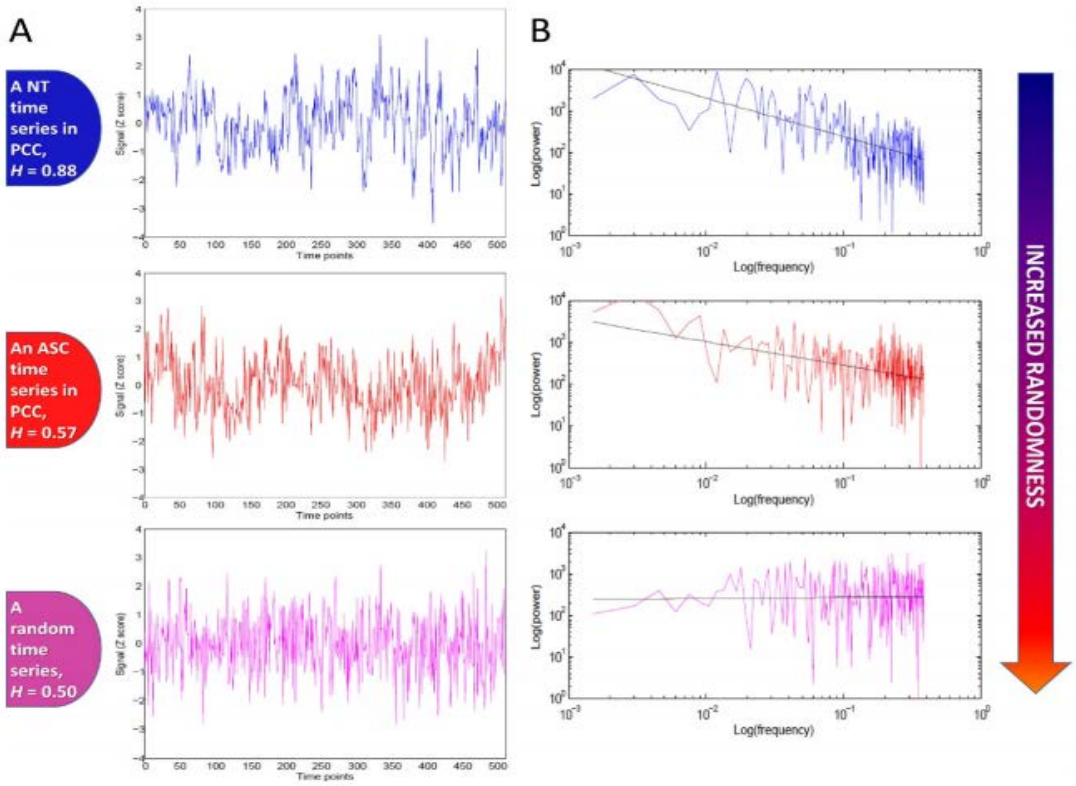

Figure 1. Illustrative functional magnetic resonance imaging (fMRI) and random time series demonstrating the concept of shift-to-randomness. Panel **(A)** shows normalized fMRI time series from a voxel in posterior cingulate cortex (Montreal Neurological Institute coordinate: −4, −36, 30) from a neurotypical (NT) (upper, blue, $H = .88$) and an autism spectrum condition (ASC) participant (middle, red, $H = .57$), as well as a simulated random (white Gaussian noise) time series (lower, purple, $H = .50$). Both fMRI time series exhibit self-similarity, but the one from the ASC participant shows less persistence, i.e., it is more similar to the random time series. Panel **(B)** illustrates the log-log plot of power spectrum for the three time series. For the NT time series, power attenuates as frequency increases (slope < 0); for the random time series, all frequencies are present with equal power in the spectrum (slope $= 0$); the ASC time series shows an intermediate slope between the NT and random time series, indicating a shift-to-randomness. *H*, Hurst exponent; PCC, posterior cingulate cortex.

Figure 2: **fMRI random time series in autism (Lai et al., 2010).**

Few studies which have investigated the temporal structure of schizophrenic patients; one of them is a study of Radulescu et al. (2012). Radulescu et al. (2012) used PSSI in order to measure the complexity of BOLD signal in SCZ. Radulescu et al. (2012) hypothesized that erroneous organization might characterize paranoid SCZ, via optimization abnormalities in the prefrontal-limbic circuit regulating emotion. To quantify dynamic regulation, researchers analyzed the PSSI of fMRI time-courses when participants were engaging in a task and computed the geometry of time-delay (Poincaré) maps, a measure of variability. PSSI is one of the complexity measures, and PSSI values (reflective of complexity) vary as a function of both input type (excitatory, inhibitory) and input density (mean number of long-range connections, or strength). Signals show pink noise (1/f) behavior when excitatory and inhibitory influences are balanced. As excitatory inputs are increased and decreased, signals shift toward white and brown noise, respectively. As inhibitory inputs are increased and decreased, signals shift toward brown and white noise, respectively. Patients and controls showed distinct PSSI in two clusters, localized to the orbitofrontal/medial prefrontal cortex (Brodmann Area 10), represented by β close to white noise in patients ($\beta \approx 0$) and in the pink noise range in controls ($\beta \approx -1$). The results from the Poincaré maps indicated less variability in patients than in controls. As there is a coupling between limbic and autonomic regulation, the patients' lowered PSSI might have some connections to the lowered heart rate variability seen in SCZ (Tolkunov et al., 2010). Brodmann Area 10 was found to be less variable in schizophrenic patients, which implicates that schizophrenic patients may have deficits of working memory, executive functioning, emotional regulation, and underlying biological abnormalities in synaptic (glutamatergic) transmission. Radulescu et al. (2012) used the formula $S(f) \propto f^{\beta}$ to calculate PSSI. The PLE β were estimated using a least-square linear fit

to the log-log power spectrum. In this case, the bigger the scaling exponent β is, the more irregular its BOLD signal. Radulescu et al. (2012) revealed that schizophrenic patients have a larger scaling exponent β (close to 0), which means they have reduced regularity in their BOLD signals while they engage in a task and they show less supple responsivity of this region (Brodmann Area 10). Rădulescu et al. (2014) insisted that measures of complexity are sensitive in detecting disease and that these measures can be potential diagnostic biomarkers. Raduescu et al. (2012) maintained that one straightforward way of characterizing complexity is the use of PSSI, which measures the relative frequency content of signals whose spectra show power-law behavior: $S(f) \propto f^{\beta}$. In this context, the scaling exponent β is 0 (white noise) at maximum entropy, with $\beta = -1, -2$ representing the increasing regularity of pink and brown noise, respectively. Several studies have applied complexity analyses to fMRI and have shown that for healthy neurobiological states, the entropy of neural time-series is characterized by roughly $\beta = -1$ ($S(f) \propto 1/f$), while neural time series in SCZ (Rădulescu et al., 2012), anxiety (Tolkunov et al., 2010), and autism (Lai et al., 2010) show a significant shift toward $\beta = 0$. Signals show pink noise ($1/f$) behavior when excitatory and inhibitory influences are balanced. In contrast, EEG signals from patients with epilepsy also deviate from the pink noise range, but in this case toward greater regularity (Bhattacharya et al., 2000; Bruzzo et al., 2008; Molteni et al., 2008; Protzner et al., 2010).

Sokunbi et al. (2014) used the Hurst exponent to examine the fMRI signals in SCZ. The researchers showed that patients with SCZ exhibited higher complexity than did the healthy controls, at mean whole brain and regional levels including mPFC. These findings suggest that patients with SCZ consistently demonstrate complex behavioral and physiological output (Sokunbi et al., 2014). In addition, both

the SampEn and the Hurst exponent agree that patients with SCZ have more complex fMRI signals than healthy controls. These results suggest that SCZ is associated with more complex signal patterns when compared to healthy controls, supporting the increase in complexity hypothesis, where system complexity increases with age or disease. They are also consistent with the notion that SCZ is characterized by a dysregulation of the nonlinear dynamics of underlying neuronal systems. This study reports global and regional differences in the SampEn and the Hurst exponent between patients with SCZ and controls while performing a social exclusion task. After adjusting for age and sex differences together, the results showed that there were differences in the SampEn and Hurst exponent values at whole brain and regional levels. In the SampEn analysis, patients with SCZ exhibited significantly higher SampEn values (higher complexity) than did the controls, while in the Hurst exponent analysis, patients exhibited significantly lower H values (higher fractal complexity) than did the controls. These significant differences indicate that patients with SCZ exhibited more complex fMRI signals than did the healthy controls. Also, the significant negative correlation ($p = 0.001$, $r = -0.606$) between the two estimates shows that as the SampEn values increase (higher complexity), the H values decrease (higher fractal complexity). This confirms that both the SampEn and the H results agree that patients with SCZ have more complex fMRI signals than do healthy controls and that the difference between the control and the patient population is actually due to real differences and not the measure employed.

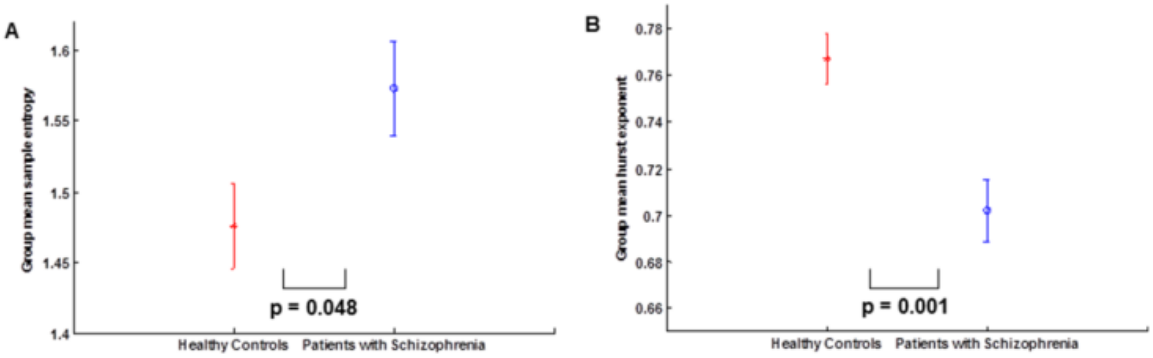

***Figure 3*: Group mean complexity differences in HC and SCZ (Sokunbi et al., 2014). (A) Group mean Sample entropy. (B) Group mean Hurst exponent. Sample entropy and Hurst exponent are similar measures to PLE.**

Furthermore, several studies focused on the alterations in the temporal structure of spontaneous brain activity in SCZ and how these relate to sensory, motor, and cognitive symptoms. Meda et al. (2015) observed reductions in activity strength within low frequency bands (0.01–0.08 Hz). These were localized to posterior cortical midline regions. Also, there might be some distinction in effects between specific ranges within these infra-slow bands. For instance, Yu et al. (2014) reported specific abnormalities within the slow-4 band (0.027–0.073 Hz) as opposed to slow-5 (0.01–0.027 Hz). Therefore, it can be suggested that there is an imbalance in the spontaneous activity's temporal structure in SCZ.

As shown above, there are few but strong results of the psychiatric studies which examined the temporal structure. However, there are not enough studies on resting-state temporal structure abnormality in mental illnesses, and none of the past studies compared different major psychiatric diseases with the same measure, which is important to differentiate them for diagnostic use. Furthermore, these past studies analyzed the BOLD signal in different frequency ranges. Also, no studies indicated which specific brain regions have these PLE differences among psychiatric patients. In this context, the current study is novel and will be helpful for future diagnostic use.

1.6. The present study

Objectives, questions and hypothesis of the present study

The primary goal of this study was to identify a potential biomarker for SCZ and also to understand functional abnormalities that occur and may contribute to the disease. The main question of the current study was whether there is an altered temporal structure in the schizophrenic brain and if the temporal structure can be a potential biomarker. The current study was conducted for better understanding of

spontaneous brain activity in SCZ by investigating the temporal structure of BOLD signals and additional measures. The general aim of the present study was to investigate the spontaneous activity's temporal structure including its different facets in schizophrenic patients from two independent datasets (GE-SCZ and TWN-SCZ) with two healthy control subjects correspondingly (GE-CON and TWN-CON) for replication of our findings. In addition, to examine whether the effect we observed was specific to SCZ, we also included another dataset with major depressive disorder (MDD) patients, bipolar disorder (BP) patients, and their control groups. Our specific aims are to investigate: (i) the LRTCs—that is, the power relationships between slower and faster frequencies indexed by PLE; (ii) temporal order and regularity as measured by LZ, ETC, and ApEn; and (iii) the correlations between measures of temporal structure and clinical parameters of psychopathological symptoms.

Based on the previous findings, we hypothesized specific changes in temporal structure in regions of the DMN, including their relationship (i.e., correlation) with clinical measures. Our hypothesis is that the schizophrenic brain has specific abnormalities in the cortical midline structures (specifically, the mPFC and the PCC) as these are related to altered self-consciousness in these patients. Specifically, based on the past studies, we hypothesized that schizophrenic patients have more complex BOLD signal patterns, which lead to reduced PLE in the mPFC and the PCC.

The current study tested whole-brain voxel wise temporal structure. The current study investigated the temporal structure using PLE, the slope of the log-power and log-frequency, which is a measure to quantify the power distribution across frequencies. It can be said that the steeper the slope for PLE, the higher the power in low frequency (Huang, 2016). Additionally, SD ratio (slow 5/slow4) analysis was performed in the current study. Slow 5 divided by slow 4 gives us the

relative contribution of each band to the temporal variability, which is suggested to reflect the temporal structure. As slow 5 over slow 4 reflects the temporal structure of the BOLD signal, this may become a new and easy way to calculate temporal structure, similar to PLE. Thus, in order to calculate the temporal structure, in addition to PLE, we calculated the SD of the ratio slow 5 divided by slow 4. Here, slow 5 and slow 4 indicate different frequency ranges. In 2004, Buzsáki and Draguhn made oscillation classes, which contain 10 frequency bands based on differences in regional property, interregional interaction, and network features in 0.02 - 600 Hz. We focused on slow 4 and 5 since past research has found altered brain signals in slow 4 and slow 5 in mental illnesses such as bipolar disorder (e.g., Magioncalda et al., 2015). We calculated the ratio as it tells us the relationship between frequency and power distribution and it indicates the relative distribution of slow 5 and slow 4, which is approximately similar to temporal structure. Therefore, in the present study, we examined two new properties: the investigation of the SD ratio (slow5/slow4), and temporal structure in SCZ in cortical midline structures. Also, slow 5 and slow 4 are the dominant sub-frequencies which are measured in fMRI. Traditional fMRI frequency is 0.01–0.1 Hz and low frequency resting-state activity normally uses a frequency of slow 4 and slow 5 (He, 2010). In addition, we performed several confirmation analyses such as complexity measures.

Identifying new ways of classifying SCZ will contribute to earlier diagnosis and improved interventions for this disease. Detailed implications are articulated in the discussion section.

2. Methods

2.1. Functional magnetic resonance imaging (fMRI)

Compared to magnetic resonance imaging, the primary target of fMRI is not anatomical discriminability but the change in tissue properties over time. The foundation of fMRI rests on the observation that activated neural tissue causes a significant vascular change in blood flow (Ogawa et al., 1990). We conducted both whole-brain and region of interest analysis in the current study.

2.2. Participants and procedures

The study consisted of three datasets (see Table 2 below). Dataset-I was collected at the University of Goettingen in Germany (GE) from 28 schizophrenic patients (GE-SCZ; 10 females; mean age = 34.04 (+/- 8.91 *SD*); age range = 21–55 years; Diagnosis: First-episode schizophrenia. CPZ mean dose = 229.39 mg/day (+/- 236.17 *SD*) and 10 healthy controls (GE-CON; 4 females; mean age = 30 (+/- 7.60 *SD*); age range = 19–35 years). 35 years or over: HC = 2 / SCZ = 13. For severity of the disease, Positive and Negative Syndrome Scale (PANSS) was used. Also, Brief Psychiatric Rating Scale (BPRS) was used to measure their symptoms. (See Appendix for raw data)

Dataset-II was collected at Taipei Medical University-Shuang-Ho Hospital in Taiwan (TWN) from 17 schizophrenic patients (TWN-SCZ; 8 females; mean age = 39.3 (+/- 11.2 *SD*); age range = 21–50 years; all medicated with CPZ), 28 major depressive disorder patients (TWN-MDD; 18 females; mean age = 37.2 (+/- 7.50 *SD*)) and 19 healthy controls (TWN-CON; 13 females; mean age = 34.3 (+/- 5.60 *SD*); age range = 25–46 years). 35 years or over: HC = 9 / SCZ = 11 / MDD = 18. Patients were recruited from the psychiatry department at that hospital. No significant difference in age or sex between healthy and schizophrenic/depression groups. For

diagnostic measures for SCZ, Positive and Negative Syndrome Scale (PANSS) was used. MDD patients were diagnosed by Beck Depression Inventory (BDI) and Montgomery–Åsberg Depression Rating Scale (MADRS) (See appendix).

Dataset-III was collected at San Martino Hospital at the University of Genoa in Italy (IT) from 73 bipolar patients and 69 healthy controls (IT-CON; 43 females; mean age = 40.1 (+/- 13.1 *SD*)). The bipolar patients comprised of 23 patients in depressive states (IT-DEP; 16 females; mean age = 45.0 (+/- 10.6 *SD*), 27 patients in euthymic phases (IT-EUT; 17 females; mean age = 45.4 (+/- 10.8 *SD*), and 23 patients in manic states (IT-MAN; 18 females; mean age = 44.6 (+/- 12.4 *SD*). 35 years or over: HC = 37 / dep = 18 / eut = 22 / manic = 18. Euthymia is defined as a normal, tranquil mental state or mood that is neither manic nor depressive. BP patients were diagnosed by DSM. This dataset was originally published by Martino et al. (2016).

The Ethics Committee of the University of Goettingen, the Taipei Medical University Institutional Review Board, and San Martino Hospital approved the study. Written informed consent was obtained from all participants. Age and sex were included as covariates in all the analysis.

Table 2

Subject Demographic Information for all three datasets. SCZ = Schizophrenia. CON = Control. MDD = Major Depressive Disorder. DEP = Depressive phase. EUT = Euthymic phase. MAN = Manic phase. Sample size, Age mean, and female number are shown from the top.

	Dataset-I (Germany)		**Dataset-II (Taiwan)**			**Dataset-III (Italy)**			
	GE-SCZ	**GE-CON**	**TWN-SCZ**	**TWN-MDD**	**TWN-CON**	**IT-DEP**	**IT-EUT**	**IT-MAN**	**IT-CON**
Sample size *n*	28	10	17	28	19	23	27	23	69
Age *mean* (SD)	34.0 (8.9)	30.0 (7.6)	39.3 (11.2)	37.2 (7.5)	34.3 (5.6)	45.0 (10.6)	45.4 (10.8)	44.6 (12.4)	40.1 (13.1)
Female *n* (%)	10 (35.7%)	4 (40.0%)	8 (47.1%)	18 (64.3)	13 (68.4%)	16 (69.6%)	17 (63.0%)	18 (78.3%)	43 (62.3%)

2.3. fMRI data acquisition

Dataset-I was acquired by a Siemens 3T scanner (standard 8-channel head coil, MAGNETOM). Gradient-echo EPI (functional) images of the whole brain were acquired (TR/TE = 2000ms = 2s/30ms; 33 slices; slice thickness = 3mm; spacing = 0; FoV = 196 x 196mm^2; flip angle = 70°; matrix = 64×64; 156 volumes; 5min 12sec). Dataset-II was acquired by a GE 3T MR750 scanner (8-channel headcoil). Gradient-echo EPI images of the whole brain were acquired (TR/TE = 1000ms/30ms; 21 slices; slice thickness = 6mm; spacing = 0; FoV = 220 x 220mm^2; flip angle = 76°; matrix = 64×64; 360 volumes; 6 min). Dataset-III was acquired by a GE 1.5T scanner (8-channel headcoil). Gradient-echo EPI images of the whole brain were acquired (TR = 2000/30ms; 33 slices; slice thickness = 4mm; spacing = 1mm; FoV = 240 x 240mm^2; flip angle = 90°; matrix = 64×64; 150 volumes; 6 min). Resting-state fMRI scanning was carried out in the dark, with participants explicitly instructed to keep their eyes closed, to relax, to stay awake, and to move as little as possible. High-resolution anatomical images were acquired at the end of the experiment. There was no other task in the scanner prior to resting-state data acquisition. For the Goettingen experiment, during the resting-state scan, subjects were told to relax and look at a fixation cross presented in the middle of the screen. In order to acquire resting-state BOLD signal, the patients do not need to maintain "default mode", as long as no specific task is given. The commonly used duration of resting-state fMRI scan varies from 5min to 20min. Here, 0.01 Hz requires 100s for one cycle. 5 min12s includes 3+ cycles. 3 cycles is the minimal requirement for reliably estimating the power-frequency.

2.4. Preprocessing of fMRI data and AFNI

Pre-processing steps were implemented in AFNI (Cox, 1996, http://afni.nimh.nih.gov/afni) and FSL (http://fsl.fmrib.ox.ac.uk/fsl/fslwiki/) including (1) slice timing correction; (2) rigid body correction/realignment within and across runs; head motion parameters were estimated and frame-wise realignment was performed using AFNI's 3dvolreg command. The magnitude of head motion for six parameters (three for shift and three for rotation) was gained for each fMRI run. The averaged head motion parameter and SD for shift and rotation were then calculated. After the estimated motion parameters were visually inspected, subjects with head motion larger than ±2 mm translation or ±2.5 degrees rotation were eliminated (Johnstone et al., 2006); (3) co-registration with high-resolution anatomical images; (4) spatial normalization into Talaraich stereotactic space (Talairach & Tournoux, 1988); (5) resampling to 3×3×3 mm^3 voxels; (6) regressing out linear and non-linear drift, head motion, and its temporal derivative, and mean time series from the white matter (WM) and cerebrospinal fluid (CSF) to control for non-neural noise (Fox et al., 2005). The WM and CSF masks were eroded by one voxel (Chai et al., 2012) to minimize partial voluming with gray matter; (7) spatial smoothing with a 6 mm full-width at half-maximum isotropic Gaussian kernel. AFNI uses the standardized brain template (named TT_N27) by using the script: @auto_tlrc, which transforms individual brain to a standardized established template. SPSS was used to calculate t-tests.

Resting-state analysis

The data were filtered with a band-pass filter reserving signals between 0.01 and 0.1 Hz, which reflects mainly neuronal fluctuations (Fox & Raichle, 2007). For the calculation of the SD ratio, we focused on two separate bands within the range of 0.01–0.1 Hz: Slow 5 (0.01– 0.027 Hz) and Slow 4 (0.027–0.073 Hz) (Hoptman et al.,

2010). After preprocessing, the time series for each voxel was filtered (bandpass, 0.01–0.1 Hz) to remove the effects of very-low-frequency drift and high-frequency noise (e.g., respiratory and heart rhythms).

2.5. Calculation of power-law exponent (PLE) and scale-free activity

Calculation of PLE

To calculate the PLE, BOLD signals need to be transformed into the form of power spectrum. In Yu et al.'s (2014) study, the preprocessed time series was transformed to a frequency domain with a fast Fourier transform (FFT), and the power spectrum was then obtained. Because the power of a given frequency is proportional to the square of the amplitude of this frequency component of the original time series in the time domain, the square root was calculated at each frequency of the power spectrum and the averaged square root was obtained across 0.01– 0.1 Hz at each voxel. This averaged square root was taken as the ALFF. Here, power is the squared value of the signal. "Power spectra" tells us which frequencies contain the signal's power. The answer is in the form of a distribution of power values as a function of frequency, where "power" is considered to be the average of the signal^2. In the frequency domain, this is the square of the FFT's magnitude. For a given signal, the power spectrum gives a plot of the portion of a signal's power (energy per unit time) falling within given frequency bins. The most common way of generating a power spectrum is by using FFT. The power spectrum indicates the energy of the signal at each frequency that it contains.

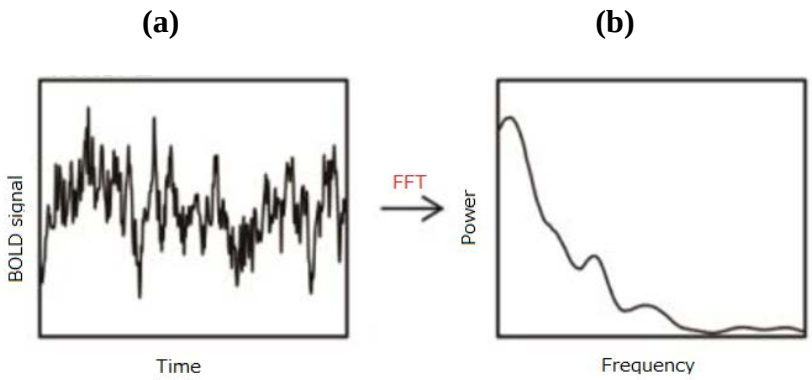

Figure 4: **Calculation of PLE. (a) – (d). (Huang et al., 2016).**

(a). BOLD signals from given regions (time course)

(b). Power spectrum of the BOLD signal for each voxel (Y: Power, X: Frequency)

Figure 4(a) indicates the BOLD signal and its time course. Figure 4(b) shows the relationship between power and frequency after the signals are transformed by using a FFT (Fast Fourier Transform), which indicates the power spectrum.

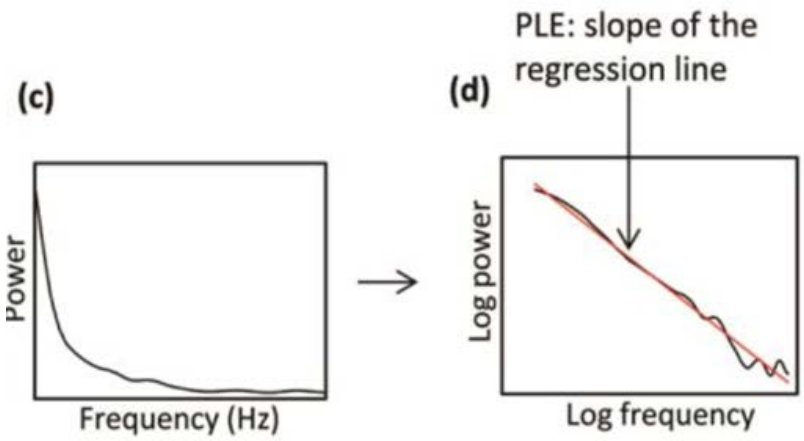

(c). The power spectra were averaged across voxels

(d). PLE was defined as the slope of the linear regression of log-power on log-frequency corresponding to the straight-line regime.

Although Yang et al. (2014) also calculated power spectra in SCZ patients, the current study proceeded to the next step in order to calculate the PLE. Figure 4(c) shows the power spectra averaged across voxels. Here, a power spectrum can be calculated using ($P \propto 1/f^{\beta:}$ Power is directly proportional to 1 over frequency to the Beta). After that, it was log-log-transformed, and Beta is now a slope of the linear regression, which is the PLE. Figure 4(d) shows the PLE defined as the slope of the linear regression of log-power on log-frequency corresponding to the straight-line. Thus, PLE tells us the pattern of the signal/relationship of frequencies of the same signal. The PLE indicates the temporal structure of neural activity by describing its self-affine pattern. So we look for some similar patterns over time.

Thus, it can be said that the PLE tells us the pattern of the BOLD signal and we can see it by seeing how steep the power spectrum is. Also, it can be said that the PLE is a power distribution across frequencies (relationship of frequencies of the same signal).

As indicated earlier, the temporal structure of the BOLD signals is mathematically calculated by a power spectrum. A power spectrum has a formula $P \propto 1/f^{\beta}$, where P is power, f is frequency, and β is the PLE (Bullmore et al., 2001). The PLE is defined as the slope of the linear regression of log-power on log-frequency corresponding to the straight-line regime (see Figure 4(d)). The power spectrum for each voxel was fitted with a power-law function $P \propto 1/f^{\beta}$ using a least-square estimation in the frequency range of 0.01–0.2 Hz (Baria et al., 2013; Rădulescu et al., 2014). The lower frequency limit was chosen to avoid signal contributions from scanner drift, whereas the higher limit was set slightly lower than the Nyquist frequency to avoid contamination from aliasing effects (Fransson et al., 2013; Huang et al., 2016).Whole-brain PLE maps were obtained for each subject (see Fig. 5).

Voxel-wise two sample *t*-tests were performed for the main contrast (control vs. SCZ) including age and sex as covariates. Unless otherwise stated, all resulting t-maps were thresholded at a corrected p-value of < 0.05 (uncorrected: *p* value at voxel level/corrected: *p* value at the cluster level). Scale-free dynamics are mathematically characterized by a power spectrum following the formula $P \propto 1/f^{\beta}$, where P is power, f is frequency, and β is the PLE (Bullmore et al., 2001). After pre-processing, the time course per voxel was normalized to zero mean and unit variance (z-value) (Stephens et al., 2013). As the variance is equal across all ROIs, all spectra have the same integrated area. Using methods previously optimized for fMRI (Rubin et al., 2013), the normalized power spectrum of the fMRI signal was computed for each voxel using the AFNI program: *3dPeriodogram*. The power spectrum of the BOLD signal was further smoothed with an optimized Hamming window of 15 neighboring frequency bins (Huang et al., 2016). The power spectrum for each voxel was fitted with a power-law function $P \propto 1/f^{\beta}$ using a least-square estimation in the frequency range of 0.01–0.2 Hz (Baria et al., 2013; Rădulescu et al., 2014).

Finally, the PLE, β, of each voxel was defined as the slope of the linear regression of log-power on log-frequency corresponding to the straight-line regime. To this end, whole-brain PLE maps were obtained for each subject (see Fig. 5 for an illustration). Voxel-wise, two sample *t*-tests were performed for the main contrast (GE-CON vs. GE-SCZ) including age and sex as covariates. Unless otherwise stated, all resulting t-maps were thresholded at a corrected *p*-value of < 0.05. That is, the multiple-comparison error was corrected using Monte Carlo simulation as implemented in AFNI program AlphaSim, yielding a family-wise error rate (FWER) at $p < 0.05$. The smoothness used in the AlphaSim was the average smoothness across subjects.

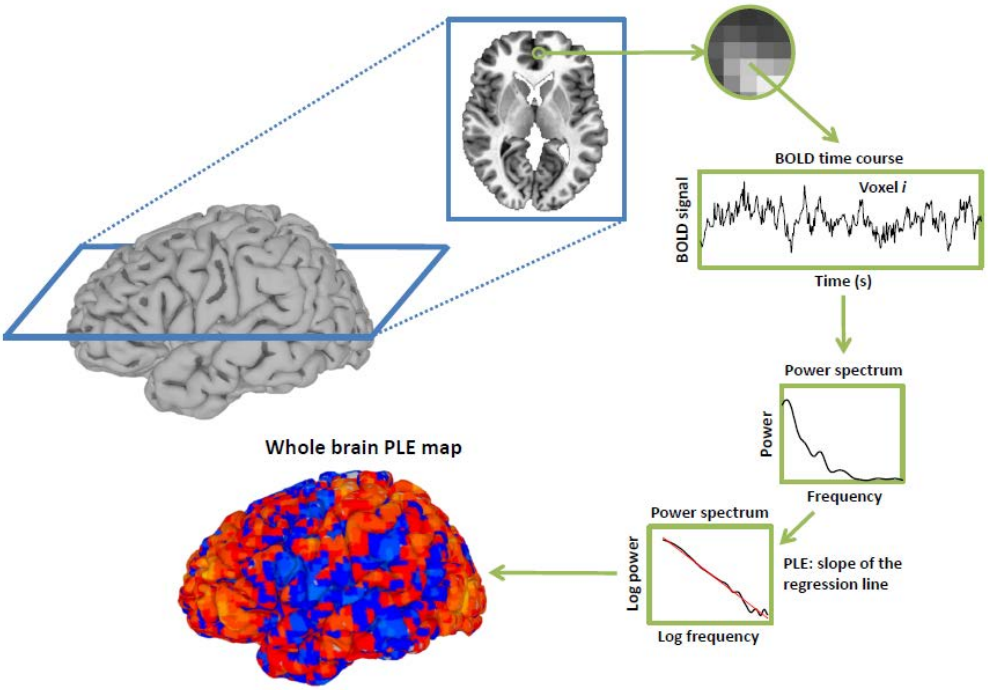

Figure 5: **Workflow of whole-brain power-law exponent (PLE) calculation. First, time series were extracted. Then, it was transformed into a frequency domain using FFT, which is a power spectrum. Finally, it was log-log transformed in order to obtain the PLE.**

2.6. Calculations of the ratio of temporal variability (SD): Whole-brain standard deviation (SD) of BOLD signal analysis — temporal variability

To calculate the temporal structure, in addition to PLE, we calculated the SD of the ratio slow 5 over slow 4. Slow 5 and slow 4 indicates different frequency ranges (0.01–0.027 Hz, 0.027–0.073 Hz respectively). Why is the ratio important? Does this mean there is a "shift" to low variability primarily in slow5? What is the function of slow5? We focused on slow 4 and slow 5 since past research has found altered brain signal in slow 4 and slow 5 in mental illnesses such as bipolar disorder (e.g., Magioncalda et al., 2015). Also, slow 5 and slow 4 are the dominant sub-frequencies which are measured in fMRI. Traditional fMRI frequency is 0.01–0.1 Hz, and low frequency resting-state normally uses a frequency of slow 4 and slow 5 (He, 2010). We adopted a definition of subfrequency bands in the BOLD signal including Slow 5 (0.01–0.027 Hz) and Slow 4 (0.027–0.073 Hz) (Huang, 2016). We calculated the ratio as it tells us the relationship between frequency and power distribution. The ratio indicates relative distribution of slow 5 and slow 4, which is approximately similar to the temporal structure measured by PLE. Thus, we can say that slow5/slow4 indicates the degree of temporal structure. In other words, it tells us the relationship between frequency and power distribution. For SD, we investigated the following four divisions: Standard frequency: 0.01–0.1 Hz, Slow 5: 0.01–0.027 Hz, Slow 4: 0.027–0.073 Hz. The ratio (Slow 5 divided by 4) is always less than 1. The small number is divided by the large number. The closer the ratio is to 1, the more similar the two signals are. Here, the ratio is important as it tells us the temporal structure: the ratio of slow 5/slow 4 tells us the relationship between frequency and power distribution. This is why we additionally used the ratio of temporal variability to calculate the temporal structure.

Thus, in the current study, we examined two new properties: the investigation of the ratio of SD and PLE measured by temporal structure in SCZ in cortical midline structures. Temporal structure can be alternatively called long-range temporal correlation. If there is a long-range temporal correlation, it means there is some similar pattern over time, and it is hypothesized that schizophrenic patients do not have this similar pattern over time.

In order to calculate the SD ratio of the BOLD signal, we used Garret et al.'s (2013) procedure. The SD of the BOLD signal across time (Garrett et al., 2010, 2011) was used to calculate the temporal variability of spontaneous brain activity across time within a particular region. The SD of the BOLD signal describes the temporal variability of fluctuations in BOLD-fMRI signals (brain activity) across time within a particular region. The SD of the resting state's BOLD signal changes were compared between a healthy group and a SCZ group for the frequency range of 0.01–0.1 Hz. All resulting t-maps were thresholded at a corrected p-value of $< .05$. We used the method of Garrett et al. (2010, 2011) to calculate the temporal variability of time series for each of our regions of interest. The SD of the BOLD signal change across the time series for each voxel was calculated to yield an SD map for each subject. The SD across time series was calculated for each subject's constructing maps of SD for each voxel. Then for each of the regions of interest, we extracted the mean SD score and calculated SD ratio of slow 5/slow4. Subject-level voxel-wise SD maps were standardized into subject-level Z-score maps (i.e., by subtracting the mean voxel-wise SD obtained for the entire brain and then dividing by the standard deviation; Zuo et al., 2010).

Definition of regions of interest (ROIs) for the mPFC mask and PCC mask

Some of the analysis in this study was based on a region of interest (ROI) analysis using established templates from the past fMRI literature (Huang et al., 2016). To calculate SD ratio and also PLE as a confirmative analysis, two masks were used: the mPFC and the PCC were chosen as regions of interest. These two regions were considered as self-consciousness relevant. These two regions are in the cortical midline structures and also in the DMN. For the whole-brain analysis of the mPFC and PCC masks, we adopted a well-established node template from a previous study (Huang et al., 2016). This template was defined according to neurobiological principles with a combination of two methods; the first was a meta-analytic (Dosenbach et al., 2006) and explored large fMRI data sets to identify voxels that showed reliable and repeated modulation when a variety of certain behaviors were demanded (e.g., button-pressing) or certain signal types were found (e.g., error-related activity). The second method utilized resting-state FC MRI (Barnes et al., 2011; Cohen et al., 2008). According to our hypotheses and past research, the scale-free dynamics of the activity in two key regions in the DMN, the mPFC and PCC, were expected to show a close relationship with SCZ deficits such as self-consciousness abnormality. Therefore, we localized the mPFC and PCC in a resting-state SD ratio analysis (De Pasquale et al., 2012; Fox et al., 2005; Greicius et al., 2003, 2009). The mPFC and PCC masks used in the previous study (Huang et al., 2016) were used in the present study. Specifically, we used a seed region in the PCC with a 12mm diameter (spherical) centered on a previously published focus (Talairach coordinates: [4, 52, 22]; Huang et al., 2016; Laird et al., 2009).

2.7. Complexity measures

Besides the PLE, three complexity measures were included in the analysis. Effort to compress (ETC) is a new complexity measure which has a greater rate of success in automatic identification and classification of short noisy sequences (Nagaraj et al., 2013). Lempel-Ziv (LZ) measures the generation rate of new patterns along a digital sequence. This is used to solve information theoretic problems and applications such as coding, data compression, and generation of test signals. Approximate entrophy (ApEn) is a regularity statistic that quantifies the unpredictability of fluctuations in a time series. This is used as a measure for classifying periodic, chaotic, and stochastic systems (Pincus et al., 1990).

2.8. Inter-subjects correlation analyses between PLE, complexity measures and clinical symptoms

To explore the association between altered temporal structure and clinical symptoms, we performed partial correlation analyses (subject-based) with a 95% confidence interval (CI) based on 1,000 bootstrap samples between PLE, complexity measures (LZ, ETC, ApEn) and scores of Brief Psychiatric Rating Scale (BPRS) subscales. Each partial correlation analysis (e.g., correlating PLE and anxiety/depression) included medication scores as a controlling factor.

3. Results-I: PLE analysis

In the following analyses, age and sex were included as covariates. Therefore all of these variables are controlled. (Medication-CPZ was not controlled).

3.1. Head motion

Head motion SD for each group (healthy and schizophrenic patients) was calculated in Excel. Shift SD for healthy and patients was 0.026mm and 0.036mm, respectively. No group difference of global mean was seen, t (36) = -1.902, p = .065. Rotation SD for healthy and patients was 0.029mm and 0.031mm, respectively. No group difference of global mean was seen, t (36) = .419, p = .678.

3.2. Whole-brain, voxel-wise PLE analysis in different frequency ranges

These figures below are showing the PLE contrast between schizophrenia and healthy controls for dataset-I. The yellow highlighted are showing the areas where HC > SCZ at p < .005 significance level.

.

Figure 6: **(a) - (d). Main PLE analysis in different frequency ranges.**

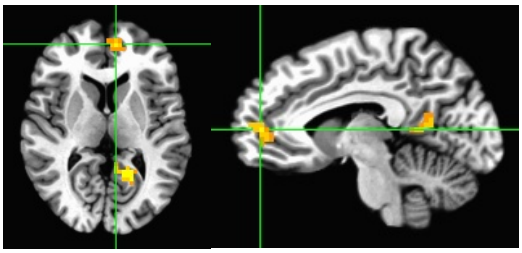

Figure 6 (a): 0.01–0.1 Hz. The yellow highlighted are showing the areas mPFC and PCC, p < .005.

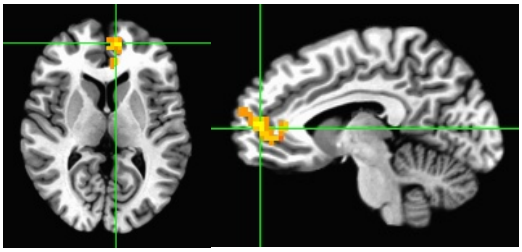

Figure 6 (b): 0.01–0.2 Hz. The yellow highlighted are showing the area mPFC, $p < .005$.

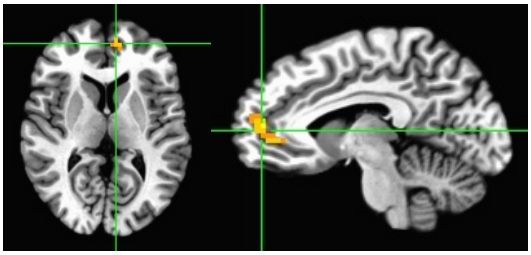

Figure 6 (c): 0.02-0.15 Hz. The yellow highlighted are showing the area mPFC, $p < .005$.

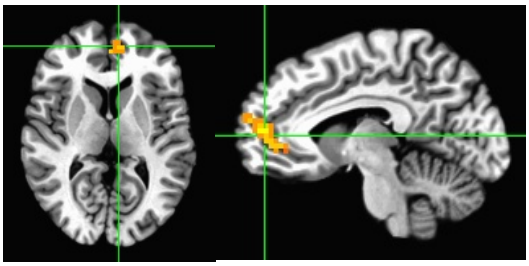

Figure 6 (d): 0.02-0.2 Hz. The yellow highlighted are showing the area mPFC, $p < .005$.

Although mPFC showed the significant differences in all of the frequency bands, the mPFC region found in 0.01–0.2 Hz (Fig. 6 (b)) showed the largest significance.

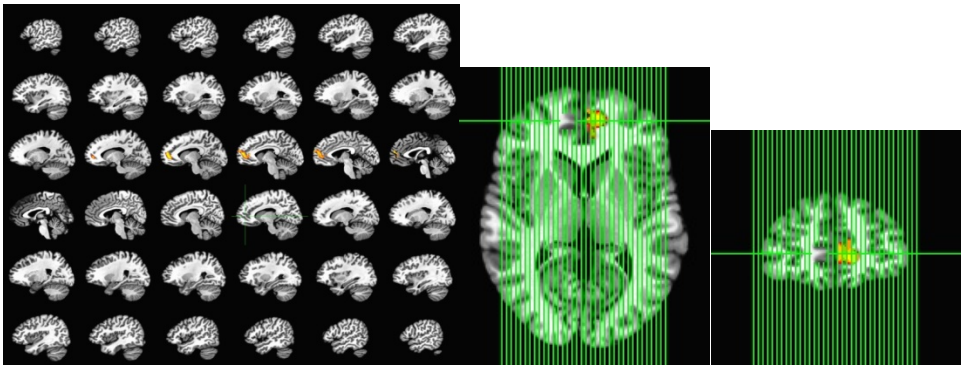

Figure 7: **Whole brain voxel-wise PLE analysis in 0.01–0.2 Hz. PLE contrast between schizophrenia and healthy controls for dataset-I. From the left: sagittal, horizontal, and coronal angles. The yellow highlighted are showing the area (mPFC) where PLE of HC > SCZ at $p < .005$.**

Here, mPFC is one of the midline regions of the brain, belonging to DMN. Unlike DLPFC, the function of mPFC does not show any hemisphere preference.; it is always bilateral instead of unilateral. The effect we saw dependents on the statistical threshold and limited number of subjects in our case. If relax the threshold, you may see bilateral. Also, one would expect that after increasing the number of subjects, the bilateral effect will be clearer.

3.3. Long-term auto-correlation (LRTC) as measured with power law exponent (PLE)

Using whole-brain PLE analysis (0.01–0.2 Hz), we compared GE-CON to GE-SCZ. Interestingly, we found GE-SCZ showed a significant decrease in PLE, which was remarkably specific in the mPFC (218 voxels; cluster center: [-7, 56, -5; MNI coordinates]) (Fig. 8). PLE: t (36) = - 3.904, p < .001*. No significant cluster was observed for GE-SCZ > GE-CON. Age and sex were included as covariates.

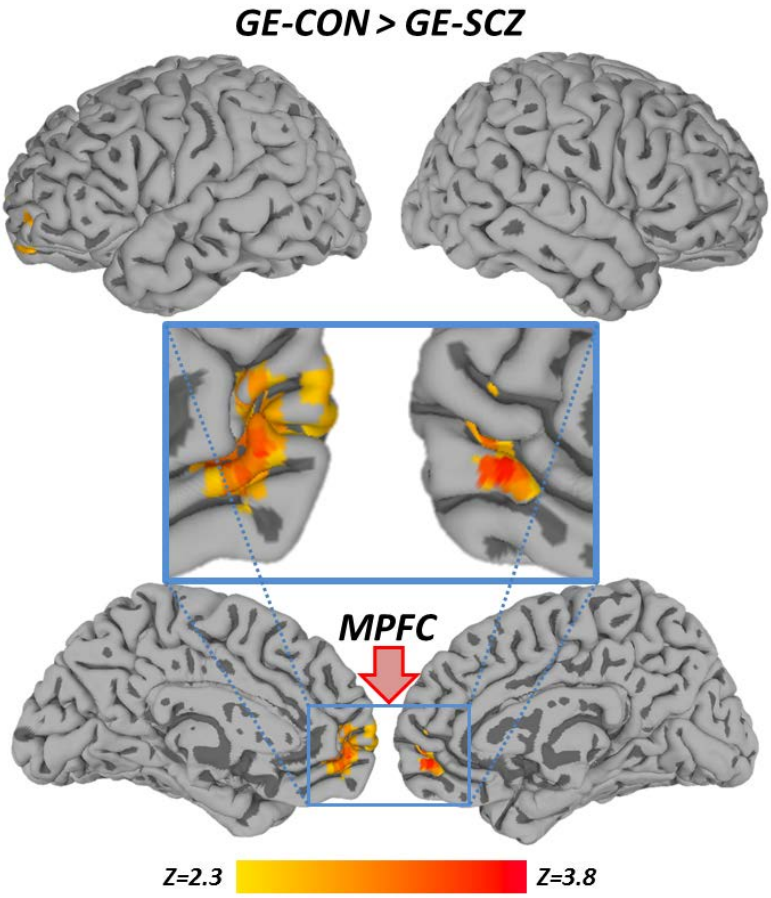

Figure 8: **Whole-brain, voxel-wise PLE results comparing GE-CON to GE-SCZ.** Z-maps were thresholded at corrected $p < 0.05$. The color bar shows voxel-wise Z-values.

3.4. Comparison of the results with additional psychiatric diseases: Depression and bipolar disorders

We thought it was important to examine whether our results are reproducible in schizophrenic populations and whether the results are specific in SCZ comparing to other mental disorders such as major depressive disorder (MDD) and bipolar disorder (BP). For this reason, we tested our results in two independent datasets (Dataset-II and Dataset-III) using region of interest (ROI) analysis. In other words, to establish diagnostic specificity of the SCZ findings, we compared them to a cohort of BP patients and MDD patients. Specifically, we defined ROIs based on an 8mm radius sphere at the center of mass of the significant clusters in the whole-brain contrast map (GE-CON vs. GE-SCZ). The PLE values for all subjects in Dataset-II and Dataset-III were extracted and submitted to second-level group analyses. A new mPFC mask (whole-brain, voxel-wise, PLE-based mask) was made for 0.01–0.2 Hz to be used as a seed region for further analysis.

Using the mPFC from above as a region of interest, we replicated our finding in Dataset-II where significant PLE reduction was seen in TWN-SCZ compared to TWN-CON: t (34) = - 3.391, p = .002*. The PLE reduction was relatively specific in SCZ, as this effect was also seen in TWN-SCZ vs. TWN-MDD t (43) = - 2.315, p = .025*, and no difference was seen in TWN-CON vs. TWN-MDD, t (45) = .855, p = .397 (n.s.). These findings were further supported by analyzing Dataset-III, where no difference was seen between IT-CON and the different bipolar disorder subtypes (IT-DEP:t (90) = .745, p = .458 (n.s.), IT-EUT: t (94) = .083, p = .934 (n.s.), and IT-MAN: t (90) = .580, p = .563 (n.s.) (See Fig. 9 below).

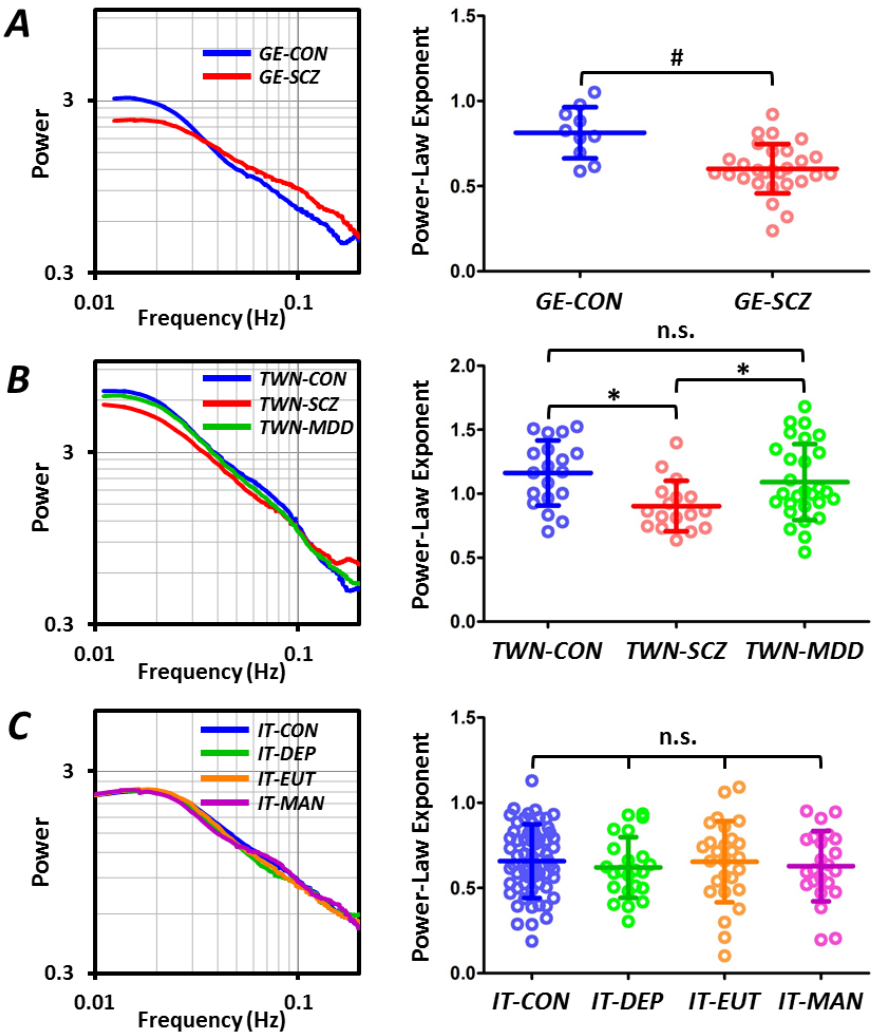

Figure 9: **The power spectra of BOLD signals and PLE values in the mPFC.** A, Comparisons between GE-CON and GE-SCZ in Dataset-I (Germany); B, Comparisons between TWN-CON, TWN-SCZ and TWN-MDD in Dataset-II (Taiwan); C, Comparisons between IT-CON, IT-DEP, IT-EUT and IT-MAN in Dataset-III (Italy). [#]No statistical analysis was performed to avoid double-dipping; *p < 0.05; n.s. no significance; Error bars indicate ±1SD. ([#]PLE: t (36) = - 3.904, p < .001*.) TWN-SCZ vs TWN-CON: t (34) = - 3.391, p = .002*. TWN-SCZ vs. TWN-MDD: t (43) = - 2.315, p = .025*, TWN-CON vs. TWN-MDD: t (45) = .855, p = .397 (n.s.). IT-DEP: t (90) = .745, p = .458 (n.s.), IT-EUT: t (94) = .083, p = .934 (n.s.), and IT-MAN: t (90) = .580, p = .563 (n.s.)

4. Result-II: Complexity measures analysis

Besides the PLE, three complexity measures were included in the analysis. Effort to compress (ETC) is a new complexity measure which has a greater rate of success in automatic identification and classification of short noisy sequences (Nagaraj et al. 2013). Lempel-Ziv (LZ) measures the generation rate of new patterns along a digital sequence. This is used to solve information theoretic problems and applications such as coding, data compression, and generation of test signals. Approximate Entrophy (ApEn) is a regularity statistic that quantifies the unpredictability of fluctuations in a time series. This is used as a measure for classifying periodic, chaotic and stochastic systems (Pincus et al., 1990).

4.1. Temporal order and regularity (LV, ETC, ApEn)

Extending the above observations, we found significant group differences (GE-CON vs. GE-SCZ) in all three complexity measures: ETC: t (36) = -2.030, p = .05*, LZ: t (36) = -2.881, p = .007*, ApEn: t (36) = -3.241, p = .003*. (See Fig. 10.) However, the data from Taiwan and Italy were all non-significant. For instance, TWN-CON vs. SCZ: ApEn: t (34) = -1.589, p = .121.(n.s.). That being said, we took out one outlier from the TWN-SCZ dataset, and then performed the simple two-sample t-test again. Although the ETC and LZ were not significant for Healthy vs. SCZ (p = .229, p = .377 respectively), the ApEn showed marginal significance, p = .055. Moreover, unfiltered data (0.0083–0.25 Hz) showed that for both the Goettingen and Taiwan SCZ datasets, ApEn showed significant differences: t (34) = -2.372, p = .023* (Taiwan). Thus, it can be suggested that ApEn is the closest measure to PLE.

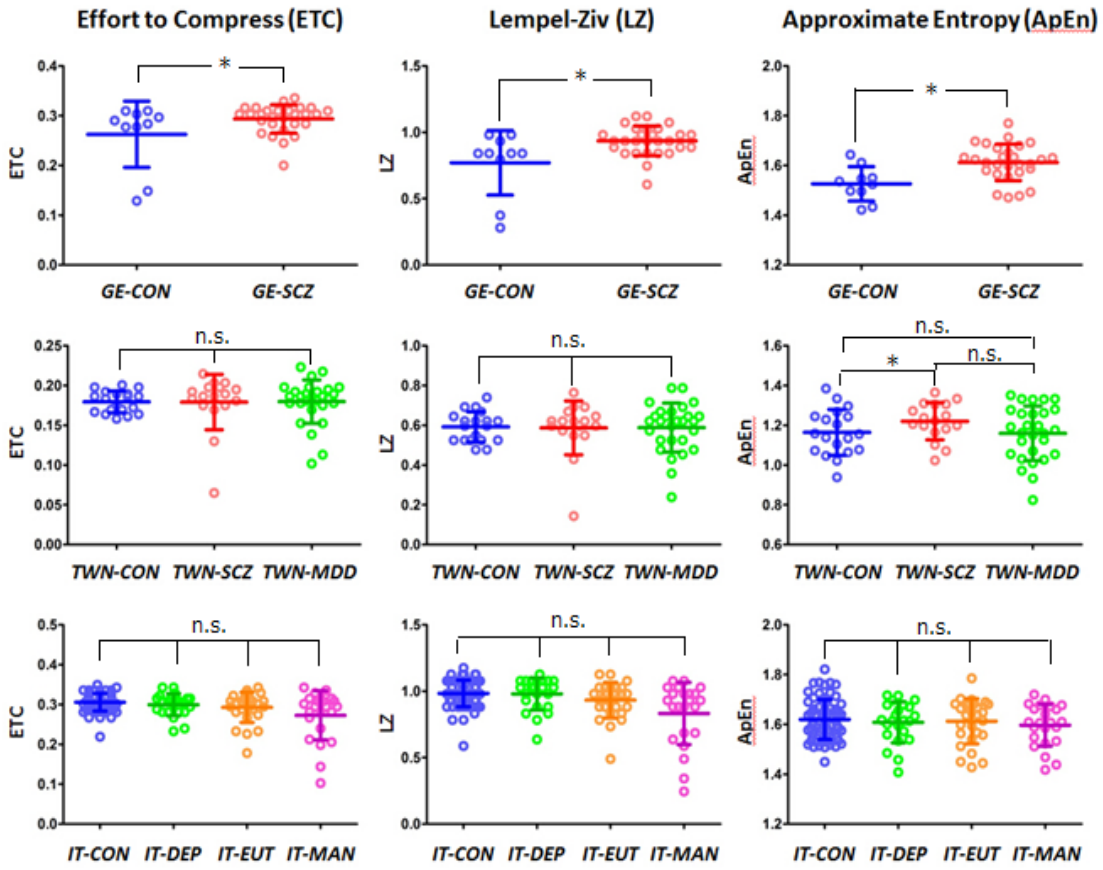

Figure 10: **Comparison of the Complexity measures in mPFC.** ETC: Effort to compress; LZ: Lempel-Ziv; ApEn: Approximate entropy. Top, Comparisons between GE-CON and GE-SCZ in Dataset-I (Germany); Middle, Comparisons between TWN-CON, TWN-SCZ and TWN-MDD in Dataset-II (Taiwan); Bottom, Comparisons between IT-CON, IT-DEP, IT-EUT and IT-MAN in Dataset-III (Italy). *$p < 0.05$; n.s. no significance; Error bars indicate ±1SD.

4.2. Correlation between different complexity measures.

A correlation analysis was conducted to see whether these different complexity measures are correlated with each other: ETC and LZ: .851, p = .000 (spearman), ETC and ApEn: r = .491, p = .002 (Spearman), LZ and ApEn: r = .519, p = .001 (Spearman). As we can see, these complexity measures are all positively correlated with each other.

5. Results-III: SD ratio analysis

From the results above, it can be suggested that PLE is related to frequency power change. In order to see which frequencies are related to this change, we then investigated the SD ratio of slow 5 over slow 4.

5.1. Global mean of SD

There was no group difference of common SD global mean of temporal variability, t (36) = -1.287, p = .206. There was no group difference of Slow 4 SD Gmean, t (36) = -1.460, p = .153. There was no group difference of Slow 5 SD Gmean, t (36) = -.992, p = .328.

5.2. SD ratio (slow 5 over slow 4): whole-brain, voxel-wise analysis

In the current study, the SD ratio of the resting state's BOLD signal changes were also compared between groups for each frequency range (standard, slow5, and 4) as the BOLD signal variability has been suggested as an indicator of cognitive deficits (Garrett et al., 2011).

5.3. The relationship between power and frequency in left mPFC

Figure 11A shows a whole-brain, voxel-wise SD ratio analysis ($p < 0.05$, corrected) comparing healthy and schizophrenic subjects. By investigating the SD ratio, we found the significant differences between healthy and schizophrenic patients.

In the figure 11A below, the color red indicates that healthy subjects shows larger SD ratio. The most voxels were found in the left mPFC (38 voxels), which is a region that is specifically implicated in self-awareness.

We picked up the region from the figure 11A **(**seen in red). For the region of the mPFC region, *t*-test was conducted for PLE, and it was found that schizophrenic patients have significantly less PLE compared to healthy controls with very high significance level. First, we investigated power spectrum and PLE and used a *t*-test to see the differences between healthy and schizophrenic patients.

Figure 11: **A–D. SD ratio (slow 5 over slow 4): whole-brain, voxel-wise analysis in Dataset-I.**

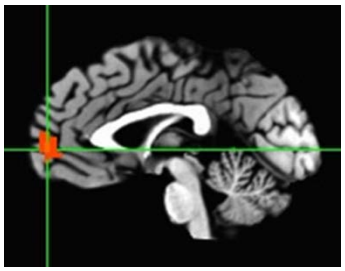

Figure 11A: **38 voxels, left mPFC. The color red is showing the area where HC > SCZ at $p < 0.05$ in Dataset-I.**

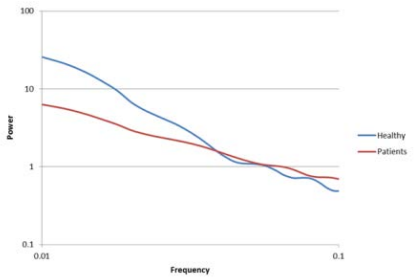

Figure 11B: **Smoothed power spectrum (FFT). X-axis indicates frequency. Y-axis indicates power.**

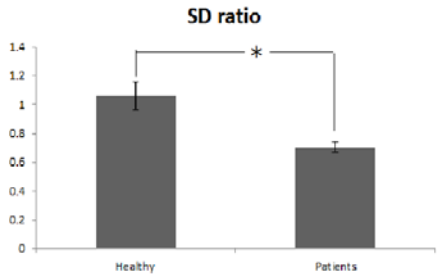

Figure 11C: **Comparison of SD ratio between HC and SCZ in left mPFC.**

t (36) = 4.344, p < .001*,

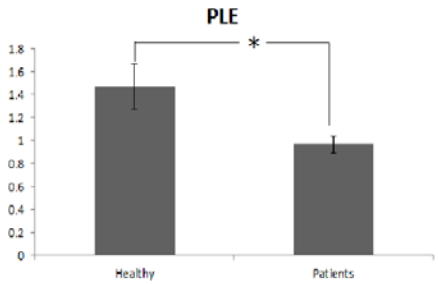

Figure 11D: **Comparison of Smoothed PLE between HC and SCZ in left mPFC.**

t (36) = 3.021, p = .005*.

Our results showed that the Slow5/slow4 SD ratio was significantly decreased in SCZ patients compared with Healthy Controls. From the results, it can be suggested that the BOLD signal network balance between slow 5 and slow 4 in mPFC is disturbed in SCZ. Thus, these results suggest that schizophrenic patients have specific abnormality in mPFC. These results were further confirmed by analyzing the regions of interest (ROIs) defined by the mPFC and PCC masks created in the previous study (See Results-IV below).

6. Results-IV: Confirmative analysis by independent ROIs: mPFC mask and PCC mask

6.1. The relationship between power and frequency in the mPFC mask

From the default mode network, the mPFC and PCC were defined as ROIs. This analysis was conducted to confirm that the altered temporal structure is specific to the mPFC and not in the PCC. The first figure (Fig. 12A) shows the mask used, the second figure shows the relationship between power and frequency in mPFC, and the third and fourth figures show the differences in SD ratio and PLE between the healthy and patient groups, respectively. As you can see, healthy subjects showed significantly larger PLE compared to patients in mPFC, while there were no differences in PCC. Therefore, we can confirm that the effects are only seen in mPFC.

Figure 12: **A–D. Confirmative analysis by independent ROIs: mPFC mask (from Huang et al., 2016) in Dataset-I.**

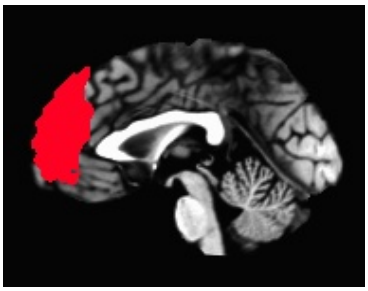

Figure 12A: **mPFC mask (Huang et al., 2016).**

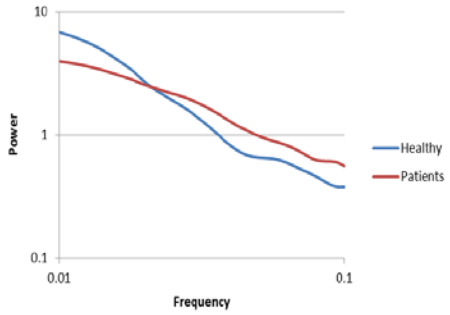

Figure 12B: **Smoothed power spectrum (FFT). X-axis indicates frequency. Y-axis indicates power.**

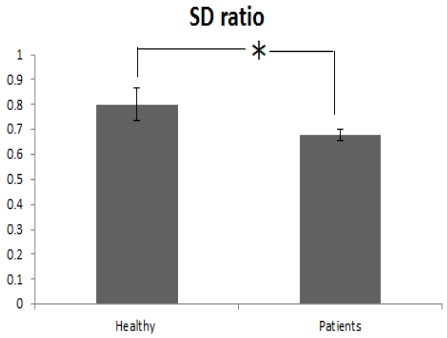

Figure 12C: **Comparison of SD ratio between HC and SCZ in mPFC mask.**

t (36) = 2.276, p = .029*.

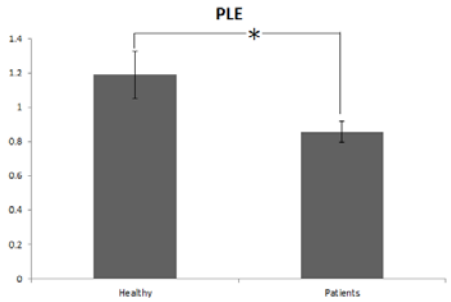

Figure 12D: **Comparison of Smoothed PLE between HC and SCZ in mPFC mask.**

t (36) = 2.579, p = .014*.

6.2. The relationship between power and frequency in the PCC mask

Figure 13: **A–D. Confirmative analysis by independent ROIs: PCC mask (from Huang et al., 2016) in Dataset-I.**

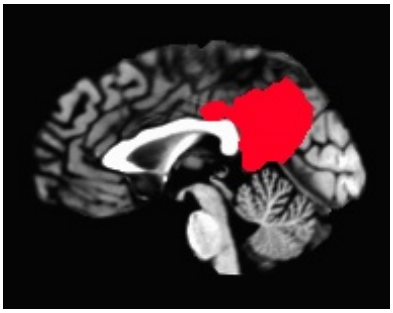

Figure 13A: **PCC mask (Huang et al., 2016).**

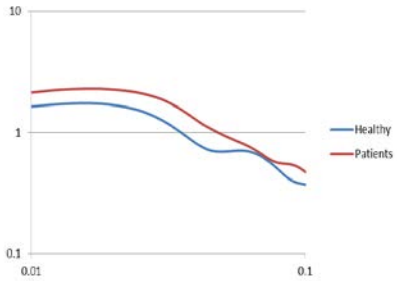

Figure 13B: **Smoothed power spectrum (FFT). X-axis indicates frequency. Y-axis indicates power.**

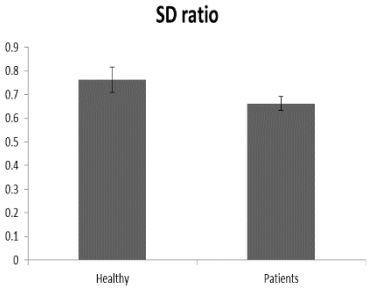

Figure 13C: **Comparison of SD ratio between HC and SCZ in PCC mask.**

t (36) = .1.655, *p* = .107 (n.s.).

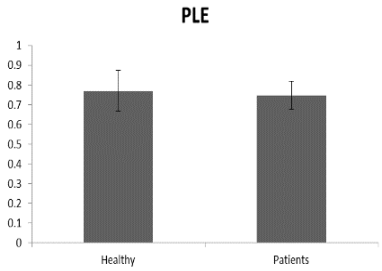

Figure 13D: **Comparison of Smoothed PLE between HC and SCZ in PCC mask.**

t (36) = 1.655, p = .107 (n.s.).

7. Result-VI: PLE and complexity measures

7.1. Correlation between PLE and complexity measures

The graphs below show the relationships between the results of these three complexity measures and PLE. All of them have somewhat negative correlations, but ApEn and PLE have the strongest negative correlations. Taken together, it can be said that ApEn is the closest measure for PLE.

1. GE-SCZ

PLE vs. ETC: r = -.521, p = .001*.

PLE vs. LZ: r = -.525, p = .001*.

PLE vs. ApEn: r = -.752, p < .001*.

2. TWN-SCZ

PLE vs. ETC: r = -.250, p = .142.

PLE vs. LZ: r = -.231, p = .175

PLE vs. ApEn: r = -.637, p < .001*.

3. TWN-MDD

PLE vs. ETC: r = -.265, p = .034*.

PLE vs. LZ: r = -.290, p = .020*.

PLE vs. ApEn: r = -.679, p < .001*.

4. IT-BP-depressive states

PLE vs. ETC: r = -.363, p < .001*.

PLE vs. LZ: r = -.479, p < .001*.

PLE vs. ApEn: r = -.759, p <.001*.

5. IT-BP-euthymic states

PLE vs. ETC: r = -.366, p <.001*

PLE vs. LZ: r = -.441, p <.001*

PLE vs. ApEn: r = -.751, p <.001*

6. IT-BP-manic states

PLE vs. ETC: r = -.285, p =.001*.

PLE vs. LZ: r = -.389, p <.001*

PLE vs. ApEn: r = -.706, p <.001*

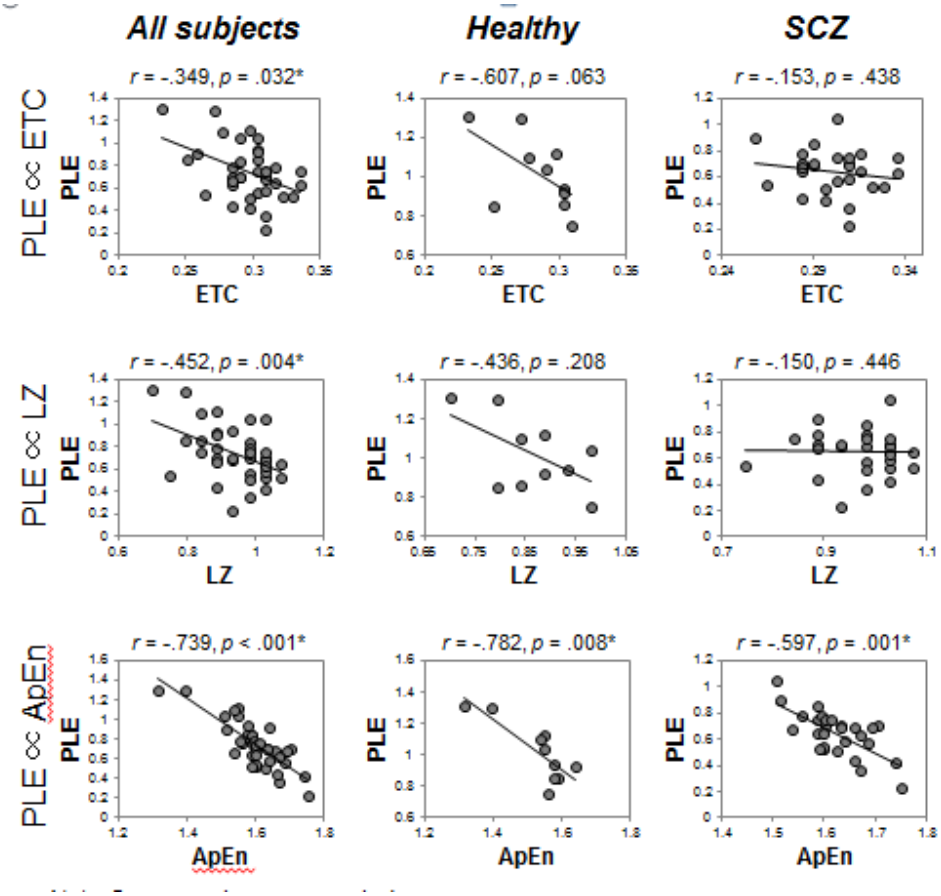

Figure 14: **Correlation analysis between PLE and complexity measures in Dataset-I. Top: Correlation between PLE and ETC. Middle: Correlation between PLE and LZ. Bottom: Correlation between PLE and ApEn.**

8. Result-VII: Relationship to clinical symptoms

To explore whether the PLE and complexity measures are associated with clinical symptoms in the SCZ patients, we correlated these measures with the scores of BPRS subscales in GE-SCZ (controlling medications). Interestingly, significant correlations were seen in LZ $\propto$ Anxiety/Depression (r = .480, p = .013*) and ApEn $\propto$ Anxiety/Depression (r = .461, p = .018*). No significant correlation was seen in ETC/PLE $\propto$ Anxiety/Depression (r = -.137, p = .514). Anxiety/Depression subscale includes 1,2,5, and 9.

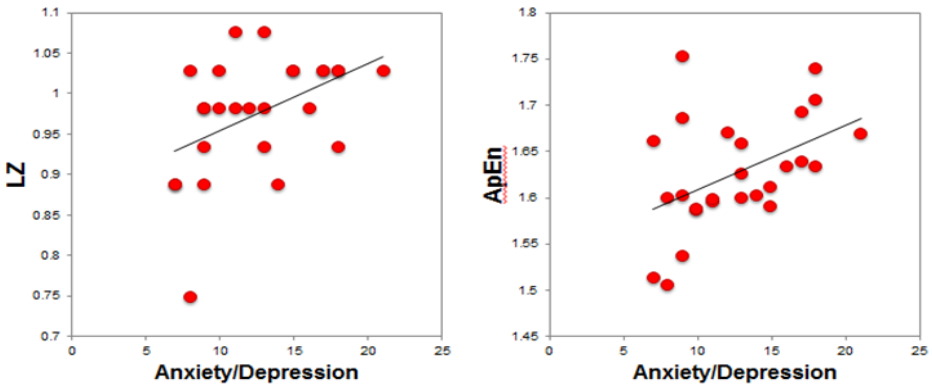

Figure 15: **Correlations between complexity measures and clinical symptoms in GE-SCZ (Dataset-I). X-axes are showing the BPRS scores of anxiety/depression. Y-axes are showing the scores of complexity measures LZ and ApEn respectively. LZ ∝ Anxiety/Depression (*r* = .480, *p* = .013*). ApEn ∝ Anxiety/Depression (*r* = .461, *p* = .018*).**

9. Discussion

As the past research has been showing inconsistent results in terms of functional connectivity and temporal variability and variance, one of the aims of the current study was to find a possible and consistent biomarker for SCZ by investigating the temporal structure between healthy and schizophrenic patients.

Our main findings showed significant reduction of the PLE in specifically the mPFC in SCZ in two independent datasets, from Goettingen and Taiwan. Both PLE and complexity measures agree that patients with SCZ have reduced long-range temporal correlations (smaller PLE) and increased complexity (larger ETC, LZ, and ApEn). This alteration is remarkably specific in the mPFC, which has been closely linked to self-related processing and self-consciousness (D'Argembeau, 2013; Gillihan & Farah, 2005, Kelley et al., 2002, Northoff et al., 2006, Supekar et al., 2010; Van der Meer et al., 2010). This may indicate that the spatiotemporal changes in the mPFC's spontaneous activity in SCZ may result in corresponding changes in the person's perception and sense of the world, but further investigation is needed. To conclude, although more detailed investigation will be needed, the current study revealed that the schizophrenic patients have altered temporal structure of spontaneous brain activity in mPFC and also it was replicated by an independent SCZ sample. Furthermore, as expected, this alteration was not seen in the depressed patients and patients with bipolar disorder. This PLE reduction in mPFC was specific for SCZ as it was neither observed in MDD nor in the three different phases of BP. Taken together, we here shown disease-specific reduction in mPFC PLE in SCZ as distinguished from both MDD and BP, which therefore may serve eventually as a biomarker.

Thus, our findings show that schizophrenic patients show decreased LRTC as indexed by lower PLE in specifically the mPFC spontaneous activity. This was replicated in a separate subset of another sample of schizophrenic patients and, even more important, it was shown to be specific for SCZ as distinguished from MDD patients and BP patients. Taken together, the observed effect in the mPFC is robust and specific in the schizophrenic patients. Hence, our main findings are the following: (i) decreased LRTCs as indexed by lower power law exponent in specifically mPFC spontaneous activity in SCZ, which was replicated in independent datasets and shown to be specific for SCZ as distinguished from MDD patients and BP patients; (ii) decreased temporal order and regularity as indexed by higher LZ, ETZ, and ApEn in mPFC spontaneous activity in SCZ; (iii) relationship–that is, correlation of abnormal temporal order and regularity with clinical symptoms like anxiety/depression. Taken together, our results show that different facets or aspects of the spontaneous activity's temporal structure are specifically altered in SCZ and related to clinical symptoms in a distinct way. As self-reference is typically reduced in SCZ as a disorder of the self (Kühn, & Gallinat, 2013), we hypothesized the brains of patients with SCZ have some abnormalities in their DMNs, especially in the mPFC; as expected, our results supported the hypothesis. Since a past study revealed that the PLE value of mPFC is correlated with private self-consciousness (Huang et al., 2016), our results for the reduced PLE value of mPFC in schizophrenic patients support the notion that schizophrenic patients have abnormal private self-consciousness. These results support the views that schizophrenic patients have disturbed self-consciousness (Northoff, 2014).

The mPFC is among those brain regions having the highest baseline metabolic activity at rest and one that exhibits decreases from this baseline across a wide variety

of goal-directed behaviors in functional imaging studies (Gusnard et al., 2001). This high metabolic rate and this behavior suggest the existence of an organized mode of default brain function, elements of which may be either attenuated or enhanced. Extant data suggest that these mPFC regions may contribute to the neural instantiation of aspects of the multifaceted "self." The presence of self-referential mental activity appears to be associated with increases from the baseline in dorsal mPFC. It has been suggested that a useful way to explore the neurobiology of the self is to explore the nature of default state activity (Northoff, 2014). DMN is the set of brain areas preferentially activated during internally focused tasks (Öngür et al., 2010). It has been found that higher levels of activity within anterior medial regions of the DMN such as mPFC are linked to a focus on internal mental contents, self-directed thoughts, and to sensations of parts of their own body (like the limbs or the face) and to bodily processes (such as the heartbeat; Vanhaudenhuyse et al., 2011). Many studies have shown that cortical midline structures (CMS) are related to self-related processing (e.g., Northoff et al., 2006; Van der Meer et al., 2010). Especially, the two regions in the CMS, the mPFC and the PCC, were shown to highly overlap with the DMN with high levels of spontaneous activity and functional connectivity during resting-state activity (e.g., Raichle et al., 2001; Wicker et al., 2003).

Gradin et al. (2012) also observed abnormalities in the mPFC of patients with SCZ. Past studies on healthy subjects have implicated the mPFC, a region involved in emotional and social information processing, in neural responses to social exclusion. Impairments in social interactions are common in SCZ; therefore they investigated the tasks which induces social exclusion. This task involves passing a "ball" between the participant and two cartoon representations of other subjects. The extent of social exclusion (ball not being passed to the participant) was parametrically varied

throughout the task. Replicating previous findings, increasing social exclusion activated the mPFC in controls. In contrast, patients with SCZ failed to modulate mPFC responses with increasing exclusion. Furthermore, the blunted response to exclusion correlated with increased severity of positive symptoms. In contrast, patients with SCZ failed to modulate mPFC responses with increasing exclusion. Their study indicates that abnormal activity of mPFC in SCZ is related to their impairments in social interactions. It will be important to see if abnormal mPFC in SCZ is reflecting their impairment in self-consciousness since it is one of the biggest features of SCZ.

Our results extend previous results from other studies that showed changes in PLE during task-evoked activity (Radulescu et al., 2012) by showing the decreased PLE in spontaneous activity. Radulescu et al. (2012) investigated PSSI while engaging in a task, which revealed less PSSI, indicating more complexity in SCZ. In addition, Sokunbi (2014) found more complexity (less regular pattern) in SCZ patients than in healthy controls using the Hurst exponent. These two are the only studies which investigated the temporal structure of schizophrenic patients' BOLD signal, but they analyzed a task-evoked brain activity instead of a resting-state brain. Since our study used resting-state data and showed that mPFC was the specific region, we can say that the present results significantly extend these previous findings. One may speculatively hypothesize that the spontaneous activity's decreased power in the extremely slow frequencies observed in the current study may then also be carried over to task-evoked or stimulus-induced activity as observed by Radulescu et al. (2012). Since the past findings of fMRI SCZ research are inconsistent, it is expected that our investigation of PLE will contribute to better understandings of abnormality of schizophrenic brain.

There are several points of novelty in the current study. First, unlike other fMRI studies of SCZ which used task-period activity, the current study analyzed the brain's spontaneous activity. In addition, the current study conducted a whole-brain analysis on three different datasets, which gives us a rigid comparison. Furthermore, the current study analyzed BOLD signals using PLE and three distinct complexity measures. The other measures of temporal order and regularity like LV, ETC, and ApEn showed significant increase in mPFC spontaneous activity in SCZ. Previous studies using mainly EEG/MEG also demonstrated abnormal complexity measures in SCZ (1–60 Hz) (Akar et al., 2016; Bachiller et al., 2014, 2015; Brookes et al., 2015; Molina et al., 2016; Sokunbi et al., 2014, Yang et al., 2015); these results are complemented by our findings that, due to measurement in fMRI, target the infraslow frequency range (0.01–0.1 Hz) rather than the higher frequencies as in EEG/MEG. These findings further support our assumption of abnormal temporal structure in spontaneous activity in SCZ where decreased LRTC are complemented by increased complexity that is, less temporal order and regularity: there seems to be a higher degree of temporal disorder and dissimilarity in spontaneous activity patterns in SCZ.

Furthermore, the current study conducted several confirmative analysis, which used ROI analysis using the mPFC mask from the main PLE analysis and the mPFC and PCC masks from the previous study. In the confirmative analyses, we used PLE and SD ratio, and both of the measures showed similar results. The results from SD ratio analysis showed that the slow5/slow4 ratio had a significantly reduced value in schizophrenic patients compared to healthy controls in vmPFC, which is involved in Brodman Area 10, which is located in the DMN. These results are consistent with Radulescu et al.'s (2012) study, which found restricted temporal variability in schizophrenic patients in Brodman Area 10. Radulescu et al. (2012) explained that

this is a prefrontal cortical region implicated as an inhibitory component of the control circuit regulating emotional arousal. Therefore, it can be assumed that SCZ patients may have impairment in this control circuit, which might have some influence on their cognitive deficits, although further investigation is needed.

Here, it is not certain why the PLE effect was only seen in mPFC: it might be a sensitivity issue, and also it is possible that mPFC might be cut off from other targets in SCZ. Limited number of subjects may reduce the possibility of seeing other significant regions. In the sense, the effect in mPFC may be the strongest, while may not be the only one. It is also possible that the mPFC is very specific. It is unknown unless using a larger sample size.

mPFC is also implicated in anxiety and cognitive function. It has been known that anxiety dissociates dorsal and ventral mPFC functional connectivity. Therefore, it can be suggested that larger PLE allows more balanced connection within mPFC, which leads to less anxiety. Also, since dysfunction in DMN is related to cognitive deficits, it can be said that reduced PLE in mPFC might be related to impaired cognitive functions.

Frequency specificity (slow 5)

In addition, our main result from PLE analysis means that, relatively considered, the power of the extremely infraslow frequency fluctuations (as measured in fMRI) like slow 5 (0.01–0.027Hz) is diminished relative to higher ones like slow 4 (0.027–0.073Hz); the bigger the power of slow 5, the bigger the PLE (slope). We can say that abnormalities of temporal variability in SCZ may depend on the specific frequency range examined. Moreover, from the SD ratio analysis, we can say that SCZ patients have lower slow 5 relative to slow 4 comparing to that of healthy

subjects. It can be assumed that slow 5 is more related to self-consciousness as it is more stable, and its reduction relative to slow 4 might be related to abnormally reduced self-consciousness in SCZ. Therefore, SCZ patients have lower slow 5 and may have lower self-consciousness. Thus, their sense of self might be influenced by surrounding things more, although further investigations are needed.

Past studies found greater brain activity in DMN in lower slow 5 band. Lower frequency oscillations like slow 5 allow for an integration of neuronal networks, which leads to impaired communication between DMN and other brain regions. Slow 5 is known to be more distributed among different regions compared to slow 4, therefore it can be considered that slow 5 is more related to self-consciousness compared to slow 4.

Our SD ratio analysis confirmed that in SCZ, slow 5 is abnormally diminished compared to slow 4. Here, although the exact physiology is not known yet, past studies give us some ideas about the reason for the reduction in slow 5.

Our result of the abnormal reduction of slow 5 is supported by past studies. According to Ebisch et al.'s (2013) study, a subdivision in different frequency bands of BOLD fluctuations suggested that differences between first episode SCZ and HC more specifically concerned the frequency range between 0.01 and 0.027 Hz (slow-5) but not the 0.027–0.07 Hz (slow-4) frequency range. In their study, ROI-based functional interaction analyses were performed focusing on the frequency band between 0.01 and 0.027 Hz (slow-5) and the frequency band between 0.027 and 0.07 Hz (slow-4). Results showed that differences in functional interaction between the healthy subjects and the SCZ group detected in the 0.009–0.08 Hz frequency band more specifically concerned the 0.01–0.027 Hz frequency band (slow-5), whereas no significant differences between the healthy subjects and SCZ group were detected in

the slow-4. Therefore, the power of slow-5 is reduced in SCZ patients at larger degrees than slow-4, which is consistent with our results.

Moreover, Garitty et al. (2007) revealed that healthy subjects had significantly more power in the lower-frequency range and SCZ patients exhibited significantly higher power at higher frequencies. A study by Calhoun et al. (2009) also found that the time courses for the temporal lobe network in SCZ patients showed a tendency toward more power at higher frequencies than those of healthy subjects. The greater fluctuations BOLD signals observed in the default mode time course components for patients in higher frequency may reflect a lower degree of interconnection between the regions in the default mode and other brain regions. Healthy subjects exhibited low-frequency oscillations (0.03 Hz), whereas patients exhibited significantly higher-frequency oscillations in the 0.08–0.24 Hz range. This result may indicate less temporal synchronicity between the brain regions involved in the DMN of patients or may even indicate impaired communication between the default mode network and other brain regions in SCZ.

From the separated analysis of different frequency, we can see that the frequency-specific investigation is important since it tells us the balance and the temporal structure of the BOLD signal.

According to Buzsaki and Draguhn (2004), oscillatory coupling of neuronal assemblies is usually examined within single frequency bands, but different oscillatory classes might carry different dimensions of brain integration since the nature of these algorithms in the brain remains to be discovered. Slow rhythms may synchronize large spatial domains and can bind together specific assemblies by the appropriate timing of higher frequency localized oscillations. Understanding the physiological mechanisms of self-emerging oscillations will provide insight into their

functions. Moreover, it may assist in the diagnosis and treatment of brain disorders and psychiatrics such as SCZ. Buzsaki and Draguhn (2004) insist that uncovering the relationship between neuronal oscillators and the much slower biochemical-molecular oscillators such as circadian rhythms should be investigated in the future.

Zuo et al. (2010) also measured ALFF and fALFF in different frequency bands. ALFF is calculated as the sum of amplitudes within a specific low frequency range (0.01–0.1 Hz). The researchers subdivided the low frequency range into four bands as previously defined (Buzsáki & Draguhn, 2004): slow-5 (0.01–0.027 Hz), slow-4 (0.027 - 0.073 Hz), slow-3 (0.073–0.198 Hz) and slow-2 (0.198-0.25 Hz). The frequencies subtended by the slow-5 and slow-4 bands are typically utilized for resting-state FC analyses (0.01–0.1 Hz). For both ALFF and fALFF measures, significant slow-4 and slow-5 oscillations were primarily detected within gray matter. In contrast, slow-3 and slow-2 oscillations were primarily restricted to white matter. This distinction of slows 2/3 vs. slows 4/5 is especially noteworthy given prior demonstrations that respiratory and aliased cardiac signals fall in the range of slows 2-3 (Cordes et al., 2001), while the oscillatory signals upon which resting-state functional connectivity is based are primarily located within slows 4 and 5 (e.g., De Luca et al., 2006). Their analyses of four previously characterized subdivisions of the power spectrum suggest that gray matter-related oscillations primarily occur in the slow-4 and slow-5 range (0.01–0.073 Hz), slow-4 fluctuations are more robust in basal ganglia than slow-5, and slow-5 is more dominant within ventromedial prefrontal cortices than slow-4. Larger ALFF in slow-5 were found in regions including ventromedial frontal gyrus in the past studies (Han et al., 2011; Zuo et al., 2010). Researchers examined changes in LFO amplitude (i.e., ALFF and fALFF) in SCZ at different frequency bands. They found that LFO amplitudes for slow-4 were

higher in cingulate cortex, basal ganglia, and midbrain, but it is lower in inferior frontal gyrus and ventromedial frontal gyrus, comparison to LFO amplitudes in slow-5. Overall, patients with SCZ showed abnormal ALFF/fALFF in regions including middle occipital gyrus, inferior parietal lobule, precunus, insula, middle temporal gyrus and medial and inferior frontal gyrus. Thus, Zuo et al.'s (2010) study tells us that reduced slow 5 in SCZ in mPFC may serve as a potential biomarker for SCZ.

In addition, Hoptman et al. (2010) showed that the patients with SCZ had widespread abnormalities of LFO amplitudes in the slow-4 frequency band. These studies suggest that the pattern of intrinsic brain activity is sensitive to specific frequency bands. Brain regions showing a significant main effect for frequency band include the anterior mPFC/anterior cingulate cortex (ACC), the PCC, the inferior parietal lobe, the occipital, the basal ganglia, the hippocampus, and the insula. Interestingly, the brain regions with higher ALFF values in the slow-5 band showed a large overlap with the components of default-mode networks (Greicius et al., 2003; Raichle et al., 2001). It was also found that the group differences in fALFF in the slow-5 band were greater than those in the slow-4. They examined changes in LFO amplitude (i.e., ALFF and fALFF) in the patients with Amnestic mild cognitive impairment (aMCI) at two different frequency bands (slow-4 and slow-5 bands). It was found that many brain regions showed significant differences in LFO amplitude (ALFF/fALFF) between slow-4 and slow-5 bands and between the aMCI patients and controls. Interestingly, it was found that several brain regions including PCC and frontal regions showed significant interaction between frequency band and group, with greater group differences in the slow-5 band than in the slow-4 band. Their results suggest that the aMCI patients had abnormal LFO amplitude in intrinsic brain activity and that the abnormalities are associated with specific frequency bands. Thus,

there were significant differences in ALFF/fALFF between two different frequency bands (slow-4 vs. slow-5). Several default-mode regions (the PCC and MPFC) showed greater ALFF/fALFF in the slow-5 band than in the slow-4 band. Many previous studies have demonstrated that these regions constitute a structurally and functionally connected neuronal network that supports the default function of the human brain (Greicius et al., 2003; Raichle et al., 2001). Previous studies have suggested that lower-frequency oscillations allow for an integration of neuronal networks (Buzsaki & Draguhn, 2004). This notion is compatible with their results of greater brain activity in the DMN in the lower slow-5 band. In this study, they also showed greater brain activity in several brain regions in the slow-4 band than in the slow-5 band. This result is consistent with a recent fMRI study showing the most significant ALFF/fALFF differences in the basal ganglia between the two bands (Zuo et al., 2010).

It has been suggested that the oscillations of the brain cover a wide range of frequencies and each of these oscillatory bands is generated by different mechanisms and has different physiological functions (Buzsaki & Draguhn, 2004). Although the origins, relation, and specific physiological functions of different frequency bands have yet to be fully clarified, neighboring bands have been found to be typically associated with different brain states and compete with each other (Buzsaki & Draguhn, 2004). Future work should discover the neurophysiological basis of the signals located at different frequency bands. Thus, it can be said that the abnormalities of brain spontaneous activity in the aMCI patients are associated with the choice of specific frequency bands. For instance, aMCI patients had greater decreases in LFO amplitude in the PCC in the slow-5 band (0.01–0.027 Hz) than in the slow-4 band (0.027–0.073 Hz). Also, Hoptman et al. (2010) showed that the patients with SCZ had

widespread abnormalities of LFO amplitudes in the slow-4 frequency band. These studies suggest that the pattern of intrinsic brain activity is sensitive to specific frequency bands. In their study, it was shown that PCC activity exhibited greater group differences in the lower slow-5 band than in the slow-4 band. As mentioned above, within the same neuronal networks neighboring bands are typically associated with different brain states (Buzsaki & Draguhn, 2004).

Future studies are important to examine whether such frequency specific fluctuations could be used for disease diagnosis. From our results imply that in SCZ, the slow-5 band could be more sensitive in detecting abnormalities of spontaneous brain activity in the mPFC region compared to other frequency bands.

Yu et al. (2014) showed that there were significant differences in ALFF/fALFF between the two bands (slow-5 and slow-4) in regions including the basal ganglia, the midbrain, and the vmPFC. The results suggest that the abnormalities of LFOs in SCZ is dependent on the frequency band and suggest that future studies should take the different frequency bands into account when measure intrinsic brain activity. Previous studies have demonstrated visual and auditory sensory processing dysfunction revealed by evoked potentials showing abnormalities at the level of lateral geniculate nucleus or primary visual cortex (Butler et al., 2008). Instead of using evoked potentials, Yu et al. (2014) found reduced LFO amplitude in occipital cortex in patients with SCZ on rs-fMRI, consistent with the hypothesis that SCZ is associated with low-level sensory functions (e.g., Butler et al., 2001, 2005). Their findings that SCZ patients exhibited larger ALFF/fALFF in mPFC provide insights into this issue by showing a high mPFC baseline in SCZ. Nevertheless, the activation pattern of mPFC in SCZ under the resting state is far from conclusive and warrants more studies.

Complexity measures and clinical symptoms

Next, our data showed a significant relationship between complexity measures and anxiety/depression. The higher the degree of complexity in spontaneous activity mPFC, the higher the degree of symptoms in anxiety/depression. This suggests that increased temporal disorder and irregularity in spontaneous activity pattern induce psychological changes like anxiety and depression. Interestingly, this relationship only holds for the complexity measures but not for PLE. Regionally, our data show findings in mPFC that has been associated with emotion processing (Etkin et al., 2011) and self-relatedness (Northoff, 2015; Northoff et al., 2006; van den Meer et al., 2010) which both show major changes in SCZ (Leube, 2008; van den Meer et al., 2014, 2015). Moreover, changes in the spontaneous activity's temporal structure may surface also in the subjects' abnormal perception of time that is, inner time consciousness, as it has often been reported in SCZ (Northoff, 2015; Stanghellini et al., 2015). Unfortunately, we did not include any measures of subjective time perception in our patients, including their relation to symptoms. Nevertheless, one can conceive our findings as first step towards establishing what recently has been introduced as "spatiotemporal psychopathology" (Northoff & Duncan, 2016).

Limitations

Some limitations in our study are worth mentioning. First, our patients in the different samples were medicated; however, we did not control the impact of medication; it was not controlled. Since CPZ in mPFC blocks dopamine and serotonin releases in that area, the results could be due to an effect of CPZ rather than SCZ. Antipsychotic drugs also attenuate glutamatergic transmission in mPFC. For efficiency and usefulness, it will be essential to design a new experiment to examine the PLE in medication-naïve SCZ patients or SCZ patients before any treatment

effects. Moreover, we observed significant difference between the control groups (GE-CON, TWN-CON and IT-CON). This is not unexpected as both TR and coil strength have been shown to affect PLE estimates (there are differences in both these factors between the three centers). There are many possible reasons that the PLE are different across dataset. It is mainly due to unmatched preprocessing (different bandpass, normalization, FFT frequency bin numbers, smooth or not, etc. Thus, there is no way to figure that out without preprocessing all the dataset in exactly the same way by the same person. Therefore, since preprocessing may impact the actual PLE values, the comparison makes sense only if there is healthy control group processed in the same way. Furthermore, our study did not investigate the actual relationship between reduced PLE in mPFC and private self-consciousness. Currently, it remains unclear how the PLE changes during self-related tasks. Since a larger PLE has been observed during resting-state activity compared with task-evoked activity (He, 2011), one would expect the PLE during the self-related task to be attenuated when compared with resting-state activity. Also, we did not examine the full spectrum of cognitive functions and social behaviors in our sample. Although we instructed participants to close their eyes during scanning, without eye tracking or other visual monitoring equipment, we cannot rule out the possibility that some participants failed to comply with this instruction during the whole resting session. It has been shown that the type of a resting condition (eyes open or eyes closed) can influence ALFF in mPFC, parahippocampal gyrus, cingulate cortex, and precuneus (Yan et al., 2009). Future studies should take the resting condition into account and investigate whether and how it influences LFOs in specific frequency band. Also, it would have been important to examine the test-retest reliability of PLE measure. For instance, the test-retest reliability of ALFF has only been examined in healthy volunteers to date (Zuo

et al., 2010), and it is unclear whether ALFF is reliable and stable over the short-term illness course in chronically treated persons with SCZ. A related measure, fractional ALFF or fALFF, measures the amount of power in the lower frequency spectrum relative to the total power in the detectable range; however, it is slightly less reliable than ALFF in healthy controls (Zuo et al., 2010). Since there are no enough studies using PLE in psychiatric patients, conducting more studies will be able to give us how reliable this PLE measure is. Moreover, we did not include any fMRI task in our sample which precluded us from drawing a relationship between spontaneous and stimulus-induced activity.

Implications and future research

Our results may hold important implications for a biomarker in diagnosing SCZ as well as other psychiatric disorders and lead to earlier interventions. Also, since the current study revealed that investigation of the temporal structure of the BOLD signal can be used to differentiate psychiatric disorders, there is a possibility that we can use temporal structures for more personalized treatments. Furthermore, although the current study only used mPFC as a seed region based on the results of SCZ patients, it will be important to investigate PLE in other brain regions other than mPFC in other psychiatric disorders. For instance, the current study did not find any significant group differences in PLE in mPFC in MDD and BP, but these patients might have reduced or increased PLE in other regions such as PCC. Therefore, future studies should apply the current analysis to investigate other disorders by focusing on other brain regions.

Regarding PLE, a past study revealed that the PLE value of mPFC is correlated with private self-consciousness (Huang et al., 2016). Therefore, our results

regarding the reduced PLE value of mPFC in schizophrenic patients support the notion that schizophrenic patients have abnormal private self-consciousness.

Based on the current study, future research could investigate further in terms of the relationship between SCZ and self-consciousness and also other mental illness. Huang et al. (2016) found a significant positive correlation between the PLE in the mPFC and private self-consciousness. This result suggests that higher degrees of long-range temporal correlations (as signified by the PLE) are specifically related to higher degrees of private self-consciousness. As SCZ is considered to be related to abnormal self-consciousness, it would be meaningful to investigate the relationship between high PLE in the mPFC and self-consciousness abnormality in SCZ patients and also in healthy subjects.

Interestingly, a study found that mPFC was activated by self-recognition tasks and also theory of mind tasks. ‘Theory of Mind’ refers to the ability to attribute mental states to oneself and other people (Premack & Woodruff, 1978). Since mPFC is an overlapping region of two distinct tasks, this region might be related to the social cognitive impairment of SCZ patients as well as the self-disturbances of SCZ. The term "social cognition" generally refers to the mental operations that underlie social interactions including the perception and interpretation of the intentions, dispositions, and behaviours of others and the generation of a response to these behaviours. More studies are needed to investigate the relationship between the self and social cognitive functions (e.g., Saxe et al., 2006). Therefore, future studies should investigate how alterations in the temporal structure of spontaneous activity relate to social cognitive functions in SCZ and also how therapies can change these outcomes.

Furthermore, in the future studies on temporal structure, an investigation of correlations with SCZ symptoms, both negative and positive, as well as sensory and

motor impairment will be important. Moreover, it remains an open question as to what specific neural mechanisms may underlie the different clusters of symptoms seen in SCZ. Thus, future studies also need to differentiate positive and negative symptoms of SCZ and also different types of SCZ.

The present study only investigated resting-state brain activity—in other words, spontaneous brain activity. Therefore, future studies should investigate task-evoked activity to find an improved biomarker. Currently, it remains unclear how the PLE changes during self-related tasks. Since a larger PLE has been observed during resting-state activity compared with task-evoked activity (He, 2011), one would expect the PLE during the self-related task to be attenuated when compared with resting-state activity. Based on the observed correspondence of higher PLE with higher sense of self in the private dimension, we assume that the PLE will be less attenuated during self-related tasks versus non-self-related tasks. Therefore, it is useful to investigate whether patients still show reduced PLE compared to healthy controls during tasks or show opposite effects. Future studies may therefore want to directly link spontaneous and task-evoked activity changes with regard to PLE.

In addition, these findings will be more useful if they are combined with data on other physiological mechanisms such as heart-rate variability and other autonomic nervous systems. Radulescu et al. (2012) suggests that although heart-rate variability has become common as a psychiatric biomarker, distinguishing SCZ from other mental illness is not well established. Therefore, combining two measures will be able to improve the biomarker. Also, future studies may want to include more sophisticated psychopathological measures like time perception and ego-pathology, among others. Furthermore, future research should investigate how SCZ patients' brain activity changes after certain types of therapies such as current simulation

(rTMS). By doing so, more effective and personalized therapy can be developed. Furthermore, the current study did not control the length of SCZ diagnosis for patients or the severity of the disease. Since there is a possibility that temporal structure changes across the progress of the disease, it is worth comparing the results. Future studies should also investigate the cause–effect relationship. We still do not know whether reduced PLE in mPFC causes SCZ or SCZ causes PLE reduction. Therefore, comparing the temporal structures of early-stage SCZ and other SCZ patients as well as testing high SCZ-type healthy subjects will be able to help.

Investigation of brain activity in SCZ will contribute to early diagnosis and improved interventions for SCZ. Also, it will encourage better understanding of temporal structures and self-consciousness. Moreover, this knowledge will be able to benefit other mental illnesses such as depression and bipolar disorder. Identifying new ways of classifying mental disorders based on observable behavior and neurobiological measures could lead to earlier interventions and improved patient outcomes. Our findings could be helpful for diagnosis and evaluation of the severity of the disease, as well as understanding the pathophysiologic mechanisms underlying cognitive dysfunction in SCZ.

In conclusion, our study showed for the first time reduced LRTC and increased complexity in spontaneous activity specifically in mPFC in SCZ. This was replicated in an independent sample, and its specificity was shown when compared to MDD and BP patients. Our findings suggest an altered temporal structure and its different aspects or facets in spontaneous activity in SCZ. This provides a novel, more temporal understanding of the brain’s spontaneous activity beyond its well-investigated functional connectivity and spatial structure.

10. References

Akar, S. A., Kara, S., Latifoğlu, F., & Bilgiç, V. (2015). Analysis of heart rate variability during auditory stimulation periods in patients with schizophrenia. *Journal of clinical monitoring and computing*, *29*(1), 153-162.

Allen, P. P., Johns, L. C., Fu, C. H., Broome, M. R., Vythelingum, G. N., & McGuire, P. K. (2004). Misattribution of external speech in patients with hallucinations and delusions. *Schizophrenia research*, *69*(2), 277-287.

Bär, K. J., Boettger, M. K., Koschke, M., Schulz, S., Chokka, P., Yeragani, V. K., & Voss, A. (2007). Non-linear complexity measures of heart rate variability in acute schizophrenia. *Clinical neurophysiology*, *118*(9), 2009-2015.

Bluhm, R. L., Miller, J., Lanius, R. A., Osuch, E. A., Boksman, K., Neufeld, R. W. J., & Williamson, P. (2007). Spontaneous low-frequency fluctuations in the BOLD signal in schizophrenic patients: anomalies in the default network. *Schizophrenia bulletin*, *33*(4), 1004-1012.

http://schizophreniabulletin.oxfordjournals.org/content/33/4/1004.full

Boly, M., Phillips, C., Tshibanda, L., Vanhaudenhuyse, A., Schabus, M., Dang-Vu, T., & Laureys, S. (2008). Intrinsic brain activity in altered states of consciousness. *Annals of the New York Academy of Sciences*, *1129*(1), 119-129.

Bradbury, T. N., & Miller, G. A. (1985). Season of birth in schizophrenia: A review of evidence, methodology, and etiology. *Psychological bulletin*, *98*(3), 569.

Bullmore, E., Long, C., Suckling, J., Fadili, J., Calvert, G., Zelaya, F., & Brammer, M. (2001). Colored noise and computational inference in neurophysiological (fMRI) time series analysis: resampling methods in time and wavelet domains. *Human brain mapping*, *12*(2), 61-78.

Butler, P. D., Silverstein, S. M., & Dakin, S. C. (2008). Visual perception and its impairment in schizophrenia. *Biological psychiatry*, *64*(1), 40-47.

http://journals2.scholarsportal.info/pdf/00219967/v501i0002/290_pvcvatnnaris.xml

Buzsáki, G., & Draguhn, A. (2004). Neuronal oscillations in cortical networks. *Science*, *304*(5679), 1926-1929.

Calhoun, V. D., Eichele, T., & Pearlson, G. (2009). Functional brain networks in schizophrenia: a review. *Frontiers in human neuroscience*, *3*, 17.

Camchong, J., MacDonald, A. W., Bell, C., Mueller, B. A., & Lim, K. O. (2011). Altered functional and anatomical connectivity in schizophrenia. *Schizophrenia bulletin*, *37*(3), 640-650.

Cox, R. W. (1996). AFNI: software for analysis and visualization of functional magnetic resonance neuroimages. *Computers and Biomedical research*, *29*(3), 162-173.

Deco, G., Ponce-Alvarez, A., Mantini, D., Romani, G. L., Hagmann, P., & Corbetta, M. (2013). Resting-state functional connectivity emerges from structurally and dynamically shaped slow linear fluctuations. *The Journal of Neuroscience*, *33*(27), 11239-11252.

DSM-5 American Psychiatric Association. (2013). Diagnostic and statistical manual of mental disorders. *Arlington: American Psychiatric Publishing*.

Ebisch, S. J., Mantini, D., Northoff, G., Salone, A., De Berardis, D., Ferri, F., & Gallese, V. (2014). Altered brain long-range functional interactions underlying the link between aberrant self-experience and self-other relationship in first-episode schizophrenia. *Schizophrenia bulletin*, *40*(5), 1072-1082. https://academic.oup.com/schizophreniabulletin/article/40/5/1072/1925034/Altered-Brain-Long-Range-Functional-Interactions

Ernst, M., Zametkin, A. J., Matochik, J. A., Pascualvaca, D., & Cohen, R. M. (1997). Low medial prefrontal dopaminergic activity in autistic children. *The Lancet*, *350*(9078),638. *http://journals2.scholarsportal.info/pdf/01406736/v350i9078/638_lmpdaiac.xml*

Etkin, A., Egner, T., & Kalisch, R. (2011). Emotional processing in anterior cingulate and medial prefrontal cortex. *Trends in cognitive sciences*, *15*(2), 85-93.

Fioravanti, M., Bianchi, V., & Cinti, M. E. (2012). Cognitive deficits in schizophrenia: an updated metanalysis of the scientific evidence. *BMC psychiatry*, *12*(1), 64.

https://bmcpsychiatry.biomedcentral.com/articles/10.1186/1471-244X-12-64

Fletcher, P., McKenna, P. J., Friston, K. J., Frith, C. D., & Dolan, R. J. (1999). Abnormal cingulate modulation of fronto-temporal connectivity in schizophrenia. *Neuroimage*, *9*(3), 337-342.

Frith, C. D., Blakemore, S. J., & Wolpert, D. M. (2000). Explaining the symptoms of schizophrenia: Abnormalities in the awareness of action. *Brain Research Reviews*, *31*(2), 357-363.

Garakh Z, Zaytseva Y, Kapranova A, Fiala O, Horacek J, Shmukler A, Gurovich IY, Strelets VB (2015): EEG correlates of a mental arithmetic task in patients with first episode schizophrenia and schizoaffective disorder. Clin Neurophysiol 126:2090–8. .

Garrett, D.D., Kovacevic, N., McIntosh, A.R., Grady, C.L., (2010). Blood oxygen leveldependent signal variability is more than just noise. *J. Neurosci. 30*, 4914–4921.

Garrett, D.D., Samanez-Larkin, G.R., MacDonald, S.W., Lindenberger, U., McIntosh, A.R., Grady, C.L., (2013). Moment-to-moment brain signal variability: a next frontier in human brain mapping? *Neurosci. Biobehav. Rev. 37* (4), 610–624.

Garrity, A. G., Pearlson, G. D., McKiernan, K., Lloyd, D., Kiehl, K. A., & Calhoun, V. D. (2007). Aberrant "default mode" functional connectivity in schizophrenia. *American journal of psychiatry*, *164*(3), 450-457.

http://ajp.psychiatryonline.org/doi/full/10.1176/ajp.2007.164.3.450

Gradin, V. B., Waiter, G., Kumar, P., Stickle, C., Milders, M., Matthews, K., & Steele, J. D. (2012). Abnormal neural responses to social exclusion in schizophrenia. *PloS one*, *7*(8), e42608.

https://www.ncbi.nlm.nih.gov/pubmed?cmd=Search&doptcmdl=Citation&defaultField=Title%20Word&term=Gradin%5Bauthor%5D%20AND%20Social%20Exclusion%20in%20Schizophrenia

Greicius, M. D., Krasnow, B., Reiss, A. L., & Menon, V. (2003). Functional connectivity in the resting brain: A network analysis of the default mode hypothesis. *Proceedings of the National Academy of Sciences*, *100*(1), 253-258.

Greicius, M. D., Supekar, K., Menon, V., & Dougherty, R. F. (2009). Resting-state functional connectivity reflects structural connectivity in the default mode network. *Cerebral cortex*, *19*(1), 72-78.

Gusnard, D. A., Akbudak, E., Shulman, G. L., & Raichle, M. E. (2001). Medial prefrontal cortex and self-referential mental activity: relation to a default mode of brain function. *Proceedings of the National Academy of Sciences*, *98*(7), 4259-4264.

Han, Y., Wang, J., Zhao, Z., Min, B., Lu, J., Li, K., & Jia, J. (2011). Frequency-dependent changes in the amplitude of low-frequency fluctuations in amnestic mild cognitive impairment: a resting-state fMRI study. *Neuroimage*, *55*(1), 287-295.

He, B. J., Zempel, J. M., Snyder, A. Z., & Raichle, M. E. (2010). The temporal structures and functional significance of scale-free brain activity. *Neuron*, *66*(3), 353-369.

He, B. J. (2011). Scale-free properties of the functional magnetic resonance imaging signal during rest and task. *Journal of Neuroscience*, *31*(39), 13786-13795.

He, Z., Deng, W., Li, M., Chen, Z., Jiang, L., Wang, Q., & Li, T. (2013). Aberrant intrinsic brain activity and cognitive deficit in first-episode treatment-naive patients with schizophrenia. *Psychological medicine*, *43*(04), 769-780.

Hong LE, Summerfelt A, Mitchell BD, McMahon RP, Wonodi I, Buchanan RW, Thaker GK (2008): Sensory gating endophenotype based on its neural oscillatory pattern and heritability estimate. Arch Gen Psychiatry 65:1008–16.

Hoptman, M. J., Zuo, X. N., Butler, P. D., Javitt, D. C., D'Angelo, D., Mauro, C. J., & Milham, M. P. (2010). Amplitude of low-frequency oscillations in schizophrenia: a resting state fMRI study. *Schizophrenia Research*, *117*(1), 13-20. http://www.sciencedirect.com/science/article/pii/S0920996409004745

Howes, O. D., & Kapur, S. (2009). The dopamine hypothesis of schizophrenia: version III—the final common pathway. *Schizophrenia bulletin*, *35*(3), 549-562. http://www.behaviorismandmentalhealth.com/wpcontent/uploads/2015/01/Howes-and-Kapur.pdf

Huang, X. Q., Lui, S., Deng, W., Chan, R. C., Wu, Q. Z., Jiang, L. J., & Gong, Q. Y. (2010). Localization of cerebral functional deficits in treatment-naive, first-episode schizophrenia using resting-state fMRI. *Neuroimage*, *49*(4), 2901-2906.

Huang, Z., Dai, R., Wu, X., Yang, Z., Liu, D., Hu, J., & Wu, X. (2014). The self and its resting state in consciousness: an investigation of the vegetative state. *Human brain mapping*, *35*(5), 1997-2008.

Huang, Z., Wang, Z., Zhang, J., Dai, R., Wu, J., Li, Y., & Zhang, J. (2014). Altered temporal variance and neural synchronization of spontaneous brain activity in anesthesia. *Human brain mapping*, *35*(11), 5368-5378.

Huang, Z., Zhang, J., Longtin, A., Dumont, G., Duncan, N. W., Pokorny, J., & Northoff, G. (2015). Is there a nonadditive interaction between spontaneous and evoked activity? Phase-dependence and its relation to the temporal structure of scale-free brain activity. *Cerebral Cortex*, bhv288.

Huang, Z., Obara, N., Davis, H. H., Pokorny, J., & Northoff, G. (2016). The temporal structure of resting-state brain activity in the medial prefrontal cortex predicts self-consciousness. *Neuropsychologia*, *82*, 161-170.

Huang, Z., Zhang, J., Wu, J., Qin, P., Wu, X., Wang, Z., & Northoff, G. (2015). Decoupled temporal variability and signal synchronization of spontaneous brain activity in loss of consciousness: An fMRI study in anesthesia. *NeuroImage*, *124*, 693-703.

Ide, J. S., Hu, S., Zhang, S., Mujica-Parodi, L. R., & Chiang-shan, R. L. (2016). Power spectrum scale invariance as a neural marker of cocaine misuse and altered cognitive control. *NeuroImage: Clinical*, *11*, 349-356. https://www.ncbi.nlm.nih.gov/pmc/articles/PMC4888196/#ec0005

Jafri, M. J., Pearlson, G. D., Stevens, M., & Calhoun, V. D. (2008). A method for functional network connectivity among spatially independent resting-state components in schizophrenia. *Neuroimage*, *39*(4), 1666-1681.

http://www.sciencedirect.com/science/article/pii/S1053811907010282

Karbasforoushan, H., & Woodward, N. D. (2012). Resting-state networks in schizophrenia. *Current topics in medicinal chemistry*, *12*(21), 2404-2414.

Kesler, S. R., Kent, J. S., & O'hara, R. (2011). Prefrontal cortex and executive function impairments in primary breast cancer. *Archives of neurology*, *68*(11), 1447-1453.

Kühn, S., & Gallinat, J. (2013). Resting-state brain activity in schizophrenia and major depression: a quantitative meta-analysis. *Schizophrenia bulletin*, *39*(2), 358-365.

Lai, M. C., Lombardo, M. V., Chakrabarti, B., Sadek, S. A., Pasco, G., Wheelwright, S. J., & MRC AIMS Consortium. (2010). A shift to randomness of brain oscillations in people with autism. *Biological psychiatry*, *68*(12), 1092-1099.

Lawrie, S. M., Buechel, C., Whalley, H. C., Frith, C. D., Friston, K. J., & Johnstone, E. C. (2002). Reduced frontotemporal functional connectivity in schizophrenia associated with auditory hallucinations. *Biological psychiatry*, *51*(12), 1008-1011. http://www.sciencedirect.com/science/article/pii/S0006322302013161

Lee, U., Oh, G., Kim, S., Noh, G., Choi, B., & Mashour, G. A. (2010). Brain networks maintain a scale-free organization across consciousness, anesthesia, and recovery: evidence for adaptive reconfiguration. *Anesthesiology*, *113*(5), 1081.

Lee, M. H., Smyser, C. D., & Shimony, J. S. (2013). Resting-state fMRI: a review of methods and clinical applications. *American Journal of Neuroradiology*, *34*(10), 1866-1872.

Leube, D., Whitney, C., & Kircher, T. (2008). The neural correlates of ego-disturbances (passivity phenomena) and formal thought disorder in schizophrenia. *European Archives of Psychiatry and Clinical Neuroscience*,*258*(5), 22-27.

Lindström, L. H., Gefvert, O., Hagberg, G., Lundberg, T., Bergström, M., Hartvig, P., & Långström, B. (1999). Increased dopamine synthesis rate in medial prefrontal cortex and striatum in schizophrenia indicated by L-(β-11 C) DOPA and PET. *Biological psychiatry*, *46*(5), 681-688.

http://www.sciencedirect.com/science/article/pii/S0006322399001092

Lynall, M. E., Bassett, D. S., Kerwin, R., McKenna, P. J., Kitzbichler, M., Muller, U., & Bullmore, E. (2010). Functional connectivity and brain networks in schizophrenia. *Journal of Neuroscience*, *30*(28), 9477-9487.

http://www.jneurosci.org/content/30/28/9477.full

Magioncalda, P., Martino, M., Conio, B., Escelsior, A., Piaggio, N., Presta, A., & Amore, M. (2015). Functional connectivity and neuronal variability of resting state activity in bipolar disorder-reduction and decoupling in anterior cortical midline structures. *Human brain mapping*, *36*(2), 666-682.

Marcelis, M., Takei, N., & van Os, J. (1999). Urbanization and risk for schizophrenia: does the effect operate before or around the time of illness onset?. *Psychological medicine*, *29*(5), 1197-1203.

Martin, B., Wittmann, M., Franck, N., Cermolacce, M., Berna, F., & Giersch, A. (2014). Temporal structure of consciousness and minimal self in schizophrenia.

Martino, M., Magioncalda, P., Huang, Z., Conio, B., Piaggio, N., Duncan, N. W., & Inglese, M. (2016). Contrasting variability patterns in the default mode and sensorimotor networks balance in bipolar depression and mania. *Proceedings of the National Academy of Sciences*, *113*(17), 4824-4829.

Micheloyannis, S., Pachou, E., Stam, C. J., Breakspear, M., Bitsios, P., Vourkas, M., & Zervakis, M. (2006). Small-world networks and disturbed functional connectivity in schizophrenia. *Schizophrenia research*, *87*(1), 60-66.

http://www.sciencedirect.com/science/article/pii/S0920996406002969

Mingoia, G., Wagner, G., Langbein, K., Maitra, R., Smesny, S., Dietzek, M., & Nenadic, I. (2012). Default mode network activity in schizophrenia studied at resting state using probabilistic ICA. *Schizophrenia research*, *138*(2), 143-149.

Moran, L. V., & Hong, L. E. (2011). High vs low frequency neural oscillations in schizophrenia. *Schizophrenia bulletin*, *37*(4), 659-663.

Nagaraj, N., Balasubramanian, K., & Dey, S. (2013). A new complexity measure for time series analysis and classification. *The European Physical Journal Special Topics*, *222*(3-4), 847-860.

Narayan, C. L., Shikha, D., & Shekhar, S. (2015). Schizophrenia in identical twins. *Indian journal of psychiatry*, *57*(3), 323.

Northoff, G., Heinzel, A., De Greck, M., Bermpohl, F., Dobrowolny, H., & Panksepp, J. (2006). Self-referential processing in our brain—a meta-analysis of imaging studies on the self. *Neuroimage*, *31*(1), 440-457.

Northoff, G. (2013). What the brain's intrinsic activity can tell us about consciousness? A tri-dimensional view. *Neuroscience & Biobehavioral Reviews*, *37*(4), 726-738.

Northoff, G. (2014). How Is Our Self Altered in Psychiatric Disorders A Neurophenomenal Approach to Psychopathological Symptoms. *Psychopathology*, *47*(6), 365-376.

Northoff, G. (2015). Is schizophrenia a spatiotemporal disorder of the brain's resting state?. *World Psychiatry*, *14*(1), 34-35.

Northoff, G., & Duncan, N. W. (2016). How do abnormalities in the brain's spontaneous activity translate into symptoms in schizophrenia? From an overview of resting state activity findings to a proposed spatiotemporal psychopathology. *Progress in Neurobiology*, *145*, 26-45.

Nuechterlein, K. H., Ventura, J., Subotnik, K. L., & Bartzokis, G. (2014). The early longitudinal course of cognitive deficits in schizophrenia. *The Journal of clinical psychiatry*, *75*(0 2), 25.

Öngür, D., Lundy, M., Greenhouse, I., Shinn, A. K., Menon, V., Cohen, B. M., & Renshaw, P. F. (2010). Default mode network abnormalities in bipolar disorder

and schizophrenia. *Psychiatry Research: Neuroimaging*, *183*(1), 59-68.

Palva, J. M., & Palva, S. (2011). 22 Roles of multiscale brain activity fluctuations in shaping the variability and dynamics of psychophysical performance. *Progress in brain research*, *193*, 335.

Palva, J. M., Zhigalov, A., Hirvonen, J., Korhonen, O., Linkenkaer-Hansen, K., & Palva, S. (2013). Neuronal long-range temporal correlations and avalanche dynamics are correlated with behavioral scaling laws. *Proceedings of the National Academy of Sciences*, *110*(9), 3585-3590.

Pincus, S. M. (1991). Approximate entropy as a measure of system complexity. *Proceedings of the National Academy of Sciences*, *88*(6), 2297-2301.

Premack, D., & Woodruff, G. (1978). Does the chimpanzee have a theory of mind?. *Behavioral and brain sciences*, *1*(4), 515-526.

Radulescu, A. R., Rubin, D., Strey, H. H., & Mujica-Parodi, L. R. (2012). Power spectrum scale invariance identifies prefrontal dysregulation in paranoid schizophrenia. *Human Brain Mapping*, *33*(7), 1582-1593.

Rădulescu, A., & Mujica-Parodi, L. R. (2014). Network connectivity modulates power spectrum scale invariance. *NeuroImage*, *90*, 436-448. http://sci-hub.cc/10.1016/j.neuroimage.2013.12.001

Rotarska-Jagiela, A., van de Ven, V., Oertel-Knöchel, V., Uhlhaas, P. J., Vogeley, K., and Linden, D. E. J. (2010). Resting-state functional network correlates of psychotic symptoms in schizophrenia. Schizophr. Res. 117, 21–30. doi:10.1016/j.schres.2010.01.001.

Salvador, R., Sarró, S., Gomar, J. J., Ortiz-Gil, J., Vila, F., Capdevila, A., & Pomarol-Clotet, E. (2010). Overall brain connectivity maps show cortico-subcortical abnormalities in schizophrenia. *Human brain mapping*, *31*(12), 2003-2014.

Saxe, R., Moran, J. M., Scholz, J., & Gabrieli, J. (2006). Overlapping and non-overlapping brain regions for theory of mind and self reflection in individual subjects. *Social cognitive and affective neuroscience*, *1*(3), 229-234.

Sekar, A., Bialas, A. R., de Rivera, H., Davis, A., Hammond, T. R., Kamitaki, N., & Genovese, G. (2016). Schizophrenia risk from complex variation of complement component 4. *Nature*, *530*(7589), 177-183.

Sokunbi, M. O., Gradin, V. B., Waiter, G. D., Cameron, G. G., Ahearn, T. S., Murray, A. D., & Staff, R. T. (2014). Nonlinear complexity analysis of brain FMRI signals in schizophrenia. *Plos One*, *9*(5), e95146. http://journals.plos.org/plosone/article?id=10.1371/journal.pone.0095146

Stanghellini, G., & Rosfort, R. (2015). Disordered selves or persons with schizophrenia?. *Current opinion in psychiatry*, *28*(3), 256-263.

Stephan, K. E., Baldeweg, T., & Friston, K. J. (2006). Synaptic plasticity and dysconnection in schizophrenia. *Biological psychiatry*, *59*(10), 929-939.

Strimbu, K., & Tavel, J. A. (2010). What are biomarkers?. *Current Opinion in HIV and AIDS*, *5*(6), 463. https://www.ncbi.nlm.nih.gov/pmc/articles/PMC3078627/

Talairach, J., & Tournoux, P. (1988). Co-planar stereotaxic atlas of the human brain. 3-Dimensional proportional system: an approach to cerebral imaging.

Turner, J. A., Chen, H., Mathalon, D. H., Allen, E. A., Mayer, A. R., Abbott, C. C., & Bustillo, J. (2012). Reliability of the amplitude of low-frequency fluctuations in resting state fMRI in chronic schizophrenia. *Psychiatry Research: Neuroimaging*, *201*(3), 253-255.

Turner, J. A., Damaraju, E., Van Erp, T. G., Mathalon, D. H., Ford, J. M., Voyvodic, J., & Potkin, S. G. (2013). A multi-site resting state fMRI study on the amplitude of low frequency fluctuations in schizophrenia. *Frontiers in neuroscience*, *7*. https://www.ncbi.nlm.nih.gov/pmc/articles/PMC3361647/

Tolkunov, D., Rubin, D., & Mujica-Parodi, L. (2010). Power spectrum scale invariance quantifies limbic dysregulation in trait anxious adults using fMRI: Adapting methods optimized for characterizing autonomic dysregulation to neural dynamic time series. *Neuroimage*, *50*, 72-80.

Tomashi, D., Shokri-Kojori, E., & Volkow, N. D. (2016). Temporal changes in local functional connectivity density reflect the temporal variability of the amplitude of low frequency fluctuations in gray matter. *PloS one*, *11*(4), e0154407. http://journals.plos.org/plosone/article?id=10.1371/journal.pone.0154407

Uhlhaas, P. J. (2013). Dysconnectivity, large-scale networks and neuronal dynamics in schizophrenia. *Current opinion in neurobiology*, *23*(2), 283-290.

van der Meer, L., Costafreda, S., Aleman, A., & David, A. S. (2010). Self-reflection and the brain: a theoretical review and meta-analysis of neuroimaging studies with implications for schizophrenia. *Neuroscience & Biobehavioral Reviews*, *34*(6), 935-946.

Welsh, R. C., Chen, A. C., & Taylor, S. F. (2010). Low-frequency BOLD fluctuations demonstrate altered thalamocortical connectivity in schizophrenia. *Schizophrenia bulletin*, *36*(4), 713-722. http://schizophreniabulletin.oxfordjournals.org/content/36/4/713.full

Whitfield-Gabrieli, S., Thermenos, H. W., Milanovic, S., Tsuang, M. T., Faraone, S. V, McCarley, R. W., Shenton, M. E., Green, A. I., Nieto-Castanon, A., LaViolette, P., et al. (2009). Hyperactivity and hyperconnectivity of the default network in schizophrenia and in first-degree relatives of persons with schizophrenia. Proc. Natl. Acad. Sci. U. S. A. 106, 1279–84. doi:10.1073/pnas.0809141106.

Yang, G. J., Murray, J. D., Repovs, G., Cole, M. W., Savic, A., Glasser, M. F., & Anticevic, A. (2014). Altered global brain signal in schizophrenia. *Proceedings of the National Academy of Sciences*, *111*(20), 7438-7443.

Yu, Q., A Allen, E., Sui, J., R Arbabshirani, M., Pearlson, G., & D Calhoun, V. (2012). Brain connectivity networks in schizophrenia underlying resting state functional magnetic resonance imaging. *Current topics in medicinal chemistry*, *12*(21), 2415-2425.

Yu, R., Chien, Y. L., Wang, H. L. S., Liu, C. M., Liu, C. C., Hwang, T. J., & Tseng, W. Y. I. (2014). Frequency-specific alternations in the amplitude of low-frequency fluctuations in schizophrenia. *Human brain mapping*, *35*(2), 627-637. https://www.researchgate.net/profile/Hsieh_Ming/publication/232813696_Frequency-Specific_Alternations_in_the_Amplitude_of_Low-Frequency_Fluctuations_in_Schizophrenia/links/02e7e516d15d80554a000000.pdf

Yu-Feng, Z., Yong, H., Chao-Zhe, Z., Qing-Jiu, C., Man-Qiu, S., Meng, L., & Yu-Feng, W. (2007). Altered baseline brain activity in children with ADHD revealed by resting-state functional MRI. *Brain and Development*, *29*(2), 83-91. http://sci-hub.cc/10.1016/j.braindev.2006.07.002

Zang, Y., Jiang, T., Lu, Y., He, Y., Tian, L., 2004. Regional homogeneity approach to fMRI data analysis. *NeuroImage 22* (1), 394–400.

Zhou, Y., Shu, N., Liu, Y., Song, M., Hao, Y., Liu, H., & Jiang, T. (2008). Altered resting-state functional connectivity and anatomical connectivity of hippocampus in schizophrenia. *Schizophrenia research*, *100*(1), 120-132. http://www.sciencedirect.com/science/article/pii/S0920996407005634

Zuo, X. N., Di Martino, A., Kelly, C., Shehzad, Z. E., Gee, D. G., Klein, D. F., & Milham, M. P. (2010). The oscillating brain: complex and reliable. *Neuroimage*, *49*(2), 1432-1445. http://fcp-indi.github.io/docs/user/alff.html

11. Appendices

11.1. BPRS (clinical symptoms) scales and complexity measures in GE-SCZ (Dataset-I). BPRS indicates Brief Psychiatric Rating Scale. AN/DP indicates Anxiety/Depression Score. LZ: Lempel-Ziv. ApEn: Approximate Entrophy.

Patients No.	BPRS (AN/DP)	LZ	ApEn
SCZ01	13	0.93	1.66
SCZ02	13	1.07	1.60
SCZ03	9	0.98	1.69
SCZ04	8	0.75	1.60
SCZ05	18	1.03	1.63
SCZ06	10	0.98	1.59
SCZ07	N/A	0.84	1.59
SCZ08	10	1.03	1.59
SCZ09	18	0.93	1.70
SCZ10	7	0.89	1.51
SCZ11	11	0.98	1.60
SCZ12	16	0.98	1.63
SCZ13	17	1.03	1.69
SCZ14	14	0.89	1.60
SCZ15	15	1.03	1.59
SCZ16	N/A	0.89	1.56
SCZ17	9	0.89	1.54
SCZ18	12	0.98	1.67
SCZ19	9	0.98	1.60
SCZ20	13	0.98	1.63
SCZ21	17	1.03	1.64
SCZ22	15	1.03	1.61
SCZ23	8	1.03	1.51
SCZ24	9	0.93	1.75
SCZ25	21	1.03	1.67
SCZ26	18	1.03	1.74
SCZ27	7	0.89	1.66
SCZ28	11	1.07	1.60

11.2. Raw data (Dataset I – III)

Dataset-I	subject	sex	age	group	restFD	restSNR	ple	ETC	LZ	ApEn
GT_con01	h01	m	42	GT_control	0.022913	76.09591	0.881739	0.2839	0.8406	1.4962
GT_con02	h02	f	29	GT_control	0.018754	79.20873	0.976575	0.2968	0.8406	1.4981
GT_con03	h03	f	35	GT_control	0.028756	65.75766	0.782254	0.129	0.2802	1.5359
GT_con04	h04	m	32	GT_control	0.025148	65.96022	0.58804	0.2903	0.8406	1.6115
GT_con05	h05	f	19	GT_control	0.02151	65.65327	0.615417	0.3097	0.934	1.6435
GT_con06	h06	m	22	GT_control	0.024051	61.87707	0.792911	0.2774	0.7939	1.4219
GT_con07	h07	f	40	GT_control	0.029356	58.79474	1.051053	0.1484	0.3736	1.5245
GT_con08	h08	m	29	GT_control	0.031452	71.41901	0.922402	0.3097	0.9807	1.5498
GT_con09	h09	m	30	GT_control	0.016931	74.11651	0.697273	0.2774	0.8406	1.4335
GT_con10	h10	m	22	GT_control	0.023893	72.18314	0.826572	0.3032	0.9807	1.5466
GT_scz01	p01	f	37	GT_scz	0.019075	77.56484	0.527781	0.3032	0.9807	1.6517
GT_scz02	p02	m	33	GT_scz	0.020904	67.24797	0.657473	0.3355	1.0274	1.6301
GT_scz03	p03	f	41	GT_scz	0.019695	74.12803	0.516244	0.3161	1.1208	1.6971
GT_scz04	p04	m	40	GT_scz	0.054213	43.24244	0.593264	0.3032	0.934	1.5993
GT_scz05	p05	m	22	GT_scz	0.025928	54.3165	0.546699	0.3161	0.9807	1.5875
GT_scz06	p06	m	29	GT_scz	0.052897	40.4153	0.777729	0.2	0.6071	1.471
GT_scz07	p07	f	21	GT_scz	0.021839	50.06733	0.591731	0.2839	0.8406	1.6801
GT_scz08	p08	m	54	GT_scz	0.027934	60.66439	0.749162	0.3032	0.8873	1.5734
GT_scz09	p09	m	35	GT_scz	0.086364	31.24004	0.563738	0.2839	0.934	1.6052
GT_scz10	p10	m	30	GT_scz	0.033011	52.00562	0.921483	0.2968	0.934	1.4932
GT_scz11	p11	m	32	GT_scz	0.060021	45.50492	0.238714	0.3161	0.9807	1.7696
GT_scz12	p12	f	40	GT_scz	0.029649	66.59527	0.646818	0.2839	0.934	1.5807
GT_scz13	p13	f	31	GT_scz	0.023908	80.76222	0.494899	0.3161	1.0274	1.7128
GT_scz14	p14	f	26	GT_scz	0.043033	55.90389	0.572912	0.3097	1.1208	1.6041
GT_scz15	p15	m	49	GT_scz	0.039772	65.1292	0.708277	0.2581	0.7472	1.4775
GT_scz16	p16	f	33	GT_scz	0.025814	72.70869	0.576377	0.3097	1.0274	1.6926
GT_scz17	p17	m	22	GT_scz	0.028496	60.89806	0.579616	0.3097	0.8406	1.5526
GT_scz18	p18	f	39	GT_scz	0.024899	77.1151	0.578517	0.3097	1.0741	1.6233
GT_scz19	p19	m	27	GT_scz	0.028121	60.07139	0.812748	0.2581	0.8406	1.6042
GT_scz20	p20	m	27	GT_scz	0.021573	72.61813	0.51176	0.329	1.0741	1.6239
GT_scz21	p21	m	25	GT_scz	0.038672	61.50479	0.810773	0.2968	0.9807	1.5646
GT_scz22	p22	f	40	GT_scz	0.015298	82.61875	0.567996	0.3032	0.934	1.6341
GT_scz23	p23	m	27	GT_scz	0.015778	74.00161	0.704109	0.271	0.8873	1.4816
GT_scz24	p24	f	27	GT_scz	0.020003	76.26776	0.605159	0.2452	0.8406	1.6337
GT_scz25	p25	m	38	GT_scz	0.035987	65.98747	0.320052	0.2903	0.8873	1.67
GT_scz26	p26	m	35	GT_scz	0.037104	78.8567	0.670133	0.3032	0.934	1.6114
GT_scz27	p27	m	38	GT_scz	0.053174	62.24969	0.394036	0.3032	0.9807	1.6319
GT_scz28	p28	m	55	GT_scz	0.024978	71.17383	0.629284	0.2645	0.8406	1.6896

***CON: Control group**

SCZ: Schizophrenia group

PLE: Power Law Exponent

ETC: Effort to compress

LZ: Lempel Ziv

ApEn: Approximate Entrophy

MDD: Major Depressive Disorder group

BP: Bipolar Disorder group

DEP: depressed phase

EUT: euthymic phase

MAN: manic phase

Dataset-II	subject	sex	age	group	restFD	restSNR	ple	ETC	LZ	ApEn
SHH_con01	mdC02	M	26	SHH_contro	0.037104	182.7942	1.003264	0.1921	0.6921	1.2443
SHH_con02	mdC03	M	46	SHH_contro	0.036275	171.0917	1.214716	0.1893	0.5966	1.0771
SHH_con03	mdC07	F	30	SHH_contro	0.026575	200.4358	1.084284	0.1695	0.525	1.1556
SHH_con04	mdC08	F	37	SHH_contro	0.036811	140.6292	1.484065	0.1638	0.4773	1.0466
SHH_con05	mdC09	F	30	SHH_contro	0.024658	170.5404	1.00444	0.1723	0.525	1.2289
SHH_con06	mdC10	F	33	SHH_contro	0.021436	178.8163	0.926989	0.1977	0.6205	1.2674
SHH_con07	mdC12	F	34	SHH_contro	0.032974	187.2329	1.347097	0.1582	0.4773	1.0638
SHH_con08	mdC14	F	43	SHH_contro	0.037136	163.5003	1.164158	0.1864	0.6205	1.135
SHH_con09	mdC16	F	30	SHH_contro	0.031679	171.6993	1.264805	0.1667	0.525	1.1385
SHH_con10	mdC22	F	30	SHH_contro	0.047398	131.909	1.314925	0.1977	0.6921	1.2432
SHH_con11	mdC24	F	39	SHH_contro	0.037333	160.4872	1.171214	0.1751	0.5489	1.0728
SHH_con12	mdC25	F	36	SHH_contro	0.034053	131.1608	1.314669	0.161	0.525	1.1588
SHH_con13	mdC26	F	42	SHH_contro	0.064767	108.2669	0.703922	0.2006	0.7398	1.3849
SHH_con14	mdC27	F	32	SHH_contro	0.027417	170.4815	1.476622	0.1864	0.6443	1.1052
SHH_con15	mdC29	F	31	SHH_contro	0.035016	160.8649	0.83389	0.1893	0.6205	1.2965
SHH_con16	mdC31	M	35	SHH_contro	0.041167	141.2528	0.780069	0.1864	0.6682	1.3349
SHH_con17	mdC32	M	25	SHH_contro	0.036562	131.8392	1.524701	0.1638	0.525	1.0212
SHH_con18	mdC36	M	35	SHH_contro	0.041487	135.2624	0.965557	0.1836	0.6205	1.2041
SHH_con19	mdC37	M	38	SHH_contro	0.042521	112.9278	1.508367	0.1695	0.5966	0.9386
SHH_scz01	mdS02	M	50	SHH_scz	0.021094	176.9505	0.864782	0.2034	0.6921	1.3059
SHH_scz02	mdS03	M	39	SHH_scz	0.030355	147.449	0.974352	0.1751	0.5489	1.1017
SHH_scz03	mdS06	F	48	SHH_scz	0.039513	118.4143	1.114847	0.2034	0.6205	1.2061
SHH_scz04	mdS07	M	25	SHH_scz	0.040696	116.6244	0.73294	0.1808	0.6443	1.2369
SHH_scz05	mdS08	F	25	SHH_scz	0.041919	96.94207	0.864037	0.1864	0.5727	1.3053
SHH_scz06	mdS09	F	34	SHH_scz	0.073697	68.71494	0.730803	0.065	0.1432	1.0232
SHH_scz07	mdS10	M	56	SHH_scz	0.032016	117.431	0.969076	0.1921	0.6205	1.1978
SHH_scz08	mdS11	M	52	SHH_scz	0.039812	118.2248	0.746279	0.1695	0.5966	1.2225
SHH_scz09	mdS12	M	30	SHH_scz	0.032636	138.6062	0.924089	0.1977	0.6682	1.2717
SHH_scz10	mdS13	M	24	SHH_scz	0.030249	151.1601	1.2096	0.1893	0.6205	1.1642
SHH_scz11	mdS14	F	53	SHH_scz	0.059002	90.23159	0.637791	0.1836	0.5489	1.1826
SHH_scz12	mdS15	M	45	SHH_scz	0.04066	131.2024	0.836307	0.1299	0.4295	1.199
SHH_scz13	mdS16	F	37	SHH_scz	0.03574	117.1494	0.820917	0.1977	0.6921	1.3335
SHH_scz14	mdS17	F	42	SHH_scz	0.05106	100.1264	0.812454	0.1949	0.6205	1.3104
SHH_scz15	mdS18	F	41	SHH_scz	0.033324	126.6153	1.398223	0.1751	0.5966	1.0709
SHH_scz16	mdS19	F	21	SHH_scz	0.040523	92.54551	1.014319	0.2147	0.7636	1.3649
SHH_scz17	mdS22	M	46	SHH_scz	0.042426	82.57683	0.702456	0.1864	0.5966	1.2481
SHH_mdd01	mdD03	M	53	SHH_mdd	0.023326	192.4872	0.858386	0.1836	0.6205	1.1755
SHH_mdd02	mdD04	F	31	SHH_mdd	0.039933	171.9696	1.018612	0.1977	0.6682	1.2621
SHH_mdd03	mdD05	F	31	SHH_mdd	0.058217	173.5708	0.90281	0.1921	0.7159	1.2564
SHH_mdd04	mdD06	F	28	SHH_mdd	0.031775	189.8112	1.014049	0.2119	0.6921	1.332
SHH_mdd05	mdD07	F	27	SHH_mdd	0.033134	189.0216	0.933033	0.1864	0.6205	1.2769
SHH_mdd06	mdD08	F	45	SHH_mdd	0.04404	190.7834	1.24978	0.178	0.525	1.0097
SHH_mdd07	mdD09	M	44	SHH_mdd	0.032098	208.6886	0.93616	0.1921	0.6443	1.1971
SHH_mdd08	mdD10	F	46	SHH_mdd	0.033757	197.676	1.477643	0.178	0.5727	1.0539
SHH_mdd09	mdD11	F	36	SHH_mdd	0.046799	205.3053	0.543593	0.113	0.358	1.1911
SHH_mdd10	mdD12	F	31	SHH_mdd	0.038076	184.1883	0.981545	0.2175	0.7875	1.3328
SHH_mdd11	mdD13	M	26	SHH_mdd	0.038666	163.3923	1.269681	0.1977	0.6443	1.161
SHH_mdd12	mdD14	F	40	SHH_mdd	0.027497	207.2415	1.045037	0.1864	0.6205	1.2578
SHH_mdd13	mdD15	F	38	SHH_mdd	0.032841	182.3981	1.561034	0.1808	0.5966	0.933
SHH_mdd14	mdD16	F	41	SHH_mdd	0.041097	187.8156	0.808314	0.2232	0.7875	1.3306
SHH_mdd15	mdD17	F	40	SHH_mdd	0.039915	192.2584	0.661546	0.1977	0.7159	1.3509
SHH_mdd16	mdD18	F	40	SHH_mdd	0.03967	170.0649	1.457858	0.1808	0.525	1.0555
SHH_mdd17	mdD20	M	36	SHH_mdd	0.042016	181.1464	1.107246	0.1864	0.6205	1.1594
SHH_mdd18	mdD23	F	45	SHH_mdd	0.03233	184.5821	1.000958	0.178	0.5727	1.1514
SHH_mdd19	mdD24	F	37	SHH_mdd	0.044092	195.699	0.724245	0.1864	0.6205	1.3291
SHH_mdd20	mdD27	F	23	SHH_mdd	0.041316	125.5765	0.95969	0.1384	0.4295	1.1989
SHH_mdd21	mdD30	M	36	SHH_mdd	0.040098	131.4734	1.681117	0.1695	0.4773	1.0301
SHH_mdd22	mdD31	F	42	SHH_mdd	0.034336	161.9219	1.433947	0.1525	0.4773	0.8239
SHH_mdd23	mdD32	M	33	SHH_mdd	0.030799	140.5401	1.321823	0.1893	0.6443	1.1268
SHH_mdd24	mdD34	M	45	SHH_mdd	0.034977	153.4769	1.349488	0.1751	0.525	1.0701
SHH_mdd25	mdD35	M	43	SHH_mdd	0.039228	112.9682	0.923428	0.1017	0.2386	0.9717
SHH_mdd26	mdD36	F	45	SHH_mdd	0.033463	174.5629	1.553276	0.1525	0.4534	1.0272
SHH_mdd27	mdD37	M	26	SHH_mdd	0.038772	111.0464	0.996336	0.1893	0.6682	1.1213
SHH_mdd28	mdD38	M	33	SHH_mdd	0.045006	96.10757	0.783682	0.1949	0.6443	1.2804

Dataset-III	subject	sex	age	group	restFD	restSNR	ple	ETC	LZ	ApEn
BP_con01	subj101	F	57	BP_control	0.035901	175.1545	0.777674	0.2192	0.5877	1.5284
BP_con02	subj102	F	36	BP_control	0.028885	179.182	0.322631	0.3288	1.1265	1.6407
BP_con03	subj103	F	51	BP_control	0.041531	164.1779	0.759138	0.2808	0.7836	1.6482
BP_con04	subj104	M	47	BP_control	0.036433	159.7257	0.957484	0.2945	0.8816	1.5752
BP_con05	subj105	F	59	BP_control	0.045318	131.8253	0.285856	0.3356	1.1265	1.7592
BP_con06	subj106	F	45	BP_control	0.021506	186.5087	0.775933	0.3151	1.0285	1.5192
BP_con07	subj108	M	52	BP_control	0.037771	180.8769	0.607855	0.3014	0.9795	1.669
BP_con08	subj109	F	46	BP_control	0.045352	153.8561	0.913626	0.2877	0.8816	1.5081
BP_con09	subj110	F	52	BP_control	0.038774	193.1942	0.187711	0.3151	1.1265	1.766
BP_con10	subj111	M	61	BP_control	0.049236	142.5464	0.836522	0.2945	0.8816	1.6104
BP_con11	subj112	F	31	BP_control	0.026297	182.9934	0.719474	0.3288	0.9795	1.577
BP_con12	subj113	M	57	BP_control	0.038089	172.4589	0.660204	0.2671	0.9795	1.5982
BP_con13	subj114	M	60	BP_control	0.037467	173.7332	0.791756	0.2808	0.9306	1.5576
BP_con14	subj115	M	34	BP_control	0.020106	182.8322	0.586722	0.2808	0.8816	1.5942
BP_con15	subj116	F	60	BP_control	0.03313	183.5593	0.853443	0.2877	0.8816	1.5136
BP_con16	subj117	M	20	BP_control	0.027948	173.352	0.490119	0.3288	1.0285	1.6397
BP_con17	subj118	F	51	BP_control	0.037983	156.0856	0.570617	0.3219	1.0285	1.518
BP_con18	subj119	F	19	BP_control	0.0375	174.981	0.579365	0.3014	0.9306	1.5215
BP_con19	subj120	F	33	BP_control	0.029296	180.3648	0.499282	0.3082	0.9306	1.6516
BP_con20	subj121	M	27	BP_control	0.034626	184.0113	0.824712	0.3014	0.8816	1.5709
BP_con21	subj122	F	50	BP_control	0.029791	188.0505	0.287719	0.3082	1.1265	1.699
BP_con22	subj123	F	30	BP_control	0.040662	140.289	0.587703	0.3082	0.9795	1.6995
BP_con23	subj124	F	30	BP_control	0.057556	128.2501	0.631487	0.2671	0.8326	1.5783
BP_con24	subj125	F	46	BP_control	0.028636	153.1917	0.689159	0.3082	0.9306	1.6254
BP_con25	subj126	F	48	BP_control	0.043741	153.9888	0.910169	0.3082	1.0775	1.5915
BP_con26	subj127	F	51	BP_control	0.032371	207.1901	0.744741	0.3356	1.0775	1.6084
BP_con27	subj128	F	55	BP_control	0.03416	201.4717	0.936969	0.3151	1.0285	1.56
BP_con28	subj129	F	59	BP_control	0.028367	214.0423	0.626196	0.2877	0.9306	1.6906
BP_con29	subj130	F	60	BP_control	0.044033	122.8479	0.88273	0.2877	0.9795	1.5944
BP_con30	subj131	F	60	BP_control	0.041978	169.6865	0.565555	0.3356	1.0285	1.7666
BP_con31	subj132	F	25	BP_control	0.033056	207.5989	0.685573	0.3014	0.8816	1.5817
BP_con32	subj133	M	42	BP_control	0.026439	176.9973	0.440849	0.3219	1.0775	1.7311
BP_con33	subj134	M	60	BP_control	0.034817	156.6714	0.786359	0.2877	0.9795	1.6421
BP_con34	subj135	M	39	BP_control	0.033816	171.8605	0.393542	0.2877	0.9795	1.645
BP_con35	subj136	M	45	BP_control	0.046842	169.9471	0.831106	0.2945	1.0775	1.5094
BP_con36	subj137	M	55	BP_control	0.037416	173.5628	0.562316	0.3356	0.9306	1.6449
BP_con37	subj138	M	32	BP_control	0.034496	157.5245	0.738638	0.3014	1.0285	1.5316
BP_con38	subj139	F	60	BP_control	0.037003	184.1958	0.437674	0.3219	1.0285	1.7251
BP_con39	subj140	F	32	BP_control	0.026223	173.9391	0.609463	0.3288	0.9795	1.7054
BP_con40	subj141	F	29	BP_control	0.031942	176.5205	0.583751	0.3493	1.0775	1.7071
BP_con41	subj142	F	35	BP_control	0.041075	156.9948	0.732521	0.2945	0.7836	1.6526
BP_con42	subj143	M	36	BP_control	0.023438	195.5442	0.965839	0.2877	0.9306	1.511
BP_con43	subj144	F	29	BP_control	0.048779	139.7086	0.806845	0.3082	0.9795	1.5517
BP_con44	subj145	M	28	BP_control	0.026562	174.5981	0.469342	0.3219	1.1265	1.6813
BP_con45	subj146	F	26	BP_control	0.03566	169.3029	0.61548	0.3288	1.0775	1.651
BP_con46	subj147	F	26	BP_control	0.032216	217.0452	0.526805	0.3288	1.1265	1.6608
BP_con47	subj148	F	26	BP_control	0.040894	174.6621	0.885254	0.3219	1.0285	1.5445
BP_con48	subj149	F	26	BP_control	0.03144	190.07	0.626348	0.3014	1.0285	1.5713
BP_con49	subj150	M	56	BP_control	0.049403	159.2784	0.634771	0.3014	1.0285	1.6643
BP_con50	subj151	F	45	BP_control	0.026277	182.5274	0.818794	0.3082	0.9795	1.53
BP_con51	subjlab101	M	29	BP_control	0.035576	181.2325	0.909092	0.3151	1.0775	1.5342
BP_con52	subjlab102	F	28	BP_control	0.025712	192.1997	0.699331	0.3425	1.0775	1.6141
BP_con53	subjlab103	M	29	BP_control	0.073548	149.1571	0.387316	0.3288	0.9795	1.7684
BP_con54	subjlab104	F	28	BP_control	0.029451	178.054	−0.16798	0.2877	1.0775	1.8213
BP_con55	subjlab105	M	22	BP_control	0.025533	176.7473	0.929328	0.3082	0.8816	1.5473
BP_con56	subjlab106	F	27	BP_control	0.026175	205.3034	0.393792	0.3356	1.1755	1.6362
BP_con57	subjlab107	F	28	BP_control	0.023557	197.8421	0.700566	0.2808	0.9795	1.5466
BP_con58	subjlab108	F	38	BP_control	0.032533	153.0275	0.505031	0.3356	1.0775	1.7604
BP_con59	subjlab109	F	29	BP_control	0.030974	179.6558	0.931495	0.3014	0.9306	1.5459
BP_con60	subjlab311	M	61	BP_control	0.053342	139.8832	1.129585	0.2808	0.9306	1.4492
BP_con61	subjlab312	F	31	BP_control	0.026856	200.9004	0.785455	0.3014	0.9306	1.6125
BP_con62	subjlab315	M	35	BP_control	0.035985	195.0133	0.527115	0.2808	0.9306	1.7136
BP_con63	subjlab321	M	29	BP_control	0.03544	168.2033	0.65587	0.2671	0.8816	1.5841
BP_con64	subjlab333	M	42	BP_control	0.044635	160.012	0.524189	0.2877	0.9306	1.7272
BP_con65	subjlab337	M	57	BP_control	0.042091	166.3832	0.399088	0.3082	0.9795	1.6599
BP_con66	subjlab338	M	33	BP_control	0.030932	156.4572	0.840131	0.3014	0.8816	1.6602
BP_con67	subjlab341	F	30	BP_control	0.035789	166.6213	0.777606	0.3082	0.9795	1.5852
BP_con68	subjlab347	F	26	BP_control	0.027163	181.0813	0.648568	0.3288	1.0775	1.5984
BP_con69	subjlab349	F	26	BP_control	0.03593	168.8674	0.793222	0.3219	1.0775	1.562

BP_dep01	subj002	F	53	BP_dep	0.049392	170.7937	0.303588	0.3151	1.0775	1.6789
BP_dep02	subj004	M	20	BP_dep	0.02755	171.5975	0.662301	0.2808	0.8816	1.5728
BP_dep03	subj005	F	56	BP_dep	0.039023	166.8433	0.837363	0.2945	0.9306	1.4076
BP_dep04	subj008	F	48	BP_dep	0.056244	137.1339	0.499816	0.2671	0.8326	1.6785
BP_dep05	subj010	M	52	BP_dep	0.018844	198.3728	0.623873	0.3219	1.0775	1.6704
BP_dep06	subj012	F	36	BP_dep	0.026853	203.1022	0.5758	0.2808	1.0285	1.6155
BP_dep07	subj013	F	56	BP_dep	0.031692	197.2109	0.480381	0.3151	1.0775	1.5953
BP_dep08	subj014	M	59	BP_dep	0.032448	175.5218	0.682994	0.3014	0.9795	1.6155
BP_dep09	subj020	F	34	BP_dep	0.040916	200.2219	0.604549	0.3151	1.0285	1.6009
BP_dep10	subj022	F	31	BP_dep	0.024718	172.3213	0.93452	0.2808	0.8326	1.5392
BP_dep11	subj029	F	49	BP_dep	0.02833	207.4083	0.593151	0.2808	0.9795	1.6176
BP_dep12	subj032	M	47	BP_dep	0.049244	143.3796	0.418747	0.3425	0.9795	1.696
BP_dep13	subj037	M	55	BP_dep	0.036376	164.9863	0.403706	0.3082	1.0775	1.7164
BP_dep14	subj041	F	39	BP_dep	0.037769	166.7021	0.636894	0.2329	0.6367	1.6135
BP_dep15	subj049	F	46	BP_dep	0.035479	180.7149	0.599334	0.3014	1.0285	1.6554
BP_dep16	subj050	F	49	BP_dep	0.038533	177.4734	0.3913	0.3151	1.0775	1.6984
BP_dep17	subj052	F	49	BP_dep	0.042829	172.5279	0.91486	0.2877	0.8816	1.4849
BP_dep18	subj053	M	60	BP_dep	0.035409	166.1263	0.730896	0.3082	1.0775	1.4578
BP_dep19	subj054	M	31	BP_dep	0.032922	155.1323	0.844238	0.3288	1.0285	1.5593
BP_dep20	subjlab226	F	40	BP_dep	0.022128	194.7108	0.505423	0.3151	1.0775	1.6374
BP_dep21	subjlab501	F	45	BP_dep	0.047465	168.2278	0.928183	0.2397	0.7836	1.5342
BP_dep22	subjlab509	F	51	BP_dep	0.123067	96.65002	0.511845	0.3425	1.1265	1.6338
BP_dep23	subjlab510	F	30	BP_dep	0.018595	180.8826	0.587148	0.3082	1.0285	1.7149
BP_eut01	subj001	M	46	BP_eut	0.047999	119.5745	0.101818	0.2945	0.8816	1.668
BP_eut02	subj009	F	45	BP_eut	0.03822	179.5347	0.859929	0.3014	0.8326	1.54
BP_eut03	subj011	M	27	BP_eut	0.028536	159.9378	0.478498	0.3288	1.0285	1.6991
BP_eut04	subj015	F	32	BP_eut	0.037303	177.4866	0.541306	0.3219	0.9795	1.6768
BP_eut05	subj017	F	56	BP_eut	0.050549	153.8133	0.560565	0.2877	0.8816	1.6641
BP_eut06	subj019	M	60	BP_eut	0.035934	149.6263	0.766664	0.226	0.7836	1.428
BP_eut07	subj025	F	60	BP_eut	0.038721	173.8748	0.657927	0.2671	0.8326	1.563
BP_eut08	subj027	F	39	BP_eut	0.028621	189.598	0.741197	0.3356	1.0775	1.648
BP_eut09	subj030	F	41	BP_eut	0.027064	167.1799	0.377642	0.3151	0.9306	1.6837
BP_eut10	subj036	M	50	BP_eut	0.039598	162.2178	1.062907	0.2329	0.7347	1.4497
BP_eut11	subj038	M	30	BP_eut	0.033622	178.5674	0.786962	0.3014	1.0285	1.6819
BP_eut12	subj043	F	50	BP_eut	0.027287	197.1417	0.490425	0.3014	1.0285	1.6812
BP_eut13	subj045	F	25	BP_eut	0.031931	189.7049	0.658109	0.2945	0.9795	1.6467
BP_eut14	subj047	F	31	BP_eut	0.034175	209.7623	0.910879	0.2808	0.8816	1.4823
BP_eut15	subj055	M	44	BP_eut	0.023578	173.1694	0.609628	0.1781	0.4898	1.6855
BP_eut16	subj056	F	60	BP_eut	0.035319	155.9438	0.892899	0.274	0.7836	1.4443
BP_eut17	subj057	M	37	BP_eut	0.042148	78.418	0.298939	0.3425	1.1265	1.785
BP_eut18	subj058	F	39	BP_eut	0.042749	199.3477	1.092057	0.3151	1.0285	1.5127
BP_eut19	subj059	F	65	BP_eut	0.045	148.6116	0.209714	0.3288	1.1265	1.6902
BP_eut20	subj060	M	52	BP_eut	0.036255	169.5205	0.571808	0.3288	0.9795	1.6363
BP_eut21	subj207	M	42	BP_eut	0.042923	165.8727	0.716449	0.3082	0.9795	1.615
BP_eut22	subj208	F	48	BP_eut	0.041586	208.4134	0.749293	0.3082	1.0285	1.5943
BP_eut23	subj210	M	52	BP_eut	0.031145	176.9279	0.883245	0.3082	0.9306	1.7024
BP_eut24	subj213	F	56	BP_eut	0.037059	177.9997	0.712488	0.2945	0.9795	1.5986
BP_eut25	subj223	F	46	BP_eut	0.031881	182.1247	0.759651	0.2329	0.8816	1.5574
BP_eut26	subjlab218	F	52	BP_eut	0.03786	149.982	0.677754	0.3082	0.9795	1.5667
BP_eut27	subjlab230	F	41	BP_eut	0.035611	111.187	0.476859	0.2877	0.9795	1.6387
BP_man01	subj003	M	42	BP_man	0.039956	156.5065	0.195853	0.3082	0.9795	1.6412
BP_man02	subj006	F	58	BP_man	0.081285	131.2912	0.784667	0.3082	0.9795	1.5482
BP_man03	subj007	M	42	BP_man	0.02744	183.5125	0.383851	0.2945	0.9795	1.6999
BP_man04	subj016	M	46	BP_man	0.02896	191.0016	0.813509	0.3151	0.8816	1.6058
BP_man05	subj018	F	52	BP_man	0.034759	152.6464	0.204348	0.3288	1.0285	1.7202
BP_man06	subj021	F	56	BP_man	0.044982	160.2273	0.765588	0.3356	1.0775	1.6102
BP_man07	subj023	F	46	BP_man	0.034909	164.1685	0.66574	0.3151	0.8816	1.6826
BP_man08	subj024	F	58	BP_man	0.040308	133.6885	0.799031	0.3151	0.9306	1.5881
BP_man09	subj026	F	40	BP_man	0.029247	179.9428	0.600003	0.1438	0.3428	1.5324
BP_man10	subj028	F	42	BP_man	0.028353	201.3313	0.606413	0.3014	0.8816	1.6769
BP_man11	subj031	F	19	BP_man	0.05304	118.4765	0.70428	0.2123	0.6367	1.5232
BP_man12	subj033	F	62	BP_man	0.035462	205.687	0.476286	0.2808	0.9306	1.6087
BP_man13	subj035	F	18	BP_man	0.032028	197.6239	0.51953	0.2945	0.9795	1.6771
BP_man14	subj039	F	46	BP_man	0.045158	145.3267	0.593077	0.3082	1.0775	1.6727
BP_man15	subj042	F	48	BP_man	0.043592	88.64259	0.541216	0.2808	0.9306	1.6068
BP_man16	subj044	F	51	BP_man	0.031523	171.8103	0.470893	0.2397	0.6857	1.5893
BP_man17	subj046	F	45	BP_man	0.034248	191.6798	0.951572	0.2808	0.8816	1.586
BP_man18	subj051	F	59	BP_man	0.051791	130.2957	0.9084	0.1986	0.4898	1.4381
BP_man19	subj211	M	27	BP_man	0.036045	134.8101	0.787611	0.3425	1.0285	1.6622
BP_man20	subj215	F	32	BP_man	0.028181	172.161	0.556453	0.2945	1.0285	1.6606
BP_man21	subjlab248	F	51	BP_man	0.039901	160.0532	0.636186	0.2671	0.6857	1.5117
BP_man22	subjlab507	F	56	BP_man	0.088481	83.2075	0.530714	0.2055	0.5877	1.4682
BP_man23	subjlab508	M	29	BP_man	0.039966	156.635	0.946041	0.1027	0.2449	1.4177

11.3. Raw Data

Dataset-I

*** CPZ: Chlorpromazine (mg/day)**

*** glu + gln: glutamate + glutamine**

subject	age	gender	CPZ (mg/day)	glu+gln
SCZ1	37	f	57	1.67
SCZ2	33	m	39	1.86
SCZ3	41	f	113	2.09
SCZ4	40	m	368	0.14
SCZ5	22	m	39	2.28
SCZ6	29	m	475	1.96
SCZ7	21	f	154	2.52
SCZ8	54	m	168	1.88
SCZ9	35	m	347	N/A
SCZ10	30	m	154	2.18
SCZ11	32	m	1128	2.09
SCZ12	40	f	197	1.73
SCZ13	31	f	225	1.80
SCZ14	26	f	52	2.01
SCZ15	49	m	52	1.79
SCZ16	33	f	99	2.18
SCZ17	22	m	312	2.15
SCZ18	39	f	17	1.62
SCZ19	27	m	308	1.75
SCZ20	27	m	39	0.14
SCZ21	25	m	308	1.82
SCZ22	40	f	96	1.72
SCZ23	27	m	394	1.80
SCZ24	27	f	39	1.96
SCZ25	38	m	266	2.92
SCZ26	35	m	669	1.77
SCZ27	38	m	208	N/A
SCZ28	55	m	104	1.92

Dataset-II

*** BDI: Beck Depression Inventory**

*** MADRS: Montgomery–Åsberg Depression Rating Scale**

*** N/A: Not Applicable**

SUBJECTS	SEX	AGE	BDI	MADRS
mdC02	M	26	1	N/A
mdC03	M	46	2	N/A
mdC07	F	30	0	N/A
mdC08	F	37	3	N/A
mdC09	F	30	11	N/A
mdC10	F	33	3	N/A
mdC12	F	34	7	N/A
mdC14	F	43	3	N/A
mdC16	F	30	12	N/A
mdC22	F	30	0	N/A
mdC24	F	39	6	N/A
mdC25	F	36	12	N/A
mdC26	F	42	8	N/A
mdC27	F	32	13	N/A
mdC28	F	32	45	N/A
mdC29	F	31	0	N/A
mdC31	M	35	9	N/A
mdC32	M	25	6	N/A
mdC33	F	38	10	N/A
mdC36	M	35	8	N/A
mdC37	M	38	14	N/A
mdD03	M	53	29	31
mdD04	F	31	41	26
mdD05	F	31	26	14
mdD06	F	28	35	31
mdD07	F	27	31	20
mdD08	F	45	27	27
mdD09	M	44	17	36
mdD10	F	46	33	37
mdD11	F	36	40	40
mdD12	F	31	28	36
mdD13	M	26	36	36
mdD14	F	40	38	29
mdD15	F	38	22	23
mdD16	F	41	21	29
mdD17	F	40	19	11
mdD18	F	40	32	31
mdD20	M	36	35	39
mdD22	F	27	30	25
mdD23	F	45	32	25
mdD24	F	N/A	39	36
mdD26	F	38	9	9
mdD27	F	23	42	32
mdD30	M	36	13	19
mdD31	F	42	34	33
mdD32	M	33	24	29
mdD34	M	45	27	31
mdD35	M	43	41	33
mdD36	F	45	38	24
mdD37	M	26	43	37
mdD38	M	33	29	20